Exploring Parasite Diversity: Taxonomic Studies of Parasites from Birds, Crocodilians, and Anurans Across Diverse Ecosystems

by

Haley Rebecca Dutton

A dissertation submitted to the Graduate Faculty of
Auburn University
in partial fulfillment of the
requirements for the Degree of
Doctor of Philosophy

Auburn, Alabama
May 10, 2025

Platyhelminthes, systematics, morphology, Alabama, Africa

Approved by

Anita M., Kelly, Chair, Extension Professor of Fisheries, Aquaculture, and Aquatic Sciences
Nathan V. Whelan, Assistant Research Professor, Director, United States Fish and Wildlife Service Southeast Conservation Genetics Lab
Luke A. Roy, Extension Professor of Fisheries, Aquaculture, and Aquatic Sciences
Timothy J. Bruce, Assistant Professor of Fisheries, Aquaculture, and Aquatic Sciences
Louis H. Du Preez, Professor in Zoology at the North-West University

Abstract

The overall objective of this dissertation was to apply modern taxonomic and molecular phylogenetic methods to understanding “hidden” (undiscovered) parasite diversity in common wildlife species. The specimens described herein were collectedly sourced from parasitological collections and expeditions in the Southeastern United States (Alabama, Louisiana, South Carolina, Georgia, Mississippi) as well as sub-Saharan Africa (Namibia, Mozambique, South Africa, Botswana).

The Southeastern United States is a center of biodiversity for numerous aquatic invertebrate and vertebrate taxa, including mollusks that are the critical first intermediate host for nearly all lineages of trematodes (Platyhelminthes, Digenea; the focus parasite group of the dissertation). We think that the parasite groups infecting these diverse aquatic hosts are correspondingly diverse. Alabama is an ideal geographic locality to study the parasites of aquatic and semi-aquatic wildlife. Because, all free living organisms have some parasites, and despite many researchers writing big grants and traveling far from the United States to collect parasites, the parasites that infect American wildlife species remain under-sampled and under-explored.

Sub-Saharan Africa is a renowned region of the world for its diversity of charismatic megafauna. It is less surveyed the parasites that infect them. This dissertation includes results from opportune necropsies of rarely examined water birds (white-backed and fulvous whistling ducks), which were infected by a new lineage (genus) of bird trematode, as well as an extremely fortunate opportunity to necropsy a fresh-killed Nile crocodile in cooperation with the Namibian Department of Conservation. Again, while the Nile crocodile is an iconic wildlife species in Africa, our examination of a single individual resulted in exciting parasitological discoveries.

Each chapter of this dissertation explores the taxonomic identity and phylogenetic interrelationships, and the Discussion sections and Taxonomic Remarks sections of the works detailed below include components of ecosystem health, ecosystem indicators, host health, biogeography, and host-parasite cophyly.

For Chapter 1, In North America, we discovered *Anativermis normdroneni* n. gen., n. sp., in a Canada goose from Alabama—the first record of a cyclocoelid in this host and region. Cyclocoelids are trematodes (Cyclocoelidae) that primarily parasitize the air sacs and body cavities of birds, particularly waterfowl. Despite their presence in common bird species, many cyclocoelids remain inadequately studied, with new genera and species still being described, underscoring the need for further research. **For Chapter 2,** In Namibia, our survey of birds in ephemeral systems led to the first record of *Dendritobilharzia pulverulenta* in sub-Saharan Africa, infecting white-backed and fulvous whistling ducks. This also marked the first description of a female of *D. pulverulenta* from the continent where it was originally described. **For Chapter 3,** Similarly, we found *Dracovermis occidentalis*, an elusive liolopid digenean, in an American alligator from Alabama after nearly half a century without mention of the species. American alligators are charismatic megafauna that have been extensively studied, making the discovery of this seldom-found trematode quite surprising. **For Chapter 4,** In Africa, we discovered *Ngubuvangandu francoisjacobsi* n. gen., n. sp., in a Nile crocodile in Namibia, expanding our knowledge of crocodilian liolopids and reshaping their taxonomic grouping. This discovery underscores how much remains to be understood about crocodilian parasitology, even in species that are frequently examined, and emphasizes the need for ongoing exploration in well-studied wildlife populations. **For Chapter 5,** Furthermore, we identified *Latergator louisdupreezi* n. gen., n. sp., infecting the eye of an alligator in Louisiana. The discovery of a

polystomatid on an alligator is significant, as it represents the first record of a polystomatid infecting a crocodilian. This broadens our understanding of the host range of these parasites and provides new insights into parasitic relationships in reptiles. **For Chapter 6,** In amphibians, we redescribed *Polystoma nearcticum* from Cope's gray treefrogs in Alabama, with molecular data suggesting the need for a new genus to accommodate North American treefrog polystomatids.

These discoveries, while occurring in different regions and hosts, share common themes: overlooked parasite diversity, host-parasite relationships that exceed geographic boundaries, and the continued need for taxonomic and molecular research to classify these organisms accurately. The fact that these parasites remained undiscovered or need to be redescribed in frequently studied animals highlights how much remains to be learned about parasite biodiversity, even in well-surveyed ecosystems. These findings underscore the vast, hidden world of parasites that remains to be explored, regardless of location.

Acknowledgments

I thank my advisor and mentor Anita M. Kelly (School of Fisheries, Aquaculture, and Aquatic Sciences [SFAAS], College of Agriculture [COA], Auburn University [AU], Auburn, AL) for sharing her expertise and experiences with me, for her patience and understanding, and guidance throughout this program. I am thankful to my committee members Nathan Whelan (United States Fish and Wildlife, SFAAS, COA, AU, Auburn, AL), Luke Roy (SFAAS), and Timothy Bruce (SFAAS) for providing comments on this dissertation, and for their help outside the dissertation in the Aquatic Animal Health field. I especially thank my committee member Louis Du Preez (North-West University, South Africa) for sharing his knowledge about polystomatids, but also for teaching me about the herpetofauna, avian fauna, and botanical diversity we encounter in the field, for being our guide through 4 different South African countries and teaching me the art of the potjie. Baie dankie.

I thank my laboratory mates that have been with me since I started my masters Micah "Brett" Warren and Steve Ksepka, but also all the new additions Triet Truong, Steve Curran, John Brule, Kamila Cajiao-Mora, and Chissy Smith. Thank you all for your friendship, for taking your time to look for parasites in whatever host that comes into the lab, and for your general excitement, your insights, energy, and conversations that make those long hours in the lab fun.

I thank my parents Tracy and Kevin Haake and Ross Dutton for talking me through the lows and celebrating with me during the highs and for their unwavering love and support. I am inspired by my Mimi (Martha Drake) for always being optimistic and joyful. She may not be able to vocalize her support anymore, but I hope she is proud of I have accomplished. Thank you to my sisters, cousins, niece, nephews, and friends for all of their kindness and support, I love you all.

I couldn't have done any of this without the support of my husband and our puppy dogs at home. For all the academic breaks that were not spent on break but in the lab or in the field, all the evening conversations talking about parasites and taxonomy, and constant encouragement to acknowledge my expertise and to have to confidence to voice it. Finally, I dedicate this document to my dog Comet, my spirit animal, she has been in my life since I started in parasitology during my undergrad at Peru State College and has been by my side through every degree, move, adventure, and new beginning we have started.

Table of Contents

List of Tables

List of Figures

CHAPTER 1: NEW GENUS AND SPECIES OF CYCLOCOELIDAE STOSSICH, 1902 (PLATYHELMINTHES: DIGENEA) INFECTING THE NASOPHARYNGEAL CAVITY OF CANADA GOOSE, *BRANTA CANADENSIS* (ANSERIFORMES: ANATIDAE) FROM WESTERN ALABAMA

***Published in Journal of Parasitology (01 August 2023)**

Authors: Haley R. Dutton, Stephen A. Bullard, and Anita M. Kelly

ABSTRACT

While surveying the parasites of birds associated with western Alabama aquaculture ponds, we collected several specimens of *Anativermis normdroneni* n. gen., n. sp. (Digenea: Cyclocoelidae) from the nasopharyngeal cavity of a Canada goose, *Branta canadensis* (Linnaeus, 1758) (Anseriformes: Anatidae). These flukes were heat-killed and fixed in neutral buffered formalin for morphology or preserved in 95% ethanol for DNA extraction. *Anativermis* resembles *Morishitium* (Witenberg, 1928) by having testes that are spheroid with smooth margins and located in the posterior quarter of the body, an anterior testis that is lateral to the midline and abuts the respective cecum, a posterior testis that is medial (testes diagonal) and abuts the cyclocoel, a genital pore that is immediately post-pharyngeal, and a vitellarium that is discontinuous posteriorly. The new genus differs from *Morishitium* and is unique among all other cyclocoelid genera by having the combination of a body that is broadest in the anterior body half, a posterior body end that is more sharply tapered than the anterior body end, an ovary that nearly abuts the posterior testis, a vitellarium that is asymmetrical and distributes from the area immediately posterior to the cecal bifurcation posteriad to approximately the level of the ovary, and uterine loops extending dorsolateral to the ceca and filling the space between the ceca and the respective body margin for nearly the entire body length. The new genus was recovered

as a distinct lineage in separate *28S, 18S*, and *ITS2* phylogenetic analyses. This is the first report of a cyclocoelid infecting the Canada goose and of a cyclocoelid from Alabama.

INTRODUCTION

While surveying the parasites of birds associated with western Alabama aquaculture ponds raising channel catfish, *Ictalurus punctatus* Rafinesque, 1818 (Siluriformes, Ictaluridae), we discovered several large trematodes infecting the nasopharyngeal cavity of a Canada goose, *Branta canadensis* (Linnaeus, 1758) (Anseriformes: Anatidae). We describe these specimens as a new species of Cyclocoelidae Stossich, 1902 (Digenea) and propose a new genus for the new species. Cyclocoelidae includes >120 species that mature in the airways, air sacs, nasopharyngeal cavity, hypothalamus, liver, and body cavity of birds (Kossack,1911; Witenberg, 1923, 1926; Baskirova, 1950; Dubois, 1959; Kanev et al., 2002). Dronen and Blend (2015) published the most recent revision of the family and accepted 6 subfamilies and 22 genera.

MATERIALS AND METHODS

An infected Canada goose was shot dead at an aquaculture farm (32°29'22.9"N 87°36'47.0"W) in Hale County, Alabama (USDA Aquatic Nuisance Species Permit), transferred to personnel of the Southeastern Cooperative Fish Parasite and Disease Laboratory, transported to Auburn University in a cooler of ice, and dissected. The goose was identified as a Canada goose by having a black head with white cheeks and chinstrap, black neck, tan breast, and brown back (Dunn, 1987). A total of 4 live trematode specimens were removed from the nasopharyngeal cavity of this goose and placed in physiological saline. Specimens intended for morphology were heat-killed on glass slides using a butane hand lighter under little or no coverslip pressure, fixed in 10% neutral buffered formalin, rinsed with distilled water, stained in

Van Cleave's hematoxylin with several drops of Ehrlich's hematoxylin, dehydrated through a graded series of EtOHs, made basic at 70% EtOH with lithium carbonate and butyl-amine, dehydrated in absolute EtOH and xylene, cleared with clove oil, and permanently mounted on glass slides using Canada balsam (Dutton et al., 2019). The resulting whole mounts were examined and illustrated with the aid of an Olympus BX53 (Olympus, Tokyo, Japan) with DIC and a drawing tube, and a Ken-A-Vision X1000 Microprojector (Ken-A-Vision, Raytown, Missouri). Measurements were obtained with a calibrated ocular micrometer (as straight lines along the course of each duct) and are reported in micrometers (μm) as the range followed by the mean, +/− standard deviation, and sample size in parentheses. Types of the new species were deposited in the National Museum of Natural History's Invertebrate Zoology Collection (Smithsonian Institution, USNM Collection Nos. 1683864–1683866). Classification and anatomical terms for cyclocoelids follow Dronen and Blend (2015).

Total genomic DNA (gDNA) was extracted from 2 cut portions of 1 EtOH-preserved specimen using DNeasy™ Blood and Tissue Kit (Qiagen, Valencia, California) as per the manufacturer's protocol with 1 exception; the proteinase-K incubation period was extended overnight, and 100 μl of elution buffer was used to increase the final DNA concentration. The *28S, 18S*, *ITS2* and *CO1* genes were amplified using the primer set and PCR amplifications according to Urabe et al. (2020). DNA sequencing was performed by Genewiz, Incorporated (South Plainfield, New Jersey). Sequence assembly and analysis of chromatograms were performed with Geneious version 2022.0.2 (http://www.geneious.com). All nucleotide sequence data were deposited in GenBank (OQ780427, OQ780428, OQ780430, OQ780431, OQ802836, OQ821763, OQ821977). The phylogenetic analyses included two identical sequences of the new species, all available *28S, 18S,* and *ITS2* sequences from Cyclocoelidae and Typhlocoelidae

Harrah, 1922, expanding on the work of Olson et al. (2003), members from Schistosomatidae Stiles and Hassall, 1898, and a haploporid comprising the outgroups. Sequences were aligned with the multiple alignment tool using fast Fourier transform (MAFFT) (Katoh and Standley, 2013) and trimmed to the length of the shortest sequence (1,179 [28S] base pairs). JModelTest 2 version 2.1.10 was implemented to perform statistical selection of the best-fit nucleotide substitution models based on Bayesian Information Criterion (BIC) (Darriba et al., 2012). Aligned sequences were reformatted (from .fasta to .nexus) using the web application ALTER (Glez-Peña et al., 2010) to run Bayesian inference (BI). BI was performed in MrBayes version 3.2.5 (Ronquist and Huelsenbeck, 2003) using substitution model averaging ("nst-mixed") and gamma distribution to model rate-heterogeneity. Defaults were used in all other parameters. Three independent runs with 4 Metropolis-coupled chains were run for 5,000,000 generations, sampling the posterior distribution every 1,000 generations. Convergence was checked using Tracer v1.6.1 (Rambaut et al., 2014) and the "sump" command in MrBayes: all runs appeared to reach convergence after discarding the first 25% of generation as burn-in. A majority rule consensus tree of the post-burn-in posterior distribution was generated with the "sumt" command in MrBayes. The inferred phylogenetic tree was visualized using FigTree v1.4.4 (Rambaut et al., 2014) and further edited for visualization purposes with Adobe Illustrator (Adobe Systems).

DESCRIPTION

Anativermis n. gen.

(Figs. 1−3)

Diagnosis: Body large, slightly dorsoventrally flat, aspinose, broadest in the anterior body half, rounded anteriorly, more sharply tapered posteriorly. Mouth subterminal, unaccompanied by a demonstrable muscular complex (oral sucker absent). Ventral sucker

absent. Pharynx well developed, immediately posterior to the mouth (hence, a so-called "prepharynx" is absent). Esophagus short, extending posteriad directly from pharynx before connecting to cecal bifurcation. Ceca elongate, sinuous, uniting in posterior body extremity to form cyclocoel. Testes spheroid (not transverse), having smooth margins (lacking lobes), in posterior quarter of body; anterior testis lateral to the midline, abutting respective cecum; posterior testis medial, abutting cyclocoel. Genital pore immediately post-pharyngeal. Ovary spherical, lacking lobes, inter-testicular, nearly abutting posterior testis. Vitellarium asymmetrical, dorsal to ceca, distributing from immediately posterior to cecal bifurcation posteriad to level of ovary, discontinuous posteriorly. Uterus extensively convoluted, dorsal to ceca, spanning breadth of body; uterine loops extending lateral to ceca and filling space between ceca and respective body margin for nearly entire body length, terminating at the level of posterior testis. Parasites of nasopharyngeal cavity of birds.

Differential diagnosis: Body broadest in the anterior body half. Testes spheroid, lacking lobes, in posterior quarter of body; anterior testis lateral to the midline, abutting respective cecum; posterior testis medial, abutting cyclocoel. Genital pore immediately post-pharyngeal. Ovary nearly abutting posterior testis. Vitellarium asymmetrical, distributing from immediately posterior to cecal bifurcation posteriad to level of ovary, discontinuous posteriorly. Uterine loops extend lateral to ceca and fill space between ceca and respective body margin for nearly the entire body length.

Taxonomic summary

Type and only known species: *Anativermis normdroneni* n. sp.

Etymology: *Anativermis*; “Anati” for the host family Anatidae and “vermis” for worm.

***Anativermis normdroneni* n. sp.**

(Figs. 1−3)

Diagnosis of adult (based on light microscopy of 3 heat-killed, stained, whole-mounted specimens): Body large, 18,500−23,800 (21,125 ± 2,650; 3) long, 3,900−5,100 (4,667 ± 666; 3) in maximum width, broadest in anterior half of the body, 4−6× (5 ± 1; 3) longer than wide, posterior end tapering. Mouth 200−250 (227 ± 25; 3) long, 370−420 (388 ± 28; 3) wide. Pharynx strongly muscular, 500−575 (535 ± 38; 3) long or 58−59% (58% ± 1%; 2) of esophagus length, 550−625 (592 ± 38; 3) wide or 6× wider than maximum esophagus width. Esophagus short, 900−1,000 (950 ± 71; 2) long, 100 (100 ± 0; 2) wide (Fig. 2). Intestinal bifurcation 820−1,370 (1,147 ± 289; 3) or 3−7% (6% ± 2%; 3) of body length from anterior body end. Cecal bifurcation to cyclocoel 16,525−22,625 (19,600 ± 3,050; 3) long or 89−95% (93% ± 3%; 3) of body length.

Testes nearly in line, not forming a strongly triangular pattern with ovary; anterior testis 1,250−1,350 (1,283 ± 58; 3) long or 5−7% (6% ± 1%; 3) of body length, 950−1,250 (1,083 ± 153; 3) wide or 21−25% (23% ± 2%; 3) of body width at level of ovary, 74−95% (82% ± 11%; 3) of posterior testis width; inter-testicular space 2075−2375 (2233 ± 151; 3) long or 10–12% (11% ± 1%; 3) of body length; posterior testis 1,350−1,625 (1,450 ± 152; 3) long or 6−8% (7% ± 1%; 3) of body length, 1,000−1,700 (1,350 ± 350; 3) wide or 26−33% (29% ± 4%; 3) of body width at level of ovary, 310−625 (462 ± 158; 3) or 1−3% (2% ± 1%; 3) length from end of posterior testis to posterior extremity (Figs. 1, 2). Anterior vas efferens emanating from ventral surface of anterior testis, extending anteriad 13,825−16,200 (14,925 ± 1197; 3) or 66−80% (71% ± 8%; 3) of body length, 30−50 (40 ± 10; 3) wide; posterior vas efferens emanating from ventral surface of posterior testis, extending anteriad 17,325−19,700 (18,342 ± 1,224; 3) or 82−97% (87% ± 9%; 3) of body length, 30−50 (40 ± 10; 3) wide, converging with anterior trunk of vas efferens in anterior 1/5 of body; vas deferens (visible in paratype USNM 1683865) 1,640 long,

50 wide. Cirrus sac oblong, 1,150 −1,300 (1,200 ± 87; 3) long or 5−6% (6% ± 0%; 3) of body length, 350−550 (440 ± 101; 3) wide or 28−49% (38% ±10%; 3) body width at level of genital pore; cirrus aspinose, 550−680 (623 ± 57; 3) long or 48−56% (52% ± 4%; 3) of cirrus sac length, 50−100 (67 ± 29; 3) wide or 4−9% (6% ± 3%; 3) of cirrus sac width (Figs. 1, 2); internal seminal vesicle coiled, 680−800 (727 ± 64; 3) long or 59−62% (61% ± 1%; 3) of cirrus sac length, 350−500 (410 ± 79; 3) wide or 90−100% (94% ± 5%; 3) of cirrus sac width.

Ovary slightly longer than wide (not transverse), 700−800 (740 ± 53; 3) long or 3−4% (4% ± 1%; 3) of body length, 640−700 (680 ± 35; 3) wide or 14−16% (15% ± 1%; 3) of body width; post-ovarian space, 2,050−2,500 (2,342 ± 253; 3) or 11−12% (11% ± 1%; 3) of body length. Oviduct diminutive, 100−150 (117 ± 29; 3) long, 15−20 (17 ± 3; 3) wide, anterior to transverse vitelline duct (Fig. 3). Oötype indiscernible in stained, whole-mounted specimens. Mehlis' gland present around oviduct. Laurer's canal not observed. Vitellarium asymmetrical, comprising a series of interconnected, continuous, small, irregularly shaped masses of follicles, distributed along ceca, follicles 100−120 (110 ± 10; 3) long, 50−60 (53 ± 6; 3) wide; dextral vitellarium begins posterior to cecal bifurcation, 4,625−5,375 (4,958 ± 382; 3) or 23−25% (24% ± 1%; 3) from anterior body end, terminating 2,375−2,775 (2,583 ± 201; 3) or 11−14% (12% ± 2%; 3) from posterior body end; sinistral vitellarium begins posterior to cecal bifurcation, 2,250−3,000 (2,683 ± 388; 3) or 11−15% (13% ± 2%; 3) from anterior body end, terminating 1,875−2,500 (2,183 ± 313; 3) or 8−12% (10% ± 2%; 3) from posterior body end; transverse vitelline duct 1,400−2,250 (1,933 ± 465; 3) in breadth, 55−100 (75 ± 23; 3) wide; primary vitelline collecting duct 150−200 (175 ± 25; 3) long, 60−70 (65 ± 5; 3) wide, inserting into oviduct ventrally. Uterus 225,500−297,500 (257,833 ± 36,566; 3) long, individual coils 200−375 (292 ± 88; 3) wide; eggs filling lumen of uterus, oblong, 120−140 (127 ± 12; 3) long, 50−60 (53

± 6; 3) wide; empty/hatched miracidia with eyespots in distal portion of uterus; metraterm absent. Common genital pore 750−1,100 (908 ± 177; 2) or 4−6% (4% ± 1%; 2) of body length from anterior end, 100−140 (120 ± 28; 2) in diameter (Fig. 1).

Excretory vesicle a vacuous chamber that can either expand (seemingly one large lobe) or contract (appearing multi-lobed) depending on condition of specimen; excretory pore, terminal 250−550 (423 ± 155; 3) wide (Fig. 3).

Taxonomic summary

Type and only reported host: Branta canadensis (Linnaeus, 1758) (Anseriformes: Anatidae), Canada goose.

Type and only known locality: An aquaculture pond (32°29'22.9"N 87°36'47.0"W) in Hale County, Alabama.

Specimens and sequences deposited: Holotype (USNM 1683864); paratypes (USNM 1683865−1683866); *28S*, *18S*, *ITS2*, and *COI* sequences (GenBank Nos. OQ780427, OQ780428, OQ780430, OQ780431, OQ802836, OQ821763, OQ821977).

Site in host: Nasopharyngeal cavity.

Prevalence and intensity: The single Canada goose examined was infected with 4 specimens of *A. normdroneni*.

ZooBank registration: urn:lsid:zoobank.org:act:38DA085F-8070-4299-BD42-90FA97E3F840

Etymology: The specific epithet *normdroneni* honors the late Professor Norman Obert Dronen (Texas A&M University, College Station, Texas) for his extensive contributions to the taxonomy of cyclocoelids.

Taxonomic remarks

We refrain from assigning our new species to a cyclocoelid subfamily because at present the most morphologically appropriate subfamily (Hyptiasminae Dollfus, 1948) is paraphyletic and no nucleotide sequence exists for the type species of the type genus of Hyptiasminae (*Hyptiasmus arcuatus* [Brandes, 1892] Kossack, 1911). Using the subfamily key in Dronen and Blend (2015), the new species was assigned to Hyptiasminae Dollfus, 1948 by having an intertesticular ovary that is nearly in a straight line with the testes, which can be tandem to nearly tandem. Using the generic key in Dronen and Blend (2015), the new species was assigned to *Morishitium* by having a postpharyngeal genital pore and a vitellarium that is not confluent posteriorly. *Anativermis* resembles *Morishitium* by having testes that are spheroid with smooth margins and located in the posterior quarter of the body, an anterior testis that is lateral to the midline and abuts the respective cecum, a posterior testis that is medial (testes diagonal) and abuts the cyclocoel, a genital pore that is immediately post-pharyngeal, and a vitellarium that is discontinuous posteriorly. However, the new genus differs from *Morishitium* and is unique among all other cyclocoelid genera by having the combination of a body that is broadest in the anterior body half, a posterior body end that is more sharply tapered than the anterior body end, an ovary that nearly abuts the posterior testis, a vitellarium that is asymmetrical and distributes from the area immediately posterior to the cecal bifurcation posteriad to approximately the level of the ovary, and uterine loops extending dorsolateral to the ceca and filling the space between the ceca and the respective body margin for nearly the entire body length.

Phylogenetic results

The *28S* sequences of the new species were identical and comprised 1,249 and 1,236 nucleotides. The *28S* phylogenetic analysis contained 1,179 aligned nucleotides and recovered the new species sister to the clade comprising *Neohaematotrephus arayae* Zamparo, Brooks,

Causey and Rodriguez, 2003 (86 nucleotide differences with *A. normdroneni*) and *Cyclocoelum mutabile* (Zeder, 1800) (95 nucleotide differences with *A. normdroneni*). Our results agree with Tkach et al. (2016), who recovered the same topology and suggested that Typhlocoelidae could be a junior subjective synonym of the Cyclocoelidae. The *18S* sequence of the new species was 1,770 nucleotides, and the phylogenetic analysis comprised 471 aligned nucleotides. The new species was recovered in the *18S* tree as sister to *Morishitium grusi* (Kocan, Waldrup, Ramakka, and Iverson, 1982) Dronen and Blend, 2015 (4 nucleotide differences with *A. normdroneni*) and within a polytomy. Based on nucleotide evidence, Sitko et al. (2016) reassigned *Cyclocoelum obscurum* Leidy, 1887 to *Harrahium* Witenberg, 1926, as *Harrahium obscurum* (Leidy, 1887) Sitko and Heneberg, 2016. They also asserted that the sequence ascribed to *C. mutabile* (AJ287494) by Cribb et al. (2001) was misidentified. They identified that sequence as belonging to *Harrahium* sp. since that sequence was distinct and unrelated to their sequence of *C. mutabile* (KU877900). There is reportedly no voucher specimen for the sequence of "*C. obscurum*" by Cribb et al. (2001), making it a nonugen as per Roberts et al. (2018), i.e., a GenBank sequence that is unaccompanied by robust morphological evidence or a museum-curated voucher specimen that underpins its taxonomic identity. The *ITS2* sequences of *A. normdroneni* were identical and comprised 1,030 and 1,036 nucleotides, and phylogenetic analysis contained 492 aligned nucleotides. The new species was recovered sister to the clade comprising *Harrahium. tringae* (Brandes, 1892), Dronen and Blend, 2015 (102 nucleotide differences) and *H. obscurum* (97 nucleotide differences) and within a polytomy. *COI* sequences of the new species comprised 631 nucleotides. The new species was 88% similar to *C. mutabile,* but a phylogenetic analysis using that marker was moot since too few cyclocoelid *CO1* sequences exist to conduct a meaningful analysis. All phylogenetic analyses recovered the new species as a distinct lineage

that shares a common ancestor with at least *Morishitium* and *Cyclocoelum*, the only genera of cyclocoelids represented by *18S, 28S,* and *ITS2* sequences. Noteworthy is that *Morishitium* is paraphyletic in the *18S* tree, with congeners *M. grusi* and *M. polonicum* in different clades (not sharing a recent common ancestor), suggesting further that paraphyletic Hyptiasminae needs revision.

DISCUSSION

Numerous authors have called attention to the fact that Cyclocoelidae needs revision (Tkach et al., 2016; Sitko et al., 2016; Urabe et al., 2020; López-Jiménez et al., 2018; Khan et al., 2019; Assis et al., 2021; Díaz et al., 2022). Using morphological comparisons across genera, Dronen and Blend (2015) provided a robust and critical review of the family, treating several subfamilies that had been recovered as paraphyletic in previous phylogenetic analyses. Dronen et al. (2017) stated that Cyclocoelidae needs additional nucleotide information more than any other trematode family. Tkach et al. (2016) and Assis et al. (2021) synonymized Typhlocoelidae with Cyclocoelidae but did not reconcile the monophyly or taxonomic status of the subfamilies.

Additional nucleotide, phylogenetic, and life cycle information (especially including robust taxonomic identifications of the snail hosts) is needed in this group to test the monophyly of the cyclocoelid subfamilies further and to revise the family. These features are likely informative regarding the natural history of the group. For example, *Cyclocoelum*, *Harrahium*, and *Hyptiasmus* Kossack, 1911 are phylogenetically related and have similar life cycles (Sitko et al., 2006; 2016; Dronen and Blend, 2015). However, obtaining the life cycle for additional species is complicated because these trematodes exploit a broad phylogenetic spectrum of molluscan hosts, i.e., species of Lymnaeidae Rafinesque, 1815; Planorbidae, Rafinesque, 1815; Physidae, Fitzinger, 1833. Cyclocoelids undergo asexual reproduction in freshwater pulmonate

snails or in xerothermic snails that serve as both first and second intermediate hosts. Miracidia, each containing a redia, hatch, in utero or water, and are either attached to or ingested by susceptible snail hosts. However, if not ingested, the miracidium attaches to the epithelium of the snail before injecting a single redia, which produces additional rediae and cercariae within primarily the connective tissue of the snail digestive gland but also in the head-foot and albumin gland (Taft, 1975; McKindsey and McLaughlin, 1995). The tail-less cercaria encysts in the same snail individual before it develops into a metacercaria that is then ingested by a bird (Taft, 1975; Dronen and Blend, 2015). A study documenting the life cycle of the new species is underway.

ACKNOWLEDGMENTS

We thank Tommy Graeter (US Department of Agriculture APHIS Wildlife Services, Greensboro, Alabama) for helping collect the goose; Steve Curran (Southeastern Cooperative Fish Parasite and Disease Laboratory, Auburn, Alabama) for mounting the worms; Anna Phillips, Chad Walter, Kathryn Ahlfeld, and William Moser (Department of Invertebrate Zoology, National Museum of Natural History, Smithsonian Institution, Washington, D.C.) for accepting our museum specimens. This study was supported by the Southeastern Cooperative Fish Parasite and Disease Project, the US Fish and Wildlife Service (Department of Interior), National Sea Grant (National Oceanic and Atmospheric Administration), United States Department of Agriculture (National Institute of Food and Agriculture), Federal Aid in Sport Fish Restoration (Alabama Department of Conservation and Natural Resources, Inland and Marine Resources Divisions), and the Alabama Agricultural Experiment Station (Auburn University, College of Agriculture).

LITERATURE CITED

Assis, J. C., D. López-Hernández, S. Favoretto, L. B. Medeiros, A. L. Melo, N. R. Martins, and H. A. Pinto. 2021. Identification of the avian tracheal trematode *Typhlocoelum cucumerinum* (Trematoda: Cyclocoelidae) in a host–parasite–environment system: diagnosis, life cycle and molecular phylogeny. Parasitology 148: 1383–1391.

Bashkirova, E. I. 1950. Family Cyclocoelidae Kossack, 1911. *In* Trematodes of Animals and Man. Vol. 4., K. I. Skrjabin (ed.). Moskva, Leningrad, U.S.S.R., p. 329–493.

Cribb, T. H., R. A. Bray, and D. T. J. Littlewood. 2001. The nature and evolution of the association among digeneans, molluscs and fishes. International Journal for Parasitology 3: 997–1011.

Darriba, D., G. L. Taboada, R. Doallo, and D. Posada. 2012. jModelTest 2: More models, new heuristics and parallel computing. Nature Methods 9: 772–772. https://doi.org/10.1038/nmeth.2109.

Díaz, E. A., G. Donoso, J. D. Mosquera, D. X. Ramírez-Villacís, G. González, S. Zapata, and D F. Cisneros-Heredia. 2022. Death by massive air sac fluke (Trematoda: *Bothriogaster variolaris*) infection in a free-ranging snail kite (*Rostrhamus sociabilis*). International Journal for Parasitology: Parasites and Wildlife 19: 155–160.

Dronen, N. O., and C. K. Blend. 2015. Updated keys to the genera in the subfamilies of Cyclocoelidae Stossich, 1902, including a reconsideration of species assignments, species keys and the proposal of a new genus in Szidatitreminae Dronen, 2007. Zootaxa 4053: 1–100.

Dronen, N. O., N. R. Al-Kassar, A. H. Ali, M. F. Abdulhameed, B. H. Abdullah, and S. H. Al-Mayah. 2017. Intraspecific variation in adult *Uvitellina iraquensis* Dronen, Ali and Al-Amura, 2013 (Cyclocoelidae: Haematotrephinae) from two collection sites of white-tailed lapwing, *Vanellus leucurus* (Lichtenstein)(Charadriiformes: Charadriidae), in Iraq. Zootaxa 4242: 1–33.

Dubois, G. 1959. Revision des Cyclocoelidae Kossack 1911 (Trematoda). Revue Suisse de Zoologie, 66: 67–147.

Dunn, Jon Lloyd.1987. National Geographic Field Guide to the Birds of North America, 2nd ed. National Geographic Society, Washington, D.C., USA, 464p.

Dutton, H. R., M. B. Warren, and S. A. Bullard. 2019. New genus and species of turtle blood fluke (Platyhelminthes: Digenea: Schistosomatoidea) infecting six-tubercled Amazon River turtles, *Podocnemis sextuberculata* (Pleurodira: Podocnemididae) from the Amazon River Basin (Peru). Journal of Parasitology 105: 671–685.

Glez-Peña, D., D. Gómez-Blanco, M. Reboiro-Jato, F. Fdez-Riverola, and D. Posada. 2010. ALTER: Program-oriented conversion of DNA and protein alignments. Nucleic Acids Research 38(Suppl. 2): W14–W18. https://doi.org/10.1093/nar/gkq321.

Kanev, I., V. Radev, and B. Fried. 2002. Family Cyclocoelidae Stossich, 1902. *In* Keys to the Trematoda, Volume 1, D. I. Gibson, A. Jones, and R. A. Bray (eds.). CABI Publishing and The Natural History Museum, London, England, p. 131–145.

Katoh, K., and D. M. Standley. 2013. MAFFT multiple sequence alignment software version 7: Improvements in performance and usability. Molecular Biology and Evolution 30: 772–780.

Khan, M. S., P. Heneberg, C. Y. Zhou, N. Muhammad, X. Q. Zhu, and J. Ma. 2019. Characterization of the complete mitochondrial genome of *Uvitellina* sp., representative of the family Cyclocoelidae and phylogenetic implications. Parasitology Research 118: 2203–2211.

Kossack, W. 1911. Über Monostomiden. Ph.D Inaugural-Dissertation, Albertus-Universität Königsberg, Königsberg, Germany i. Press, 32pp.

López-Jiménez, A., M. García-Varela, and J. S. Hernández-Orts. 2018. Review of five species of cyclocoelids (Digenea: Cyclocoelidae) from aquatic birds in Mexico with notes on their interspecific variation. Systematic Parasitology 95: 921–942.

McKindsey, C. W., and J. D. McLaughlin. 1995. Species-and size-specific infection of snails by *Cyclocoelum mutabile* (Digenea: Cyclocoelidae). Journal of Parasitology 81: 513–519.

Olson, P. D., T. H. Cribb, V. V. Tkach, R. A. Bray, and D. T. J. Littlewood. 2003. Phylogeny and classification of the Digenea (Platyhelminthes: Trematoda). International Journal for Parasitology 33: 733–755.

Rambaut, A., M. A. Suchard, D. Xie, and A. J. Drummond. 2014. FigTree v1.4.3. http://tree.bio.ed.ac.uk/software/figtree. Accessed 7 August 2022.

Roberts, J. R., K. M.Halanych, C. R. Arias, S. S. Curran, and S. A. Bullard. 2018. A new species of *Spirorchis* MacCallum, 1918, (Digenea: Schistosomatoidea) and *Spirorchis scripta* Stunkard, 1923, infecting river cooter, *Pseudemys concinna* (Le Conte, 1830), (Testudines: Emydidae) in the Pascagoula River, Mississippi, USA, including an updated phylogeny for *Spirorchis* spp. Comparative Parasitology 85: 120–132.

Ronquist, F., and J. P. Huelsenbeck. 2003. MrBayes 3: Bayesian phylogenetic inference under mixed models. Bioinformation 19: 1572–1574.

Sitko, J., A. Faltýnková, and T. Scholz. 2006. Checklist of the trematodes (Digenea) of birds of the Czech and Slovak Republics. Academia, Prague, Czech Republic, 112 p.

Sitko, J., J. Bizos, and P. Heneberg. 2016. Central European parasitic flatworms of the Cyclocoelidae Stossich, 1902 (Trematoda: Plagiorchiida): Molecular and comparative morphological analysis suggests the re- classification of *Cyclocoelum obscurum* (Leidy, 1887) into the *Harrahium* Witenberg, 1926. Parasitology 144: 368–383.

Taft, S. J. 1975. Aspects of the life history of *Cyclocoelum brasilianum* Stossich 1902 (Trematoda: Cyclocoelidae). Journal of Parasitology 61: 1041–1043.

Tkach, V. V., O. Kudlai, and A. Kostadinova. 2016. Molecular phylogeny and systematics of the Echinostomatoidea Looss, 1899 (Platyhelminthes: Digenea). International Journal for Parasitology 46: 171–185.

Urabe, M., N. E. N. Hashim, S. Uni, T. Iwaki, M. R. A. Halim, M. E. Marzuki, A. S. M. Udin, N. A. Zainuri, H. Omar, T. Agatsuma, et al. 2020. Description and molecular characteristics of *Morishitium polonicum malayense* Urabe, Nor Hashim and Uni, n. subsp.(Trematoda: Cyclocoelidae) from the Asian glossy starling, *Aplonis panayensis strigata* (Passeriformes: Sturnidae) in Peninsular Malaysia. Parasitology International 76: 102074. doi:10.1016/j.parint.2020.102074.

Witenberg, G. 1923. The trematodes of the family Cyclocoelidae and a new principle of their systematics. Trudy Gosudarstvennogo Institute Ceksperimental'noaei Veterinarii 1: 84–141.

Witenberg, G. 1926. Die trematoden der familie Cyclocoelidae Kossack 191: Beitrage zur Kenntnis der Helminthenfauna Russlands. . Zoologische Jahrbücher Abteilung für Systematik, Geographie und Biologie der Tiere 52: 103–186.

FIGURE LEGENDS

Figures 1−3. *Anativermis normdroneni* n. gen., n. sp. from the nasopharyngeal cavity of a Canada goose, *Branta canadensis* (Anseriformes: Anatidae) from an aquaculture pond in Hale County, Alabama. (**1**) Body of holotype showing mouth (m), pharynx (ph), common genital pore (cgp), ceca (c), uterus (u), anterior testis (at), ovary (o), posterior testis (pt), and excretory vesicle (ev). Ventral view. (**2**) Anterior end of holotype, showing features labeled in Figure 1 in addition to esophagus (e), cirrus (ci), and cirrus sac (cs). Ventral view. (**3**) Posterior end of holotype, showing features labeled in Figure 1 in addition to vitellarium (v), vasa efferentia (ve), transverse vitelline duct (tvd), Mehlis' gland (mg), primary vitelline collecting duct (pvd). Ventral view.

Figure 4. Large subunit ribosomal DNA (*28S*) Bayesian phylogeny. Values aside nodes are posterior probability. Scale bar is in substitutions per site. GenBank numbers are in parentheses following each taxon. Subfamily names color coded following taxa. Color version available online.

Figures 5, 6. (**5**) Small subunit ribosomal DNA (*18S*) Bayesian phylogeny. Values aside nodes are posterior probability. (**6**) Internal transcribed spacer 2 region of nuclear ribosomal DNA (*ITS2*) Bayesian phylogeny. Color version available online.

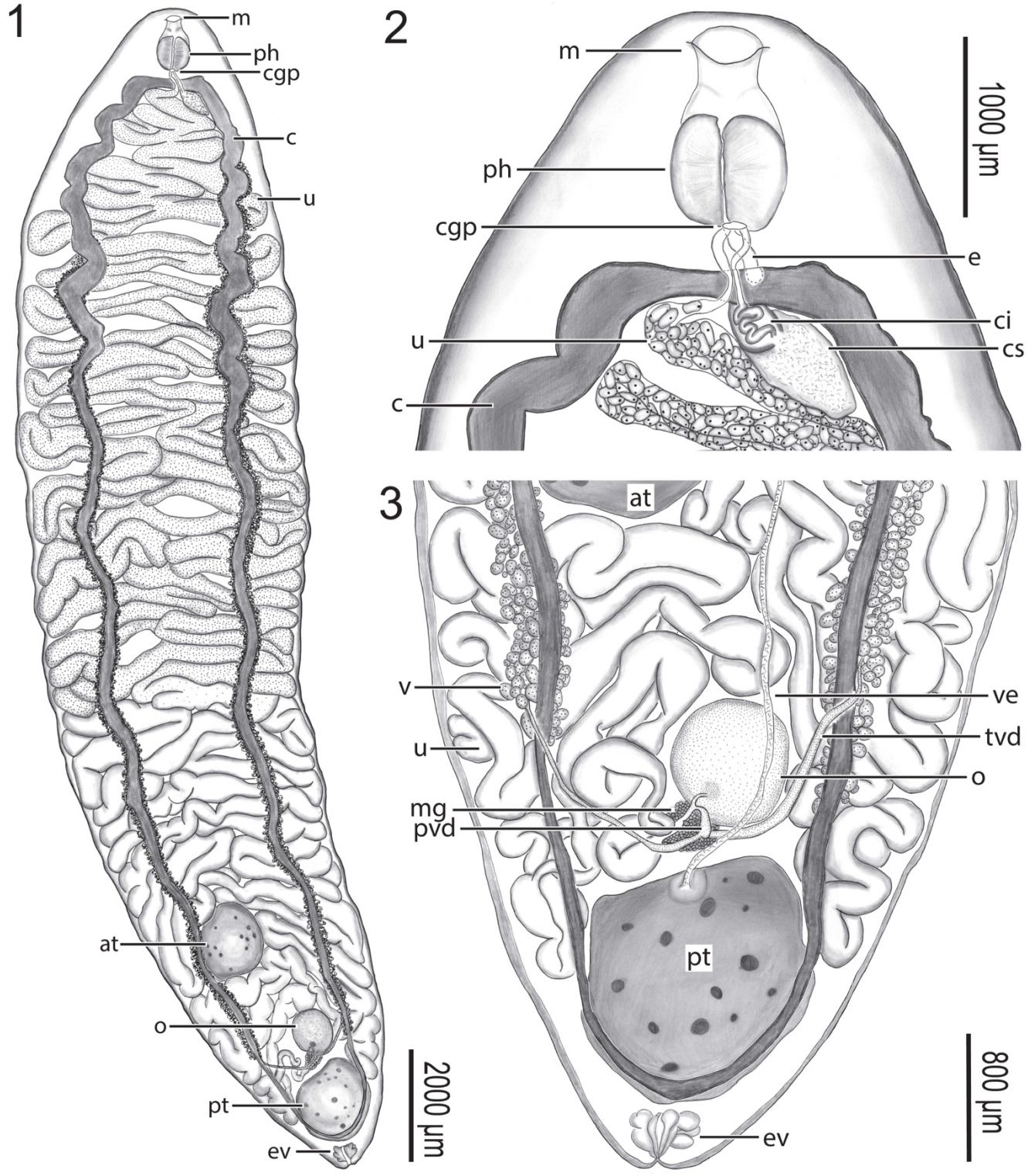
1
m
ph
cgp
c
u
at
o
pt
ev
2000 µm
2
m
ph
cgp
e
ci
cs
u
c
1000 µm
3
at
v
ve
tvd
u
o
mg
pvd
pt
ev
800 µm

4

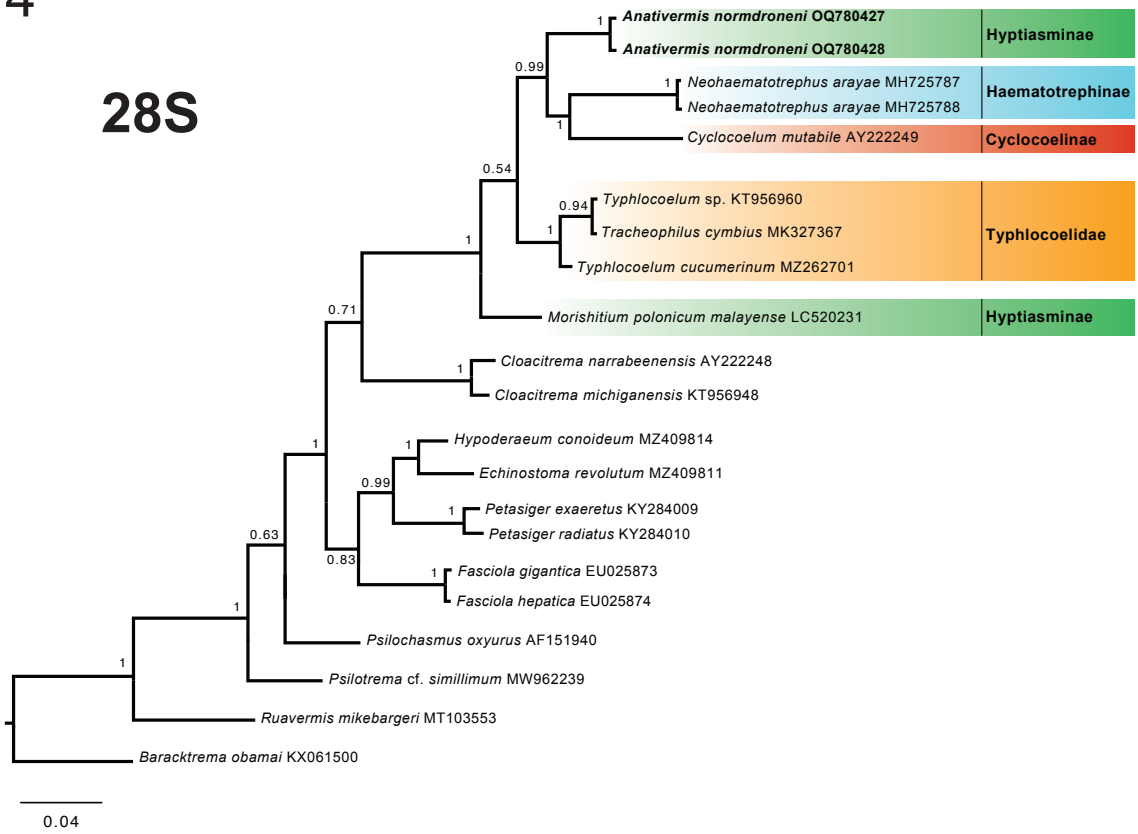
28S
Anativermis normdroneni OQ780427
Anativermis normdroneni OQ780428
Hyptiasminae
Neohaematotrephus arayae MH725787
Neohaematotrephus arayae MH725788
Haematotrephinae
Cyclocoelum mutabile AY222249
Cyclocoelinae
Typhlocoelum sp. KT956960
Tracheophilus cymbius MK327367
Typhlocoelum cucumerinum MZ262701
Typhlocoelidae
Morishitium polonicum malayense LC520231
Hyptiasminae
Cloacitrema narrabeenensis AY222248
Cloacitrema michiganensis KT956948
Hypoderaeum conoideum MZ409814
Echinostoma revolutum MZ409811
Petasiger exaeretus KY284009
Petasiger radiatus KY284010
Fasciola gigantica EU025873
Fasciola hepatica EU025874
Psilochasmus oxyurus AF151940
Psilotrema cf. simillimum MW962239
Ruavermis mikebargeri MT103553
Baracktrema obamai KX061500
0.04

5

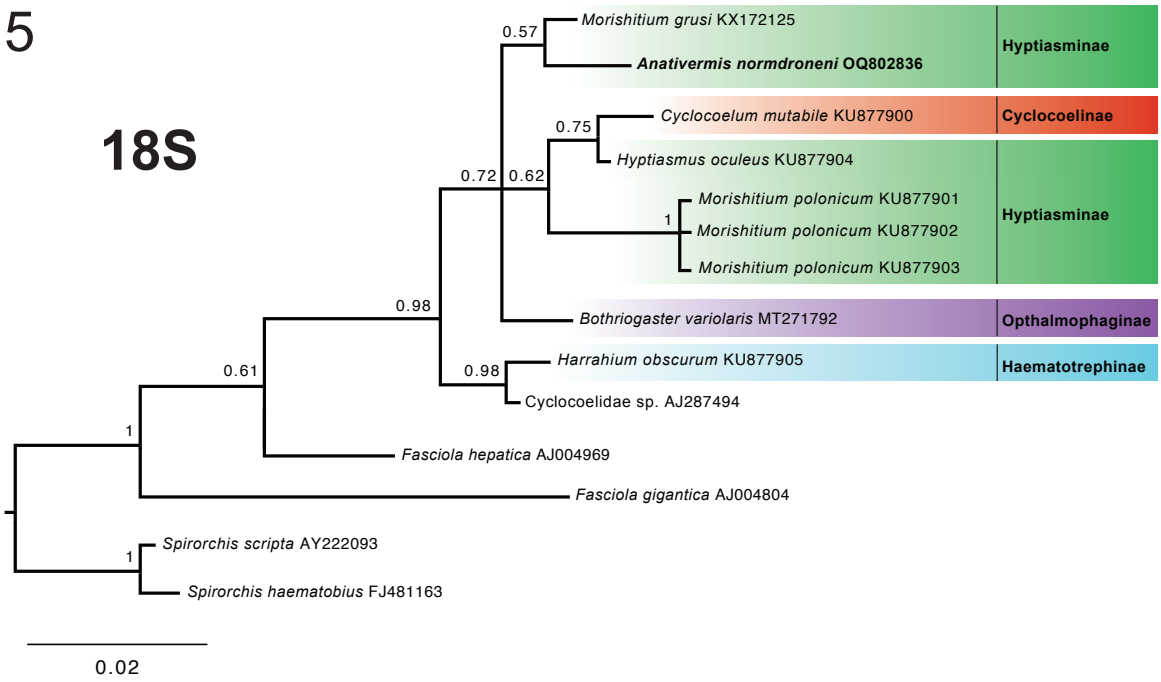
18S
Morishitium grusi KX172125
Anativermis normdroneni OQ802836
Cyclocoelum mutabile KU877900
Hyptiasmus oculeus KU877904
Morishitium polonicum KU877901
Morishitium polonicum KU877902
Morishitium polonicum KU877903
Bothriogaster variolaris MT271792
Harrahium obscurum KU877905
Cyclocoelidae sp. AJ287494
Fasciola hepatica AJ004969
Fasciola gigantica AJ004804
Spirorchis scripta AY222093
Spirorchis haematobius FJ481163
Hyptiasminae
Cyclocoelinae
Hyptiasminae
Opthalmophaginae
Haematotrephinae
0.57
0.75
0.72
0.62
1
0.98
0.61
0.98
1
1
0.02

6

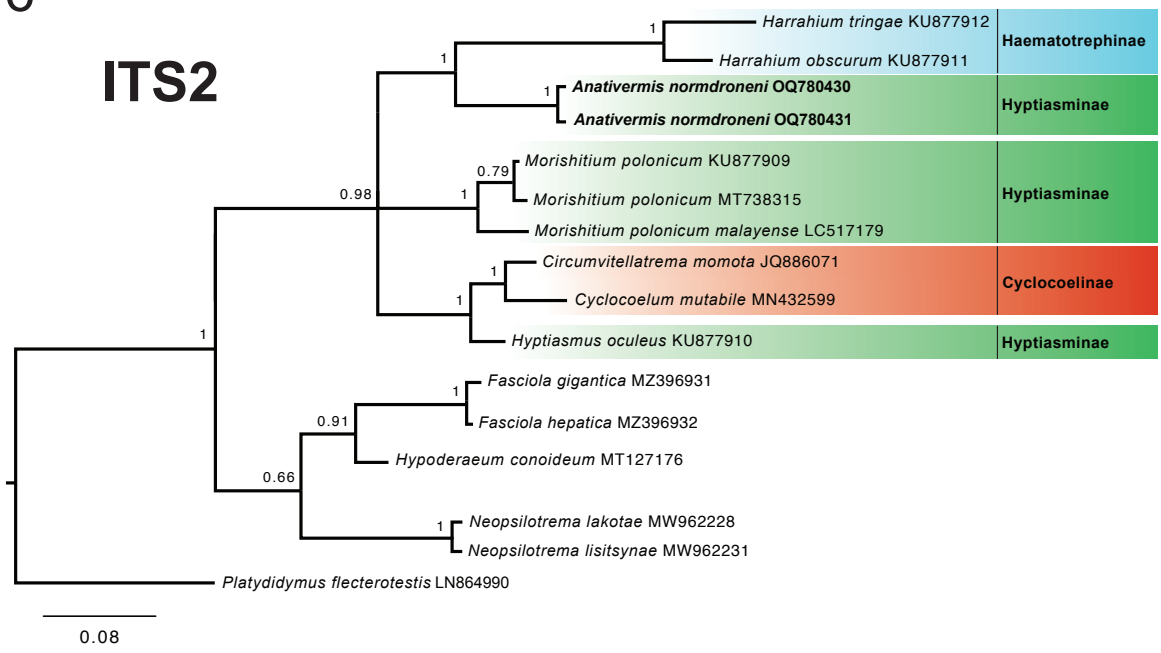
ITS2
Harrahium tringae KU877912
Harrahium obscurum KU877911
Anativermis normdroneni OQ780430
Anativermis normdroneni OQ780431
Morishitium polonicum KU877909
Morishitium polonicum MT738315
Morishitium polonicum malayense LC517179
Circumvitellatrema momota JQ886071
Cyclocoelum mutabile MN432599
Hyptiasmus oculeus KU877910
Fasciola gigantica MZ396931
Fasciola hepatica MZ396932
Hypoderaeum conoideum MT127176
Neopsilotrema lakotae MW962228
Neopsilotrema lisitsynae MW962231
Platydidymus flecterotestis LN864990
Haematotrephinae
Hyptiasminae
Hyptiasminae
Cyclocoelinae
Hyptiasminae
1
1
1
0.79
0.98
1
1
1
1
0.91
0.66
1
0.08

CHAPTER 2: DESCRIPTION OF FEMALE *DENDRITOBILHARZIA PULVERULENTA* (BRAUN, 1901) SKRJABIN, 1924 FROM TWO NEW AVIAN HOSTS IN NAMIBIA WITH PHYLOGENETIC ANALYSES AND COMMENTS ON SEVERAL TAXONOMICALLY UNCERTAIN AVIAN SCHISTOSOME SEQUENCES

***Published in Journal of Parasitology (17 April 2024)**

Authors: Haley R. Dutton, Louis H. DuPreez, Edward C. Netherlands, Bernard J. Jordaan, and Stephen A. Bullard

ABSTRACT

During a 2021 parasitological survey of birds in the Nyae Nyae-Khaudum Dispersal Area (Kavango-Zambezi Transfrontier Conservation Area, Namibia), we collected 9 specimens of *Dendritobilharzia pulverulenta* (Braun 1901) Skrjabin 1924 infecting the blood (heart lumen) of a white-backed duck, *Thalassornis leuconotus* (Eyton, 1838) (Anseriformes: Anatidae) and a fulvous whistling duck, *Dendrocygna bicolor* (Vieillot, 1816) (Anatidae). These flukes were fixed for morphology and preserved for DNA extraction. We assigned our specimens to *Dendritobilharzia* Skrjabin and Zakharow, 1920 because they were strongly dorso-ventrally flattened in both sexes and had an intestinal cyclocoel with a zig-zag common cecum with lateral dendritic ramifications, numerous testes posterior to the cyclocoel and flanking the dendritic ramifications, and a tightly-compacted convoluted ovary as well as lacking an oral sucker, ventral sucker, and gynaecophoric canal. Further, our specimens were morphologically identical to previously published descriptions of *D. pulverulenta*. Sequences of the *28S* from our specimens were nearly identical to those identified as *D. pulverulenta* from North America (New Mexico), and our *28S* phylogenetic analysis recovered *D. pulverulenta* within a polytomy of other Gigantobilharziinae spp. The *CO1* phylogenetic analysis recovered a monophyletic *Dendritobilharzia* and, with low taxon sampling, a monophyletic *Gigantobilharzia*. This is the

first record of a species of *Dendritobilharzia* infecting these ducks as well as the first record of an adult *Dendritobilharzia* from sub-Saharan Africa. The original description of adult *D. pulverulenta* (type locality: northern Sudan) was based on 2 males only, and hence the present study is the first description of female *D. pulverulenta* from Africa (the continent of the type locality). We reassign 2 Gigantobilharziinae spp. based on morphology and nucleotide evidence: *Gigantobilharzia ensenadense* (Lorenti, Brant, Gilardoni, Diaz, and Cremonte, 2022) Dutton and Bullard, n. comb. and *Gigantobilharzia patagonense* (Lorenti, Brant, Gilardoni, Diaz, and Cremonte, 2022) Dutton and Bullard, n. comb. We also comment on several avian schistosome sequences whose identities need confirmation or that likely have been misidentified.

INTRODUCTION

Dendritobilharzia Skrjabin and Zakharow, 1920 is little studied (Vande Vusse, 1980), depauperate (only 2 accepted species), ecologically unique (maturing in the arterial system of aquatic birds [Brant et al., 2011]), and morphologically divergent (lack of ventral sucker; lack of gynaecophoric canal; reduced body shape; and sexual dimorphism [Vande Vusse, 1980; Loker and Brant, 2006]). Considering the taxonomic record for *Dendritobilharzia* and until a morphology-based study eclipses the depth and breadth of the studies reviewed below (especially Vande Vusse [1980]), we accept 2 species of *Dendritobilharzia*: the type species *Dendritobilharzia pulverulenta* (Braun, 1901) Skrjabin, 1924 (the focus of the present study) and *Dendritobilharzia rionegrensis* Martorelli, 1981 (see Martorelli, 1981). Because few species of this rather unusual schistosome genus have been discovered and circumscribed with morphology, any record of either nominal species from a new geographic region and from a new bird host(s) is of interest to our knowledge of the natural history of *Dendritobilharzia* and of the

Schistosomatidae Stiles and Hassall, 1898. Previous to the present study, no adult specimen of *D. pulverulenta* had been collected from Africa since the species was described 122 yr ago. That description was based on 2 adult males only (Braun, 1901, 1902). Hence, no female of *D. pulverulenta* was previously known from Africa. Further, no nucleotide sequence is tethered to an adult of *D. pulverulenta* (type species for *Dendritobilharzia*) from Africa, the continent that includes its type locality (Dongola, northern Sudan). *Dendritobilharzia* and the type genus *Gigantobilharzia* Odhner, 1910 (type species *Gigantobilharzia acotylea* Odhner, 1910) are the only genera of Gigantobilharziinae Mehra, 1940 that we accept (see below).

Herein, we detail an opportune finding of male and female specimens of *D. pulverulenta* from water birds captured within the Nyae Nyae-Khaudum Dispersal Area (NNKDA) (Namibia). This region is essentially unexplored for bird parasites, and to the best of our knowledge the present study is the first record of a bird parasite from that area. We also comment on several avian schistosome sequences whose identities need confirmation or that likely have been misidentified.

MATERIALS AND METHODS

During December 2021, we conducted a parasitological survey of birds in the NNKDA (19º45’41.8”S; 20º28’21.5”E). Birds were captured by hand, euthanized, and examined for the presence of parasites. The heart, lung, kidney, liver, intestine, and mesentery of each bird was excised intact, isolated in containers of physiologic saline, left undisturbed for a few minutes, and ultimately examined in the field with the aid of a stereo-dissecting microscope with fiber optic and substage light sources. Resulting schistosomes were rinsed in saline to remove tissue debris and examined alive before being fixed in 10% neutral buffered formalin for morphology or preserved in 95% EtOH for DNA extraction.

Live specimens intended for morphology were fixed in the field by wet-mounting each live specimen on a slide under a coverslip (no pressure), heat-killed with heat from a butane hand lighter, and fixed in formalin. In the laboratory, the fixed specimens were removed from formalin, stained overnight in Van Cleave's and Ehrlich's hematoxylins (~500:1), rinsed in water, dehydrated in a graded series of EtOHs, placed in a basic solution (3 ml 70% EtOH + 4 drops lithium carbonate cold-saturated in 70% EtOH + 2 drops butylamine [99.5%]) for 10 min at 70% EtOH, completely dehydrated, cleared in clove oil, and whole-mounted in Canada balsam. The resulting whole-mounts were examined and illustrated with the aid of an Olympus BX53 (Olympus, Tokyo, Japan) with differential interference contrast optical components and a drawing tube. Measurements were obtained with a calibrated ocular micrometer (as straight lines along the course of each duct) and are reported in micrometers (μm) as the range followed by the mean, +/− standard deviation, and sample size in parentheses. The number of features measured is provided if the number measured diverged from the total number of worms measured. Seven voucher specimens of *D. pulverulenta* were deposited in the National Museum of Natural History's Invertebrate Zoology Collection (USNM, Smithsonian Institution, Washington, D.C. Nos. 1606776–1606782). Classification and anatomical terms follows Ulmer and Vande Vusse (1970) and Dutton et al. (2019).

The specimen for DNA extraction (from the white-backed duck, *Thalassornis leuconotus* Eyton, 1838 [Anseriformes: Anatidae]) was preserved in 95% EtOH. Total genomic DNA was extracted using the DNeasy™ Blood and Tissue Kit (Qiagen Incorporated, Valencia, California). The *28S*, *COI*, and *ITS1* were targeted for amplification by polymerase chain reaction (PCR) using a Peltier Thermal Cycler (Bio-Rad Corporation, Hercules, California). The 3′ end of the *18S* and complete *ITS1* was amplified using primers BD1 (5′-GTCGTAACAAGGTTTCCGTA -

3′) and 4S (5′-TCTAGATGCGTTCGAARTGTCGATG-3′) (Bowles and McManus, 1993). The *COI* region was amplified using Cox1_Schisto_5' (5′-TCTTTRGATCATAAGCG-3′) and Cox1_Schisto_3' (5′-TAATGCATMGGAAAAAAACA-3′), and the partial *28S* gene was amplified using the primers U178 (5′-GCACCCGCTGAAYTTAAG-3′) and L1642 (5′-CCAGCGCCATCCATTTTCA-3′) (Lockyer et al., 2003). For the *28S* and *ITS1*, thermocycling consisted of an initial denaturing step for 4 min at 94 C, followed by 40 cycles of 3 steps: (1) 40 sec denaturing at 94 C; (2) 30 sec annealing at 50 C; (3) 2 min extension at 72 C; followed by a final extension step for 7 min at 72 C and maintained at 5 C until run through electrophoresis. For the *COI* region, thermocycling consisted of an initial denaturing step for 2 min at 94 C, followed by 40 cycles of 3 steps: (1) 30 sec denaturing at 94 C; (2) 30 sec annealing at 52 C; (3) 2 min extension at 72 C; followed by a final extension step for 7 min at 72 C and maintained at 5 C until run through electrophoresis. PCR reactions were performed with a total volume of 50 µl (34 µl purified water, 10 µl 5X Taq buffer [Promega Corporation, Madison, Wisconsin], 1 µl 10 µM dNTP [Promega Corporation], 1 µl 10 µM forward primer, 1 µl 10 µM reverse primer, 0.3 µl GoTaq DNA polymerase [Promega Corporation], 2 µl DNA extract). PCR products were visualized using gel electrophoresis and then purified using the QIAquick PCR purification kit (Qiagen Incorporated). Purified DNA concentration was estimated using a Nano-Drop-1000 spectrophotometer (Thermo Scientific Corporation, Nanodrop Technologies, Waltham, Massachusetts). Purified DNA samples were prepared for sequencing with a total volume of 15 µl (2 µl 10 µM primer + purified DNA + purified water) with volumes of purified DNA and water depending on DNA sample concentration. DNA sequencing was conducted by GENEWIZ (Azenta Life Sciences, South Plainfield, New Jersey). Sequence assembly and analysis of chromatograms were assembled using MAFFT component (Katoh and Standley, 2013) in

Geneious Prime Software version 2023.0.4 (Geneious Corporation, Auckland, New Zealand). All nucleotide sequences were deposited in GenBank (OR496295, OR50238, OR502382, OR504453).

The phylogenetic analyses included 16 schistosomes and was rooted by 3 turtle blood flukes of Atamatamidae Bullard and Dutton, 2022 (see Bullard et al., 2019; Bullard and Dutton, 2022). Sequences were aligned with the multiple alignment tool using fast Fourier transform (MAFFT) (Katoh and Standley, 2013) and trimmed to the shortest sequence. JModelTest 2 version 2.1.10 selected the best-fit models of nucleotide substitution based on Bayesian Information Criterion (BIC) (Darriba et al., 2012). Aligned sequences were reformatted (from .fasta to .nexus) with ALTER (Glez-Peña et al., 2010). Bayesian inference (BI) was performed in MrBayes version 3.2.5 (Ronquist et al., 2012) using substitution model averaging ("nst-mixed") and a gamma distribution to model rate-heterogeneity (defaults used for all other parameters). Three independent runs with 4 Metropolis-coupled chains were run for 5,000,000 generations, sampling the posterior distribution every 1,000 generations. Convergence was checked using Tracer v1.6.1 (Rambaut et al., 2014) and the "sump" command in MrBayes: all runs reached convergence after discarding the first 25% of generation as burn-in. A majority rule consensus tree of the post burn-in posterior distribution was generated with the "sumt" command in MrBayes. The inferred phylogenetic trees were visualized using FigTree v1.4.4 (Rambaut et al., 2014) and edited with Adobe Illustrator (Adobe Systems).

RESULTS

***Dendritobilharzia pulverulenta* (Braun 1901) Skrjabin 1924**

(Figs. 1−3)

Diagnosis of adult male (based on light microscopy of 3 whole-mounted specimens from the white-backed duck, Thalassornis leuconotus *(Eyton, 1838) (Fig. 1)):* Body slightly more tapered anteriorly than posteriorly, 4,250−6,525 (5,567 ± 1,179; 3) long, 500−600 (533 ± 58; 3) in maximum width at middle of testes field, 9−12× longer than wide, aspinous (Fig. 1); oral sucker absent; mouth subterminal (Fig. 1). Ventral sucker absent. Nerve commissure 175−243 (209 ± 34; 3) or 3−4% (4% ± 1%; 3) of body length from anterior body end. Pharynx absent. Esophagus 435−791 (612 ± 178; 3) long or 9−13% (11% ± 2%; 3) of body length, 33−70 (49 ± 19; 3) wide or 7−12% (9% ± 3%; 3) of body width, with wall approximately 10−15 (13 ± 3; 3) thick, slightly sinuous, medial, lacking esophageal swellings or out-pockets, ventral to nerve commissure; esophageal gland presenting as a contiguous field of gland cells surrounding esophagus from immediately posterior to mouth and terminating at level of or beyond cecal bifurcation to mid-level of seminal vesicle, limited to intercecal space posteriorly, 580−1,150 (810 ± 300; 3) long or 115−145% (131% ± 15%; 3) of esophagus length, 150−190 (167 ± 21; 3) wide or 271−485% (363% ± 110%; 3) of esophagus width (Fig. 1). Intestine having an anterior portion comprising paired ceca and cyclocoel plus a posterior portion comprising a single common cecum extending posteriad, lacking anteriorly directed ceca, bifurcating 440−707 (589 ± 136; 3) or 10−12% (11% ± 1%; 3) of body length from anterior body end, 115−160 (132 ± 25; 3) in breadth or 31−44% (36% ± 7%; 3) of body width at cecal bifurcation, extending posteriad approximately in parallel with respective lateral body margin and flanking seminal vesicle, having numerous shallow lobes or short diverticula, uniting to form pre-gonadal cyclocoel 1,125−1,850 (1,559 ± 383; 3) or 26−29% (28% ± 1%; 3) of body length from anterior body end, subsequently extending posteriad as a single common cecum from cyclocoel; cyclocoel 690−1,300 (1,003 ± 305; 3) long or 16−20% (18% ± 2%; 3) of body length, 185−225 (200 ± 22;

3) wide or 37−38% (38% ± 1%; 3) of body width; common cecum having short laterally-directed diverticula, extending 2,875−4,675 (3,992 ± 975; 3) long or 68−75% (71% ± 4%; 3) of body length posteriad from cyclocoel (Fig. 1).

Testicular field 2,875−4,950 (4,042 ± 1,061; 3) long or 68−76% (72% ± 4%; 3) of body length, distributing from cyclocoel to near posterior body end, dorsal to ceca, not extending laterally beyond nerve cords; each testis oblong, 75−118 (99 ± 22; 10) long, 63−75 (71 ± 7; 10) wide, having lobed margins; pre-testicular distance 1,175−1,725 (1,506 ± 292; 3) long or 26−28% (27% ± 1%; 3) of body length (Fig. 1). Vas deferens extending anteriad 635 −850 (773 ± 120; 3) long or 13−15% (14% ± 1%; 3) of body length from antero-ventral surface of testes field, 7−8 (8 ± 1; 3) wide, crossing midline and turning posteriad upon forming seminal vesicle 610−990 (854 ± 212; 3) or 14−16% (15% ± 1%; 3) of body length from anterior body end (in anterior ¼ of intra-cyclocoel space); seminal vesicle directed entirely posteriad, convoluted, ventral to dextral portion of intestine, 325−455 (393 ± 65; 3) in total length or 38−63% (52% ± 13%; 3) of vas deferens length, 80−100 (90 ± 10; 3) in maximum width in middle portion of seminal vesicle; cirrus aspinous, everting on surface of a tegumental mound, dextral, opening sub-marginally 1,020−1,453 (1,249 ± 218; 3) or 20−25% (23% ± 3%; 3) of body length from anterior body end, 125−200 (163 ± 38; 3) long or 31−51% (42% ± 10%; 3) of seminal vesicle length, 35−45 (42 ± 6; 3) in maximum width or 44−50% (46% ± 3%; 3) of seminal vesicle maximum width; cirrus sac indistinct. Vestigial/rudimentary female genital pore (ventral opening or pit) ventral, sinistral to esophagus, 200 −500 (376 ± 157; 3) or 5−8% (7% ± 2%; 3) of body length from anterior body end, 25−30 (27 ± 3; 3) in diameter (Fig. 1). Excretory vesicle Y-shaped, with sub-terminal pore, 35 −50 (41 ± 8; 3) long.

Diagnosis of adult female (based on light microscopy of 3 specimens from the white-backed duck and 1 specimen from the fulvous whistling duck, Dendrocygna bicolor *(Vieillot, 1816)) (Fig. 2):* As in male with following exceptions. Body 4,975−7,00 (6,156 ± 853; 3) long, 630−775 (708 ± 67; 4) in maximum width at level of the vitellaria field, 8−10× longer than wide (Fig. 2). Nerve commissure 190−275 (230 ± 35; 4) from anterior body end or 4% of body length. Esophagus 570−780 (690 ± 95; 4) long or 11−12% (11% ± 0%; 4) of body length, 25−50 (39 ± 11; 4) wide or 4−7% (5% ± 1%; 4) of body width, with wall approximately 10−20 (15 ± 4; 4) thick, medial to female genital pore; esophageal gland presenting as a contiguous field of gland cells surrounding esophagus from immediately posterior to mouth to cecal bifurcation, 450−850 (673 ± 169; 4) long or 68−114% (98% ± 22%; 4) of esophagus length, 130−300 (203 ± 71; 4) wide (Fig. 2). Intestine bifurcating 580−800 (705 ± 93; 4) or 11−12% (11% ± 0%; 4) of body length from anterior body end, 140−350 (248 ± 105; 4) in breadth or 30−63% (51% ±15%; 4) of body width at cecal bifurcation, extending posteriad approximately in parallel with respective lateral body margin and flanking uterus, forming cyclocoel 1,750−2,425 (2,038 ± 282; 4) or 31−35% (33% ± 2%; 4) of body length from anterior body end; cyclocoel 1,150−1,580 (1,320 ± 183; 4) long or 20−23% (22% ± 2%; 4) of body length, 300−540 (395 ± 103; 4) wide or 48−74% (55% ± 11%; 4) of body width; common cecum 3,250−4,650 (4,156 ± 623; 4) long or 65−69% (67% ± 2%; 4) of body length (Fig. 2).

Ovary comprising a tightly-compacted convoluted mass, not extending laterad beyond nerve cord, occupying intercecal space between oötype and oviducal seminal receptacle; ovarian mass 310−460 (414 ± 70; 4) long or 6−7% (7% ± 0%; 4) of body length, 225−420 (320 ± 80; 4) wide or 36−56% (45% ± 9%; 4) of body width; post-ovarian space 3,500−4,550 (4,206 ± 478; 4) or 62−71% (69% ± 4%; 4) of body length (Fig. 2). Oviduct short, 10−25 (17 ± 6; 4) wide,

extending 420−650 (560 ± 102; 4) postero-mediad from posterior margin of ovary, passing connection of seminal receptacle and extending anteriad along sinistral margin of ovary and connecting to oötype, anterior to seminal receptacle; seminal receptacle comprising a large blind-ending sac (not an oviducal seminal receptacle), connecting to oviduct at midline immediately posterior to ovary, transverse, originating in dextral half of body, crossing midline and extending anteriad to connect with oviduct, 160−190 (175 ± 12; 4) in maximum breadth, 56−110 (77 ± 24; 4) in maximum wide; common vitelline collecting duct emerging from antero-medial margin of vitellarium posterior to cyclocoel, extending anteriad 450−730 (601 ± 115; 4) before connecting to ventral surface of oötype, 10−30 (19 ± 10; 4) wide; oötype slightly sinistral or medial, intercecal, pre-ovarian, occupying space between ovary and uterus, 50−66 (58 ± 9; 4) long, 15−30 (24 ± 6; 4) wide, 1,280−1,650 (1,408 ± 170; 4) or 21−26% (23% ± 2%; 4) of body length from anterior body end (Fig. 2). Mehlis' gland diffuse, well-stained (basophilic), surrounding oötype. Laurer's canal originating from proximal portion of oviduct in sinistral half of body immediately posterior to ovary, 40−100 (60 ± 27; 4) long, 8−13 (10 ± 2; 4) wide, with dorsal pore (Fig. 2). Vitellarium comprising a series of interconnected small, irregular-shaped masses of vitelline follicles, dorsal and ventral to common cecum and filling spaces between its dendritic branches, posterior to cyclocoel, extending laterad ventral to nerve cords, 3,425−4,650 (4,206 ± 537; 4) long or 66−70% (68% ± 1%; 4) of body length, 470−650 (568 ± 77; 4) wide; vitelline follicles 18−38 (27 ± 10; 10) long, 13−25 (19 ± 6; 10) wide. Uterus filling intercecal space anterior to oötype, extensively convoluted, comprising proximal and distal portions; proximal uterus extensively convoluted, intercecal, occupying space between cecal bifurcation and oötype, filling a space 450−700 (525 ± 119; 4) long or 7−10% (9% ± 1%; 4) of body length, 230−290 (258 ± 25; 4) wide or 33−39% (36% ± 2%; 4) of maximum body width; distal uterus

approximately three-fourths esophagus length, extending 450−570 (518 ± 54; 4) anteriad before connecting to female genital pore, lacking a muscular wall (no evidence of metraterm is present), glandular at distal most portion; uterine eggs distributing throughout uterus, oblong, lacking surface features discernible with light microscopy, 25−31 (28 ± 4; 10) long, 20−25 (23 ± 4; 10) wide (Fig. 2). Female genital pore in same relative location as 'rudimentary female genital pore' of male, sinistral, adorned with tegumental palps, opening at approximate middle section of esophagus, 320 −440 (370 ± 51; 4) or 5−6% (6% ± 0%; 4) of body length from anterior end, 40−75 (54 ± 15; 4) in diameter. Excretory vesicle as in male, 40−125 (68 ± 39; 4) long (Fig. 2).

Taxonomic summary

Type host: Garganey, *Spatula querquedula* (del Hoyo and Collar, 2014) (Anseriformes: Anatidae).

New hosts reported herein: White-backed duck, *Thalassornis leuconotus* (Eyton, 1838) (Anatidae) and fulvous whistling duck, *Dendrocygna bicolor* (Vieillot, 1816) (Anatidae).

Type locality: Dongola, northern Sudan.

New locality reported herein: Nyae Nyae-Khaudum Dispersal Area, Namibia (19º45'41.8"S, 20º28'21.5"E).

Specimens and sequences deposited: USNM: 1606776–1606782, GenBank: OR496295, OR50238, OR502382, OR504453.

Site in host: Arterial circulation; heart.

Prevalence and intensity: 2 of 2 (100%) white-backed ducks had 5 specimens of *D. pulverulenta* (3 males and 1 female fixed in formalin plus 1 male preserved in 95% EtOH) and 3 specimens of *D. pulverulenta* (2 females fixed in formalin; 1 female preserved in 95%

EtOH), respectively; 1 of 3 (33%) fulvous whistling ducks was infected with 1 female specimen of *D. pulverulenta* fixed in formalin.

Taxonomic remarks

Braun (1901) described and redescribed (Braun, 1902) *D. pulverulenta* (as *Bilharziella* Looss, 1899) based on 2 males excised from a garganey originally captured from Dongola, northern Sudan. These specimens were collected by the explorers/zoologists Christian Gottfried Ehrenberg and Wilhelm Friedrich Hemprich (Braun, 1901; Lazarus and Jahn, 1998) during an expedition that began in the lower reaches of the Nile River (1820) before going to the upriver city of Dongola and ultimately to the Red Sea (1823). This expedition resulted in ~4,000 animal specimens that were donated to the Berlin Zoological Museum; among those materials were the type specimens of *D. pulverulenta* that Braun described 74 yr later (Lazarus and Jahn, 1998). To the best of our knowledge, this stands as the only record of an adult of *Dendritobilharzia* from Africa, with no previous description of a female of *Dendritobilharzia* from Africa (hence, nor of a female of *D. pulverulenta* from Africa) (Braun 1901; 1902). Moreover, the present record is the first record of an adult of *Dendritobilharzia* from sub-Saharan Africa (Vande Vusse, 1980).

Ulmer and Vande Vusse (1970) carefully considered *Dendritobilharzia* and studied the morphology of the type species *D. pulverulenta*. These authors made no mention of the location or disposition of a type specimen of *D. pulverulenta*, and we assume they did not study Braun's types. We made an attempt to locate these specimens but they were inaccessible to us (or perhaps lost) at the time of the writing of this paper. Ulmer and Vande Vusse (1970) emphasized that prior to their work, species of *Dendritobilharzia* had been described or studied using a single specimen or few specimens of a single sex. Their study comprised 131 males and 81 females of *D. pulverulenta* collected from birds in northwest Iowa (North America), including

measurements, histological sections, and detailed illustrations of the male and female reproductive systems. This study firmly circumscribed the morphological features of *D. pulverulenta*, and our specimens conform to that description in all regards except that our specimens do not appear to have an obvious, strongly muscular metraterm.

Ten years later, Vande Vusse (1980) reviewed *Dendritobilharzia*, provided a taxonomic history of its species, and listed all known bird hosts and geographic localities for *Dendritobilharzia* spp. He morphologically diagnosed the genus as having dendritic branches arising from the common cecum, and this autapomorphy remains diagnostic to date, i.e., no other schistosomatid has such a dendritic common cecum. He asserted that this genus of schistosome was among the least well known of the family and conducted a detailed morphological study of all available specimens of each species of *Dendritobilharzia* that existed at the time. He regarded *Dendritobilharzia loossi* Skrjabin, 1924 and *Dendritobilharzia anatinarum* Cheatum, 1941 as junior subjective synonyms of *D. pulverulenta* (see also Macko [1959], who synonymized *D. anatinarum* with *D. pulverulenta*). The World Register of Marine Species lists *D. anatinarum* as an accepted species, citing the checklist of Iranian digeneans by Nazarbeigy et al. (2021). Vande Vusse (1980) summarized that Skrjabin (1924) regarded *Dendritobilharzia odhneri* Skrjabin and Zakharow, 1920 as a junior subjective synonym of *D. pulverulenta* and accepted that synonymy (Skrjabin and Zakharow, 1920). He also designated *Dendritobilharzia asiatica* Mehra, 1940 as a *species inquirenda* and *Dendritobilharzia fedtschencowi* Skrjabin, 1923 as a *nomen nudum*.

A year later, Martorelli (1981) described 8 males and 7 females of *D. rionegrensis* from a red-fronted coot, *Fulica rufifrons* Philippe and Landbeck, 1861 in Argentina. He diagnosed *Dendritobilharzia* by having a body that is elongate and dorsoventrally strongly flattened in both sexes, lacking suckers and gynaecophoric canal, a cuticle lacking spines and tubercles, an

intestine comprising a cyclocoel in the anterior one-third of the body and a "zig-zag" dendritic common cecum, numerous testes that are posterior to the cyclocoel and flank the dendritic branches of the common cecum, a sinistral male genital pore in the anterior half of the body, a "spiraled" (we interpret it as tightly-compacted, convoluted) intercecal ovary, and numerous vitelline follicles co-distributing with the common cecum. We regard this diagnosis by Martorelli (1981) as the most comprehensive to be entered into the literature. Martorelli (1981) differentiated his new species (*D. rionegrensis*) from *D. pulverulenta* by features associated with the body, mouth, uterus, and relative lengths of the cyclocoel. The World Registry of Marine Species omitted *D. rionegrensis* at the time of writing this manuscript.

Phylogenetic remarks

The amplified *28S* rDNA fragment of *D. pulverulenta* comprised 1,639 nucleotides, and the *28S* rDNA dataset comprised 1,065 aligned nucleotide positions with 1 bp difference between our sequence of *D. pulverulenta* and 2 other *28S* sequences (AF167090 of Snyder and Loker [2000]; AY157241 of Lockyer et al. [2003]). These latter sequences were recovered in a polytomy with our sequence of *D. pulverulenta* (Fig. 3). AF167090 and AY157241 have long been assumed to represent *D. pulverulenta.* The molecular systematics studies of Snyder and Loker (2000) and Lockyer et al. (2003) did not detail how any of their specimens were identified and no voucher specimen exists. As such, there are no means with which to confirm the identity of either of these sequences nor, for that matter, any sequence sourced from Snyder and Loker (2000) and Lockyer et al. (2003) (see below). Because these sequences are nonugens (= GenBank sequences unaccompanied by morphological evidence or a museum-curated voucher specimen that underpins the identification of the sequence; Roberts et al. [2018]) and because they were nearly identical to our sequences, we provisionally regard them as *Dendritobilharzia*

sp. until a study of morphological evidence confirms their species-level identity. The *28S* analysis recovered the clade including *D. pulverulenta* in a polytomy with Gigantobilharziinae sp. (AY157242; previously *Gigantobilharzia huronensis* Najim, 1950 of Lockyer et al. [2003]; see Najim [1950; 1956]) and the clade comprising *Gigantobilharzia ensenadense* (Lorenti, Brant, Gilardoni, Diaz, and Cremonte, 2022) Dutton and Bullard, n. comb. and *Gigantobilharzia patagonense* (Lorenti, Brant, Gilardoni, Diaz, and Cremonte, 2022) Dutton and Bullard, n. comb. (see below for justification of synonymies) (Fig. 3). All aforementioned taxa were recovered sister to *Gigantobilharzia melanoidis* Schuster, Aldhoun, and O'Donovan, 2014 (JX875068) (no *28S* sequence of *D. rionegrensis* exists).

The amplified *COI* fragment of *D. pulverulenta* comprised 1,128 nucleotides. Our *COI* sequence of *D. pulverulenta* differed by 69 bp (6.2%) from the only other GenBank-accessioned *COI* sequenced associated with *D. pulverulenta* (AY157187 of Lockyer et al. [2003]). AY157187 is a nonugen, and the relatively large percent difference between our *COI* sequence of *D. pulverulenta* and AY157187 calls into question the identity of AY157187, which we herein provisionally identify as *Dendritobilharzia* sp. pending a sequence derived from a morphologically diagnosed adult specimen (Fig. 3). Another problem with the nonugen sequences AY157187 and AY157241 is that we cannot know if those sequences came from the same specimen or different specimens. If they were sourced from the same specimen, given that the *28S* sequence from Lockyer et al. (2003) was nearly identical to ours, we could conclude that the differences in the *COI* comprise intraspecific variation or potentially species-level differences. Without morphology, it is equivocal and presumptive to choose one or the other. Schuster et al. (2014) morphologically diagnosed specimens of *G. melanoidis* represented by the *COI* sequence JX875069, and voucher specimens exist for both *G. huronensis* (KF738949) of

Sweazea et al. (2015) and *Dendritobilharzia* sp. (W499) ex '*Gyraulus* NM' (KX302892) of Brant et al. (2017) (Fig. 4).

The amplified *ITS1* fragments of *D. pulverulenta* comprised 826 and 816 nucleotides that were identical to each other from a single specimen of *D. pulverulenta*. These sequences differed by 2 bp (0.5%) from an *ITS1* sequence derived from a cercariae of *D. pulverulenta* shed from ash gyro, *Gyraulus parvus* (Say, 1817) (Planorbidae) from Albuquerque, New Mexico (HM125958 of Brant et al. [2011]). Only 2 other *ITS1* sequences alleged to be "*D. pulverulenta*" exist in GenBank: KJ438954 and OP737753 were both referenced in an abstract by Dolka and colleagues wherein a mute swan, *Cygnus olor* (Gmelin, 1789) (Anatidae) from Poland was reported as the host. These *ITS1* sequences differed from each other by 16 bp (1.8%). Our *ITS1* sequences of *D. pulverulenta* differed by 152 bp and 151 bp (21.1% and 22.4%) and 145 bp and 146 bp (20.6% and 20.9%) from KJ438954 and OP737753, respectively. Because the sequences submitted by Dolka are nonugens, we regard them as Gigantobilharziinae spp. until their identities can be confirmed with morphology of adult specimens. Our *ITS1* data indicate that Dolka's sequences are not *D. pulverulenta*.

Noteworthy is that Schuster et al. (2014) and Lorenti et al. (2022) asserted that *Gigantobilharzia* needed revision because AY157242 (Gigantobilharziinae sp.; a nonugen as "*G. huronensis*") did not share a recent common ancestor with JX875068 (morphologically confirmed by Schuster et al. [2014] as *G. melanoidis*). The identity of AY157242 needs confirmation with morphological detail and specimen vouchers. In addition, the type species *G. acotylea* needs to be sequenced.

A total of 6 gigantobilharziine GenBank sequences are based on a morphological diagnosis and/or a voucher specimen(s) (i.e., all other gigantobilharziine sequences in GenBank

evidently are nonugens): a critical *ITS1* sequence from cercariae morphologically diagnosed as *D. pulverulenta* provided by Brant et al. (2011); the sequences of *G. melanoidis* furnished by Schuster et al. (2014) from the United Arab Emirates; the *CO1* sequence of *G. huronensis* from Sweazea et al. (2015); a *CO1* sequence of *Dendritobilharzia* sp. from Brant et al. (2017); the sequences of *G. ensenadense* and *G. patagonense* from Lorenti et al. (2022) in Argentina; and the sequences from the present study for adult *D. pulverulenta*.

DISCUSSION

Dendritobilharzia differs from *Gigantobilharzia* most notably by having a dendritic common cecum and a flattened body, whereas *Gigantobilharzia* has a non-dendritic common cecum and a 'thread like' (cylindrical) body. We accept *Gigantobilharzia* and *Dendritobilharzia* but consider *Marinabilharzia* Lorenti, Brant, Gilardoni, Diaz, and Cremonte, 2022 and *Riverabilharzia* Lorenti, Brant, Gilardoni, Diaz, and Cremonte, 2022 junior synonyms of *Gigantobilharzia* because i) we herein reassign their respective type species to *Gigantobilharzia* (see above), ii) the molecular sequence data do not reject the synonymy (Figs. 3, 4), and iii) the diagnoses of these genera are not distinct from that of *Gigantobilharzia* (see below). Including many features of the subfamily diagnosis for Gigantobilharziinae of Khalil (2002), the text of these diagnoses differs only in the distribution of tegumental papillae and the outline of the body ends (Lorenti et al., 2022). Regarding papillae, they reportedly cover "*the entire body surface*" of *Riverabilharzia*, whereas *Marinabilharzia* reportedly has papillae *"around the mouth and posteriorly.*" No papilla was imaged or drawn for *Riverabilharzia*, and the presence/absence and anatomical detail of homologous tegumental papillae in related schistosomes is indeterminate. Regarding the body ends, *Marinabilharzia* was diagnosed as having an anterior end that is rounded (both sexes) and a posterior end that is rounded (males) or "*often spatulated*" (this

character state is variable among conspecific females and overlapping with *Riverabilharzia*). *Riverabilharzia* was diagnosed as having an anterior end that is relatively more tapered and a posterior end that is "*rounded or spatulate without protrusions*" (overlapping with *Marinabilharzia*). The illustrations for these taxa show that the anterior and posterior ends are respectively not markedly distinct and that they match the general shape of those respective body ends in *Gigantobilharzia* spp. In comparing the descriptions of *G. ensenadense*, *G. patagonense*, and *G. acotylea*, we agree with Lorenti et al. (2022) in that the relative location of the cyclocoel and seminal vesicle are useful in distinguishing closely related species of *Gigantobilharzia*: *G. ensenadense* has terminal male genitalia that are posterior to the cyclocoel; the terminal male genitalia of *G. patagonense* is near the cecal bifurcation anteriorly; and that of *G. acotylea* is immediately anterior to the posterior reunification of the ceca (cyclocoel).

The Nyae Nyae-Khaudum Dispersal Area (NNKDA) of the Kavango Zambezi Transfrontier Conservation Area (KAZA-TFCA) has not been subjected to any systematic biodiversity study, including that for parasites. Established in 2011, the KAZA is the world's largest TFCA (~520,000 km^2) and includes 36 formally-proclaimed protected areas that comprise myriad game and forest reserves, wildlife and game management areas, and communal lands (Stoldt et al., 2020). KAZA-TFCA is an area of extremely high estimated biodiversity. It is also a critical area for megafaunal migrations as well as critical open range habitat for carnivores, birds, snakes, and amphibians (Hines, 1993). The parasites, potential pathogens, and potential zoonotic agents that infect these free-living inhabitants remain largely un-surveyed; the present study is the first record of an avian parasite from the NNKDA.

ACKNOWLEDGEMENTS

We thank Dr. Francois Jacobs (Chief Fisheries Biologist, Kamutjonga Research and Training Institute, Ministry of Fisheries and Marine Resources [Divundu, Namibia]) and Piet Beytell (Chief Conservation Scientist of Wildlife Research, Directorate of Scientific Services, Ministry of Environment, Forestry, and Tourism [Windhoek, Namibia]) for informing us about the biology of the NNKDA, for facilitating permits and logistics, and for providing personnel to help collect hosts within the NNKDA. We also thank Anna Phillips, Chad Walter, Kathryn Ahlfeld, and William Moser (all Department of Invertebrate Zoology, National Museum of Natural History, Smithsonian Institution, Washington, D.C.) for curating our museum specimens. This study was supported by the Southeastern Cooperative Fish Parasite and Disease Project, the US Fish and Wildlife Service (Department of Interior), National Sea Grant (National Oceanic and Atmospheric Administration), United States Department of Agriculture (National Institute of Food and Agriculture), Federal Aid in Sport Fish Restoration (Alabama Department of Conservation and Natural Resources, Inland and Marine Resources Divisions), and the Alabama Agricultural Experiment Station (Auburn University, College of Agriculture).

LITERATURE CITED

Bowles, J., and D. P. McManus. 1993. Rapid discrimination of *Echinococcus* species and strains using a polymerase chain reaction-based RFLP method. Molecular and Biochemical Parasitology 57: 231–224.

Brant, S. V., C. A. Bochte, and E. S. Loker. 2011. New intermediate host records for the avian schistosomes *Dendritobilharzia pulverulenta*, *Gigantobilharzia huronensis*, and *Trichobilharzia querquedulae* from North America. Journal of Parasitology 97: 946–949.

Brant, S. V., E. S. Loker, L. Casalins, and V. Flores. 2017. Phylogenetic placement of a schistosome from an unusual marine snail host, the false limpet (*Siphonaria lessoni*) and gulls (*Larus donincanus*) from Argentina with a brief review of marine schistosomes from snails. Journal of Parasitology 103: 75–82.

Braun, M. 1901. Zur Revision der Trematoden der Vogel. Zentralblatt fur Bakteriologie, Parasitenkunde, Infektionskrankheiten und Hygiene Abt. I: Orig. 29: 560–568, 895–897, 941–948.

Braun, M. 1902. Fascioliden der vögel. Fischer. Zoologische Jahrbücher Abteilung für Systematik, Geographie und Biologie der Tiere 16: 1–62.

Bullard, S. A., and H. R. Dutton. 2022. Resolving the paraphyletic turtle blood flukes: Revision of Spirorchiidae Stunkard, 1921 and proposal of Carettacolidae Yamaguti, 1958, Hapalotrematidae (Stunkard, 1921) Poche, 1926, Baracktrematidae n. fam., Plattidae n. fam., and Atamatamidae n. fam. Journal of Parasitology 108: 553–564.

Bullard, S. A., J. R. Roberts, M. B. Warren, H. R. Dutton, N. V. Whelan, C. F. Ruiz, T. R. Platt, V. V. Tkach, S. V. Brant, and K. M. Halanych. 2019. Neotropical turtle blood flukes: Two new genera and species from the Amazon River Basin with a key to genera and comments on a marine-derived parasite lineage in South America. Journal of Parasitology 105: 497–523.

Darriba, D., G. L. Taboada, R. Doallo, and D. Posada. 2012. jModelTest 2: More models, new heuristics, and parallel computing. Nature Methods 9: 772. https://doi.org/10.1038/nmeth.2109

Dutton, H. R., M. B. Warren, and S. A. Bullard. 2019. New genus and species of turtle blood fluke (Platyhelminthes: Digenea: Schistosomatidae) infecting six-tubercled Amazon River turtles, *Podocnemis sextuberculata* (Pleurodira: Podocnemididae) from the Amazon River Basin (Peru). Journal of Parasitology 105: 671–685.

Glez-Peña, D., D. Gómez-Blanco, M. Reboiro-Jato, F. Fdez- Riverola, and D. Posada. 2010. ALTER: program-oriented format conversion of DNA and protein alignments. Nucleic Acids Research 38 (Suppl. 2): W14–W18. doi:10.1093/nar/ gkq321.

Hines, C. J. H., 1993. Temporary wetlands of Bushmanland and Kavango, north-east Namibia. Madoqua 1993: 57–69.

Khalil, L. F. 2002. Family Schistosomatidae Stiles & Hassall, 1898. *In* Keys to the Trematoda: Volume 1 (pp. 419-432). Wallingford UK: CABI Publishing.

Katoh, K., and D. M. Standley. 2013. MAFFT Multiple sequence alignment software version 7: Improvements in performance and usability. Molecular Biology and Evolution 30: 772–780.

Lazarus, D., and R. Jahn. 1998. Using the Ehrenberg Collection. Diatom Research 13: 273–291.

Lockyer, A. E., P. D. Olson, P. Østergaard, D. Rollinson, D. A. Johnston, S. W. W. Attwood, V. R. Southgate, P. Horak, S. D. Snyder, T. H. Le, et al. 2003. The phylogeny of the Schistosomatidae based on three genes with emphasis on the interrelationships of *Schistosoma* Weinland, 1858. Parasitology 126: 203–224.

Loker, E. S., and S. V. Brant. 2006. Diversification, dioecy and dimorphism in schistosomes. Trends in Parasitology 22: 521–528.

Lorenti, E., S. V. Brant, C. Gilardoni, J. I. Diaz, and F. Cremonte. 2022. Two new genera and species of avian schistosomes from Argentina with proposed recommendations and discussion of the polyphyletic genus *Gigantobilharzia* (Trematoda, Schistosomatidae). Parasitology 149: 675–694.

Macko, J. K. 1959. Zur Revision der Systematic der Trematode *Dendritobilharzia anatinarum* Cheatum, 1941. Helminthologia 1: 133–137.

Martorelli, S. R. 1981. *Dendritobilharzia rionegrensis* sp. nov. (Digenea: Schistosomatidae) parasita de las venas mesentericas de *Fulica rufifrons* (Aves: Rallidae). Neotropica 27: 171–177.

Najim, A. T. 1950. *Gigantobilharzia huronensis* sp. nov., bird blood-fluke from the goldfinch. Journal of Parasitology 36(Suppl): 19.

Najim, A. T. 1956. Life history of *Gigantobilharzia huronensis* Najim, 1950. A dermatitis-producing bird blood fluke (Trematoda: Schistosomatidae). Parasitology 46: 443-469.

Nazarbeigy, M., A. Halajian, and A. Amadi. 2021. Checklist of digenean trematodes of Iran. Veterinary Parasitology: Regional Studies and Reports 24: 1–36.

Rambaut, A., M. A. Suchard, D. Xie, and A. J. Drummond. 2014. FigTree v1.4.3. Available from: http://tree.bio.ed.ac.uk/software/figtree. Accessed 5 January 2023.

Roberts, J. R., K. M. Halanych, C. R. Arias, S. S. Curran, and S. A. Bullard. 2018. A new species of *Spirorchis* MacCallum, 1918 (Digenea: Schistosomatoidea) and *Spirorchis scripta* Stunkard, 1923, infecting river cooter, *Pseudemys concinna* (Le Conte, 1830), (Testudines:

Emydidae) in the Pascagoula River, Mississippi, U.S.A., including an updated phylogeny for *Spirorchis* spp. Comparative Parasitology 85: 120–132.

Ronquist, F., M. Teslenko, P. Van Der Mark, D. L. Ayres, A. Darling, S. Höhna, B. Larget, L. Liu, M. A. Suchard, and J. P. Huelsenbeck. 2012. MrBayes 3.2: Efficient Bayesian phylogenetic inference and model choice across a large model space. Systematic Biology 61: 539–542.

Schuster, R. K., J. A. Aldhoun, and D. O'Donovan. 2014. *Gigantobilharzia melanoidis* n. sp.(Trematoda: Schistosomatidae) from *Melanoides tuberculata* (Gastropoda: Thiaridae) in the United Arab Emirates. Parasitology Research 113: 959–972.

Skrjabin, K. I. 1924. Etiudy po izucheniiu paraziticheskikh chervei ptits Rossii. Trudy Gosudarstvennogo Instituta Eksperimental'noi Veterinarii 2: 149–157.

Skrjabin, K. I., and N. P. Zakharow. 1920. Zwei neue Trematodengattungen aus den Blutgefässen der Vögel. Izvestiya Donskogo Veterinarnago Instituta 2: 1–5.

Snyder, S. D., and E. S. Loker. 2000. Evolutionary relationships among the Schistosomatidae (Platyhelminthes: Digenea) and an Asian origin for *Schistosoma*. Journal of Parasitology 86: 283–288.

Stoldt, M., T. Göttert, C. Mann, and U. Zeller. 2020. Transfrontier conservation areas and human-wildlife conflict: the case of the Namibian component of the Kavango-Zambezi (KAZA) TFCA. Scientific Reports 10: 1–16.

Sweazea, K. L., A. Simperova, T. Juan, A. Gadau, S. V. Brant, P. Deviche, and C. Jarrett. 2015. Pathophysiological responses to a schistosome infection in a wild population of mourning doves (*Zenaida macroura*). Zoology 118: 386–393.

Ulmer, M. J., and F. J. Vande Vusse. 1970. Morphology of *Dendritobilharzia pulverulenta* (Braun, 1901) Skrjabin, 1924 (Trematoda: Schistosomatidae) with notes on secondary hermaphroditism in males. Journal of Parasitology 56: 67–74.

Vande Vusse, F. J. 1980. A review of the genus *Dendritobilharzia* Skrjabin and Zakharow 1920 (Trematoda: Schistosomatidae). Journal of Parasitology 66: 814–822.

FIGURE LEGENDS

Figures 1,2. *Dendritobilharzia pulverulenta* (Braun 1901) Skrjabin 1924 from the heart of a white-backed duck, *Thalassornis leuconotus* Eyton, 1838 (Anseriformes: Anatidae) from the the Nyae Nyae-Khaudum Dispersal Area, Namibia. Scale values aside each bar. (**1**) Anterior end of male voucher (USNM 1606779) showing mouth (m), esophagus (e), nerve commissure (nc), female genital pore (fgp), esophageal gland (eg), seminal vesicle (sv), cirrus (ci), vas deferens (vd), and testis (t). Ventral view. (**2**) Anterior end of female voucher (USNM 1606776), showing features labeled in Fig. 1 in addition to distal portion of uterus (du), uterus (u), oötype (oö), vitelline duct (vtd), ovary (o), Laurer's canal (Lc), and seminal receptacle (sr), vitellarium (v). Dorsal view.

Figures 3,4. Phylogenies. (**3**) Large subunit ribosomal DNA (*28S*) Bayesian phylogeny. Values aside nodes are posterior probability. New sequences are shown in bold. Scale bar is in substitutions per site. GenBank numbers are in parentheses following each taxon. (**4**) Cytochrome oxidase subunit 1 mitochondrial gene (*CO1*) Bayesian phylogeny.

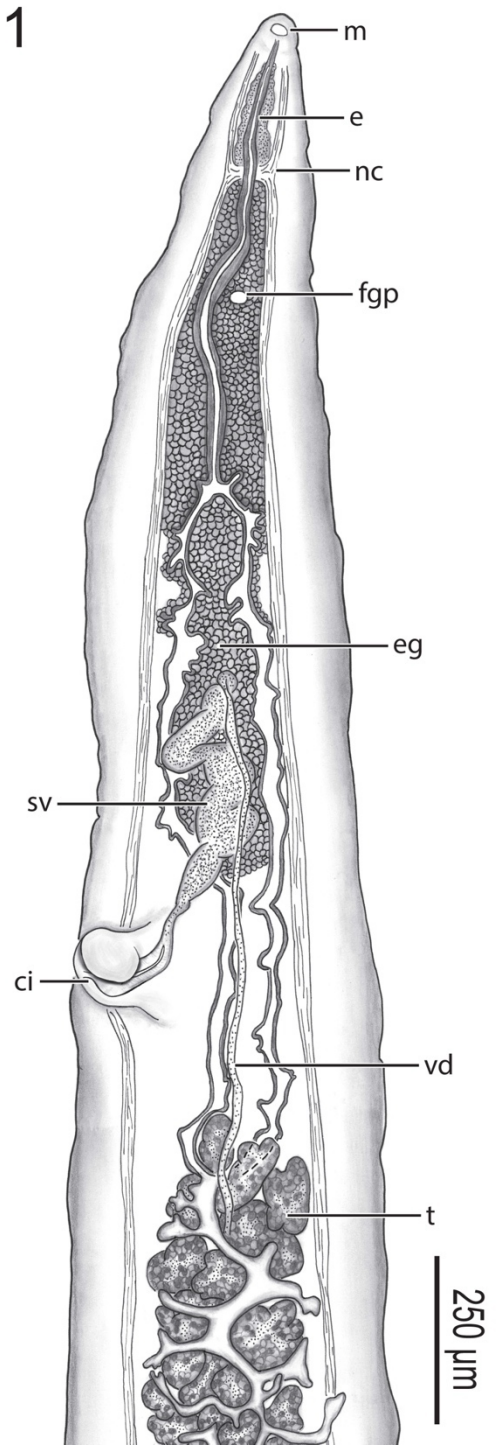
1
m
e
nc
fgp
eg
sv
ci
vd
t
250 µm

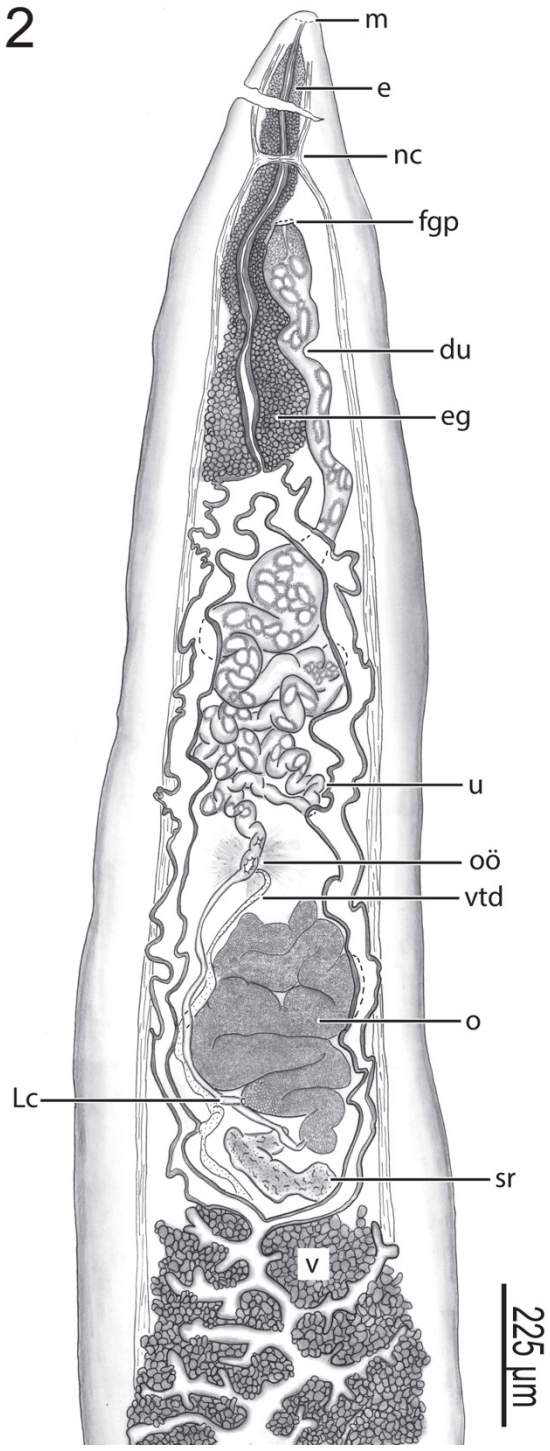
2
m
e
nc
fgp
du
eg
u
oö
vtd
o
Lc
sr
v
225 µm

3

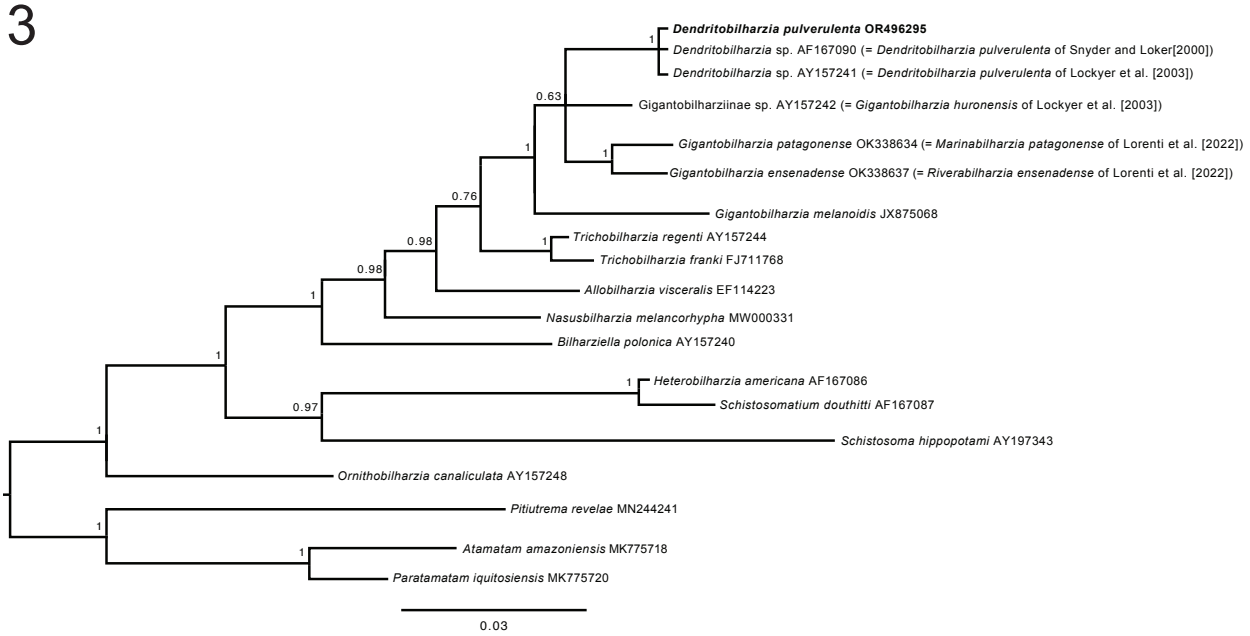
***Dendritobilharzia pulverulenta* OR496295**
Dendritobilharzia sp. AF167090 (= *Dendritobilharzia pulverulenta* of Snyder and Loker[2000])
Dendritobilharzia sp. AY157241 (= *Dendritobilharzia pulverulenta* of Lockyer et al. [2003])
Gigantobilharziinae sp. AY157242 (= *Gigantobilharzia huronensis* of Lockyer et al. [2003])
Gigantobilharzia patagonense OK338634 (= *Marinabilharzia patagonense* of Lorenti et al. [2022])
Gigantobilharzia ensenadense OK338637 (= *Riverabilharzia ensenadense* of Lorenti et al. [2022])
Gigantobilharzia melanoidis JX875068
Trichobilharzia regenti AY157244
Trichobilharzia franki FJ711768
Allobilharzia visceralis EF114223
Nasusbilharzia melancorhypha MW000331
Bilharziella polonica AY157240
Heterobilharzia americana AF167086
Schistosomatium douthitti AF167087
Schistosoma hippopotami AY197343
Ornithobilharzia canaliculata AY157248
Pitiutrema revelae MN244241
Atamatam amazoniensis MK775718
Paratamatam iquitosiensis MK775720
0.03

4

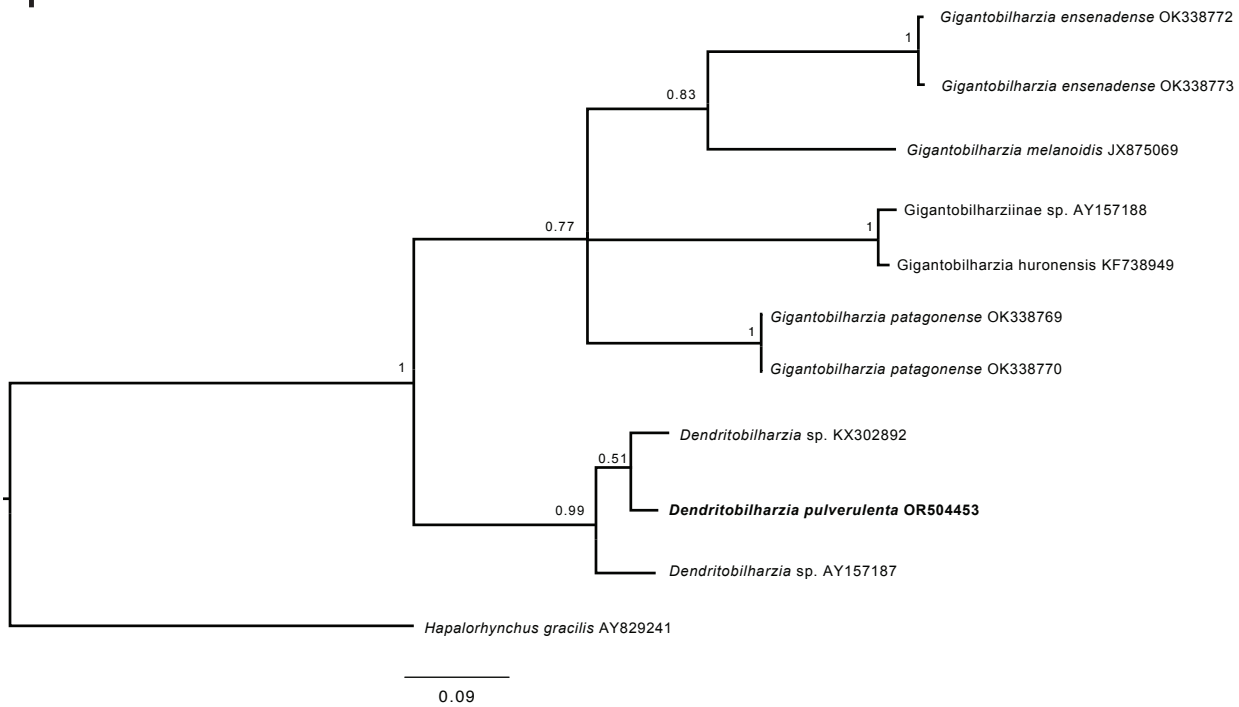
Gigantobilharzia ensenadense OK338772
Gigantobilharzia ensenadense OK338773
Gigantobilharzia melanoidis JX875069
Gigantobilharziinae sp. AY157188
Gigantobilharzia huronensis KF738949
Gigantobilharzia patagonense OK338769
Gigantobilharzia patagonense OK338770
Dendritobilharzia sp. KX302892
***Dendritobilharzia pulverulenta* OR504453**
Dendritobilharzia sp. AY157187
Hapalorhynchus gracilis AY829241
0.09

CHAPTER 3: Redescription of *Dracovermis occidentalis* (Digenea: Liolopidae) infecting American alligator, *Alligator mississippiensis* from the Bon-Secour River (Mobile–Tensaw River Delta, Alabama, USA) and a revised phylogeny for Liolopidae

***Published in Parasitology Research (19 September 2024)**

Authors: Haley R. Dutton, Stephen A. Bullard, John H. Brule, and Anita M. Kelly

Abstract

We examined several American alligators, *Alligator mississippiensis* (Daudin, 1802) (Crocodilia: Alligatoridae) from Louisiana, Alabama, and South Carolina in August 2022. The intestine of one alligator from Alabama was infected by *Dracovermis occidentalis* Brooks and Overstreet, 1978 (Platyhelminthes: Digenea: Liolopidae Odhner, 1912), a seldom collected and incompletely described trematode that lacks a representative nucleotide sequence. Liolopidae comprises 5 genera and 15 species: *Liolope* spp. infect giant salamanders; *Helicotrema* spp. infect turtles and lizards; *Harmotrema* spp. infect snakes; *Paraharmotrema* spp. infect turtles; and *Dracovermis* spp. infect crocodilians. Based on our study of the newly collected specimens and the holotype of *D. occidentalis*, we redescribe *D. occidentalis*, correct errors in its original description, and provide an updated phylogeny for Liolopidae that, for the first time, includes *Dracovermis* Brooks and Overstreet, 1978. Our specimens were identified as *D. occidentalis* by having testes in the posterior 1/3 of the body, a pretesticular cirrus sac, a spined and eversible cirrus, a bipartite seminal vesicle, and a post-acetabular vitellarium. A phylogenetic analysis of the D1–D3 domains of the nuclear large subunit ribosomal DNA (*28S*) recovered Liolopidae as monophyletic; however, low taxon sampling in the group precludes hypothesis-testing about liolopid-vertebrate cophyly. This is the first collection for morphological study of the type species for *Dracovermis* since the genus was proposed 46 years ago, the first record of a liolopid from Alabama, and the first phylogenetic analysis that includes *Dracovermis*.

Introduction

The American alligator, *Alligator mississippiensis* (Daudin, 1802) (Crocodilia: Alligatoridae), hereafter "alligator", is the largest predatory reptile in North America. Historically abundant and ranging across coastal/estuarine waters and semi-inland riverine systems throughout the southeastern USA, alligators were hunted/poached for their skin and nearly driven to extinction in the early 1900s. They remained considered threatened as late as the 1960s but proper management has allowed alligator populations to recover relatively rapidly, with the US Fish and Wildlife Service in 1979 downlisting the alligator from CITES Appendix I to Appendix II; allowing for some legal international trade of alligator skins (Ashley and Caldwell, 2013; Elsey and Woodward, 2010; Jelden et al., 2014; PIJAC, 2013; Throbjarnarson et al., 1992). Regarding captive stocks of alligators, a survey conducted in 2013 revealed that >100 commercial farms in the US maintained ~790,000 alligators, with 20,000 hatchlings being produced from these facilities annually. Based on these facts, along with the cultural and conservation value of alligators in the wild, as well as the commercial value of the large standing stock of alligators in aquaculture ponds, we assert that infectious diseases and parasites are relevant to alligator population health and captive husbandry/maintenance. This is in addition to the general interest in parasites of crocodilians regarding parasite-host cophyly and crocodilian natural history.

Although alligators are among the most iconic and well-studied reptiles in North America regarding their life history and general biology, studies on the taxonomy and life cycles of their parasites have been relatively limited. This could be in part due to the difficulty in obtaining permission to sample alligators legally, logistical challenges associated with dissecting and processing large alligators in the field, as well as the technical challenges of extracting, handling,

and fixing live, minute trematodes in the field. During a state-sponsored alligator hunt in coastal Alabama, we necropsied fresh-killed alligators during the hunter registration of alligator carcasses with natural resource agency personnel. From those collections, we herein provide a redescription for *Dracovermis occidentalis* Brooks and Overstreet, 1978 and place it in a phylogenetic analysis for the first time using the large subunit ribosomal DNA (*28S*) to test relationships and monophyly of the Liolopidae Odhner, 1912.

Materials and methods

Alligators were sampled at a coastal registration station (30°40'19.3"N 87°56'06.6"W) operated by the Alabama Division of Wildlife & Freshwater Fisheries for the annual Alabama alligator season hunt during August 2022. We encountered *D. occidentalis* infecting the intestine of 1 alligator. The infected male alligator (Tag 1329) measured 2.52 m long and was caught by a baited line in the Bon Secour River, Alabama, by Jarrod Pettie. The digestive tract was excised intact, sliced longitudinally to expose the lumen, rinsed in saline, and decanted and placed into acrylic settling columns before the sediment was observed in a petri dish under the dissecting scope and examined for live flukes.

Trematodes intended for morphology as whole-mounts were observed microscopically and fixed following Dutton et al. (2022). Whole mounts were examined and illustrated using an Olympus BX53 microscope (Olympus Corporation, Shinjuku City, Tokyo, Japan) equipped with differential interference contrast, measured using an ocular micrometer, and illustrated using a drawing tube. Measurements are reported in micrometers (μm) as the range followed by the mean, +/− standard deviation, and sample size in parentheses. Measurements of the holotype (USNM 1370158) are provided in brackets. Vouchers were deposited in the National Museum of

Natural History's Invertebrate Zoology Collection (Smithsonian Institution, USNM Collection Nos. 1718009, 1718010, 1718012–1718015). Classification and anatomical terms for liolopids follow Brooks and Overstreet (1978) and Dutton et al (2022).

Total genomic DNA was extracted from 1 EtOH-preserved specimen. The specimen was microscopically identified by the presence of the cirrus spines and genitalia in posterior third of the body as *D. occidentalis*. The specimen was extracted using DNeasy™ Blood and Tissue Kit (Qiagen, Hilden, Germany) as per the manufacturer's protocol, except that the proteinase-K incubation period was extended overnight, and 50 μL of elution buffer was used to increase the final DNA concentration. Amplification and sequencing of the *28S*, *18S*, *ITS2* and the *COX1* used the following primer sets: *28S* (LSU-5 [5′-TAGGTCGACCCGCTGAAYTTAAGCA-3′] and 1500R [5′-GCTATCCTGAGGGAAACTTCG-3′]), *18S* (WormA [5′-GCGAATGGCTCATTAAATCAG-3′] and Worm B [5′-CTTGTTACGACTTTTACTTCC-3′] [Littlewood and Olson, 2001]), *ITS2* (GA1 [5′-AGAACATCGACATCTTGAAC-3′] [Anderson and Barker, 1998] and ITS2.2 [5′-CCTGGTTAGTTTCTTTTCCTCCGC-3′] [Cribb et al., 1998]), *COX1* (JB3 [5′-TTTTTTGGGCATCCTGAGGTTTAT-3′] [Bowles and McManus, 1993] and CO1-R trema [5′-CAACAAATCATGATGCAAAAGG-3′] [Miura et al., 2005]). PCR reactions were performed with a total volume of 50 μL (34 μL purified water, 10 μL 5X Taq buffer [Promega Corporation, Madison, Wisconsin], 1 μL 10 mM dNTP [Promega Corporation], 1 μL 10 mM forward primer, 1 μL 10 mM reverse primer, 0.3 μL GoTaq DNA polymerase [Promega Corporation], and 2 μL DNA extract). The thermocycling profile for the *28S* comprised 4 min at 94 ºC for denaturation, 40 repeating cycles at 94 ºC for 40 sec for denaturation, 56 ºC for 30 sec for annealing and 72 ºC for 2 min for extension followed by a final 5 min at 72 ºC for extension. The *18S* and *ITS2* follow the same profile except 50 ºC for 30 sec

for annealing, and 72 ºC for 1 min for extension. The *COX1* thermocycling profile comprised 2 min at 94 ºC for denaturation, 40 repeating cycles at 94 ºC for 30 sec for denaturation, 52 ºC for 30 sec for annealing, and 72 ºC for 2 min for extension followed by a final 7 min at 72 ºC for extension. All PCR reactions were carried out in a ProFlex PCR System (Applied Biosystems, Waltham, MA). PCR products (10 µL) were verified on a 1% agarose gel and stained with ethidium bromide. PCR products were purified with the QIAquick PCR Purification Kit (Qiagen) according to the manufacturer's protocols except that the last elution step was performed with autoclaved nanopure H2O rather than with the provided buffer. Purified DNA concentration was estimated using a NanoDrop™ One Microvolume UV-Vis Spectrophotometer (Thermo Fisher Scientific Inc., Waltham, Massachusetts). Purified DNA samples were prepared for sequencing with a total volume of 15 ml (2 µL 10 mM primer + purified DNA + purified water) with volumes of purified DNA and water depending on DNA sample concentration. DNA sequencing was conducted by GENEWIZ (Azenta Life Sciences, South Plainfield, New Jersey). All assembled contiguous nucleotide sequences were deposited in GenBank (PQ186364, PQ186366, PQ186369, PQ187446).

The *28S* phylogenetic analysis included the single sequence from the current study and the other taxa used in Dutton et al. (2022). Sequences were aligned with the multiple alignment tool using fast Fourier transform (MAFFT) (Katoh and Standley, 2013) and trimmed to the length of the shortest sequence presented herein (1,237 base pairs [bp]) in Geneious Prime Software version 2023.0.4 (Geneious Corp., Auckland, New Zealand). Aligned sequences were reformatted and exported from .fasta to .phy to run a maximum likelihood tree (ML). The ML was inferred with IQTREE v.1.16.12 (Nguyen et al., 2015). Substitution model testing was done with ModelFinder (Kalyaanamoorthy et al., 2017) as implemented in IQTREE. After model

testing, tree inference was done using best-fitting substitution models (Chernomor et al., 2016). Default tree search parameters were used, except perturbation strength was set to 0.2, and 500 iterations had to be unsuccessful to stop the tree search. Tree inference was performed 20 times with only the tree with the best log-likelihood score reported. Support for relationships was measured with 1000 ultrafast bootstrap replicates (UFBoot) (Hoang et al., 2018). The inferred phylogenetic tree was visualized using FigTree v1.4.4 (Rambaut et al., 2014) and further edited with Adobe Illustrator (Adobe Systems) for visualization purposes. With only 4 sequences available for the *28S*, 2 sequences available for the *18S* and *ITS2*, and 1 sequence for the *CO1* we have chosen not to run the individual trees for each region but continue to create a genetic library for future use.

Results

Dracovermis occidentalis Brooks and Overstreet, 1978 emend. Dutton and Bullard, 2024 (Figs. 1 and 2)

Based on light microscopy of 6 heat-killed, stained whole-mounted adult specimens (USNM 1718009, 1718010, 1718012–1718015) and the holotype (USNM 1370158).

Body linguiform in heat-killed specimens (Fig. 1), pyriform or slightly ovoid in outline in holotype, 2,125−2,965 (2,659 ± 327; 6) [1,150] long, 370−650 (536 ± 98; 6) [480] in maximum width at the level of genital pore, 4−6× (5 ± 1; 6) [2.4×] longer than wide, with clear ventral concavity only observed in specimens having ventrally curved edges; forebody (anterior to ventral sucker) 35−47% (40% ± 5%; 6) [30%] of total body length, spinose; forebody spines scattered about ventral surface of forebody [absent or indistinct in holotype, perhaps related to poor condition of specimen]; body surfaces lacking papillae. Oral sucker bowl shaped, 43−69

(57 ± 12; 5) [45] long or 2−3% (2% ± 0%; 5) [4%] of body length, 57−80 (72 ± 10; 5) [50] wide or 10−15% (13% ± 2%; 5) [10%] of maximum body width, 1: 1.1−1.5× (1.3 ± 0.2; 5) [1.8×] pharynx width, aspinose. Ventral sucker thin and delicate (Fig. 1), 135−160 (143 ± 9; 6) [125] long or 5−6% (5% ± 1%; 6) [11%] of body length, 120−141 (132 ± 8; 6) [115] wide or 36−48% (43% ± 6%; 4) [38%] of maximum body width; 1.8−2.2× (1.9 ± 0.2; 5) [2.3×] oral sucker width. Nerve commissure 87−120 (103 ± 13; 5) [70] or 3−4% (4% ± 0%; 5) [6%] of body length from anterior body end. Pharynx 55−84 (68 ± 11; 5) [43] long, 49−70 (56 ± 8; 5) [28] wide. Esophagus short 45−150 (86 ± 45; 4) long, 13−20 (16 ± 4; 4) wide; esophageal gland absent. Intestine comprising a cecal bifurcation and paired ceca, each extending posteriad approximately in parallel with respective lateral body margin, blind ending in posterior body end, symmetrical; cecal bifurcation 120−231 (172 ± 51; 4) [70] or 5−8% (6% ± 1%; 4) [6%] of body length from anterior body end; wall of ceca thickening markedly at level immediately anterior to ventral sucker (Fig. 1).

Anterior testis (Figs. 1, 2) 110−175 (148 ± 26; 6) [118] long or 4−6% (6% ± 1%; 6) [10%] of body length, 125−217 (179 ± 33; 6) [188] wide or 24−51% (34% ± 9%; 6) [39%] of body width at level of genital pore or 60−146% (110% ± 30%; 6) [130%] of posterior testis width; inter-testicular space 15−113 (71 ± 34; 6) [33] long or 1−4% (3% ± 1%; 6) [3%] of body length; posterior testis 115−225 (167 ± 39; 6) [133] long or 5−8% (6% ± 1%; 6) [12%] of body length, 130−210 (168 ± 30; 6) [145] wide or 27−40% (32% ± 5%; 6) [30%] of body width at level of genital pore, 125−197 (163 ± 29; 6) [75] or 5−7% (6% ± 1%; 6) [7%] of body length from posterior body end; anterior trunk of vasa efferentia emanating from ventral surface of anterior testis, extending directly into posterior end of seminal vesicle; posterior trunk of vasa efferentia emanating from ventral surface of posterior testis, extending anteriad 125−275 (203

±75; 3) [155], seemingly connecting to seminal vesicle directly (vas deferens indistinct). Cirrus sac elongate, slightly curved ("semilunar") (Figs. 1, 2), 305−610 (496 ± 106; 6) [240] long or 14−21% (18% ± 2%; 6) [21%] of body length, 295−561 (443 ± 114; 6) [188] wide or 10−23% (17% ±5%; 6) [39%] body width at level of genital pore; internal seminal vesicle bipartite, comprising proximal and distal portions; proximal portion of seminal vesicle 105−270 (186 ± 81; 6) [125] long or 4−11% (7% ± 3%; 6) [11%] of body length, 46−176 (125 ± 45; 6) [65] wide, 1× (1 ± 0; 6) [0.52×] longer than wide; distal portion of seminal vesicle ovoid in outline, 100−161 (133 ± 22; 6) [100] long or 4−7% (5% ± 1%; 6) [9%] of body length, 45−145 (112 ± 36; 6) [100] wide, 1× (1 ± 0; 6) [1×] longer than wide; cirrus comprises a coiled duct ("ejaculatory duct" of Brooks and Overstreet [1978]) that leads to spined cirrus (Figs 1,2), 75−132 (105 ± 20; 6) [75] long or 14−37% (25% ± 8%; 6) [31%] of cirrus sac length, 53−130 (75 ± 28; 6) [73] wide; cirrus spines curved, tapering distally, 28−37 (31 ± 4; 7) [25] long; pars prostatica surrounding cirrus; common genital atrium present.

Ovary entire (Figs. 1, 2), 84−140 (111 ± 18; 6) [95] long or 3−5% (4% ± 1%; 6) [8%] of body length, 93−130 (111 ± 15; 6) [95] wide or 14−34% (22% ± 7%; 6) [20%] of body width; post-ovarian space 225−405 (357 ± 68; 6) [200] or 11−15% (13% ± 1%; 6) [17%] of body length. Oviduct 43−123 (98 ± 30; 6) [88] long or 2−5% (4% ± 1%; 6) [8%] of body length, 38−66 (47 ± 11; 6) [50] wide, posterior to transverse vitelline duct, laterally expanding before becoming confluent with oötype. Laurer's canal not observed. Oötype 50−107 (70 ± 22; 6) long, 20−63 (39 ± 18; 6) wide, between ovary and posterior testis. Uterus convoluted, 255−684 (415 ± 154; 6) [413] long, 33−115 (75 ± 31; 6) [75] wide; uterine seminal receptacle present; uterine eggs elongate, 70−122 (99 ±23; 6) [113] long, 28−80 (61 ± 19; 6) [75] wide, numbering 1−7 (4 ± 3; 6) [1] per specimen. Metraterm 158−230 (178 ± 27; 6) [100] long, 31−117 (67 ± 31; 6) [63]

wide, thick walled, surrounded by small glandular cells; total uterus+metraterm length 413−914 (586 ± 179; 6) [350] or 18−31% (22% ± 5%; 6) [30%] of body length. Common genital pore 485−872 (728 ± 131; 6) [450] or 23−36% (27% ± 5%; 6) [39%] of body length from posterior body end, 38−70 (54 ± 13; 6) [20] in diameter. Vitellarium comprising a series of small, irregular shaped follicles, distributing along ceca and excretory branches from level of ventral sucker or slightly anterior to end of body (Fig. 1); confluence of vitellarium 7−70 (28 ± 29; 6) [58] or 0−3% (1% ± 1%; 6) [5%] from posterior body end; transverse vitelline duct dorsal, 245−426 (307 ± 67; 6) [225] in breadth, 15−41 (25 ± 11; 6) [38] wide; primary vitelline collecting duct 40−147 (100 ± 45; 6) [73] long, 45−75 (56 ± 10; 6) [38] wide, anterior to oötype. Excretory system having extracecal and intercaecal tubules (Fig. 1), 1,970−2,744 (2,481 ± 312; 6) [1050] long; intracecal branches joining at level of cecal tips; excretory pore subterminal.

Taxonomic summary

Type and only known host: American alligator, *Alligator mississippiensis* (Daudin, 1802) (Crocodilia: Alligatoridae).

Type locality: Cameron Parish, Louisiana, USA.

Other localities: Horn Island, Jackson County, Mississippi, USA; Chambers, Jefferson, and Liberty counties in southeast Texas, USA; Bon Secour River (present study), Alabama, USA.

Prevalence and intensity of infection: 1 of 8 (20%) alligators from Alabama were infected by 7 specimens of *D. occidentalis*, 0 of 15 (0%) alligators from Rockefeller Wildlife Refuge, Cameron Parish, Louisiana, and 0 of 20 (0%) alligators from South Carolina were infected with *D. occidentalis*.

Specimens deposited: Vouchers (USNM 1718009, 1718010, 1718012–1718015).

Other specimens examined: Holotype USNM 1370158.

Site of infection: Intestine.

Taxonomic remarks

Our specimens were identified as *D. occidentalis* by having testes in the posterior 1/3 of the body, a pretesticular cirrus sac, a spined and eversible cirrus, a bipartite seminal vesicle, and a post-acetabular vitellarium. While not all of these features were clearly described in its original description, we confirmed the presence of these features in our newly collected specimens and the holotype. Noteworthy also is that our specimens of *D. occidentalis* were collected adjacent to the type locality for this species in the northern Gulf of Mexico.

Brooks and Overstreet's (1978) specimens were contracted upon fixation, whereas ours were heat-killed and formalin-fixed, and we herein correct several errors related to *D. occidentalis* in Brooks and Overstreet (1978) that were due to the poor quality of the types. First, Brooks and Overstreet (1978) stated that the body surface of *Dracovermis* spp. lacks spines; however, in our specimens of *D. occidentalis* we observed spines scattered about the ventral surface of the forebody. These spines were absent or indistinct in the holotype of *D. occidentalis*, perhaps related to poor specimen condition. Second, the body shape of *Dracovermis* spp. is elongate, having equally broadly rounded anterior and posterior ends. This pattern is obscured in the original published description of *D. occidentalis* because of the poor quality of the types. The body shape of *D. occidentalis* depicted in Brooks and Overstreet (1978) is misleading in that the body appears compact and pyriform (similar to many other trematodes), not elongate and linguiform like in other heat-killed specimens of Liolopidae. Our heat-killed and formalin fixed specimens of *D. occidentalis* demonstrate the natural habitus of the species. Third, the ventral

sucker is relatively thin and delicate with muscle fibers visible along the periphery of the sucker. Brooks and Overstreet (1978) erroneously stylized the ventral sucker as being thick-walled and extensively muscular, when in fact, the sucker appears similar to that of other liolopids. Fourth, the metraterm in heat-killed and formalin-fixed specimens is straight and strongly muscular. The holotype of *D. occidentalis* is strongly contracted such that the metraterm presents as a compressed coil, whereas in heat-killed specimens the metraterm is straight because the specimen is not contracted. Brooks and Overstreet (1978) diagnosed *D. occidentalis* as having a "folded metraterm." Fifth, the vitellarium in our specimens of *D. occidentalis* is patchily distributed, having gaps among clusters of vitelline follicles. Brooks and Overstreet (1978) highly stylized the vitellarium as a contiguous and evenly distributed field. Although typical for some trematode groups, it is taxonomically significant that the vitellarium of *D. occidentalis* is patchy (not evenly distributed) and can be confluent posteriorly or not confluent posteriorly. Lastly, we were unable to measure the esophagus and oötype in the type specimen due to the contracted nature of the holotype specimen.

Dutton et al. (2022) omitted the following species from their table listing records of liolopids: *Harmotrema indica* Chattoparhyaya, 1970 from "*Enhydrina schistosa*" (= *Hydrophis schistosus* Daudin, 1803) (Squamata: Elapidae) from off of the coast of Bombay, Mumbai, India (Chattoparhyaya, 1970); *Harmotrema microchis* Bhutta and Khan, 1975 from *Gavialis gangeticus* (Gmelin, 1789) (Crocodilia: Gavialidae) from the Sutlej River, Pakistan (Bhutta and Khan, 1975); and *Harmotrema linguiforme* Wang, 1987 from *Hydrophis cyanocinctus* Daudin, 1803 (Squamata: Elapidae) from Fujian, China (Wang, 1987).

Phylogenetic analysis

Our *28S* sequence of *D. occidentalis* comprised 1,270 nucleotides (PQ186364 GenBank No.). It differed from that of *Paraharmotrema karinganiense* Dutton and Bullard, 2022 (OL413003 GenBank No.; 1,623 bp) by 100 bp (8%), from *Liolope copulans* (Cohn,1902) Baba, Hosoi, Urabe, Shimazu, Tochimoto, and Hasegawa, 2011 (AB551568 GenBank No.; 1,303 bp) by 46 bp (4%), and from *Harmotrema laticaudae* Yamaguti, 1933 (OL413009 GenBank No.; 1,303 bp) by 44 bp (4%). The phylogenetic analysis recovered Liolopidae as monophyletic, with *P. karinganiense* sister to the remaining liolopids. *Dracovermis* (represented only by our sequence of *D. occidentalis*) was recovered sister to the clade comprising *H. laticaudae* and *L. copulans* (Fig. 3).

Discussion

We accept 3 nominal species of *Dracovermis*: *D. occidentalis, D. brayi* Brooks and Overstreet, 1978*,* and *D. rudolphii* (Tubangui and Masilungan, 1936) Brooks and Overstreet, 1978. We regard *D. nicolli* (Mehra, 1936) Brooks and Overstreet, 1978 as *incertae sedis* because it has a pyriform, relatively sharply-tapering anterior body end (vs. the accepted species of *Dracovermis* all having body ends that are equally rounded) and a vitellarium that extends from the cecal bifurcation to the posterior body end (vs. distributing from the level of the acetabulum or from slightly anterior to the acetabulum to the posterior body end in the accepted species of *Dracovermis*). It also has a diminutive oral sucker rather than the well-developed, bowl-shaped oral sucker of accepted *Dracovermis* spp. Based on the combination of these features, *D. nicolli* could represent a new genus of Liolopidae.

Dutton et al. (2022) stated that previous studies lacked adequate taxon sampling to assess liolopid phylogenetic relationships and liolopid-vertebrate cophyly. That situation has not

changed because currently only 4 species (1 from each genus) have been sequenced (Fig. 3). The tree recovered herein again is equivocal regarding vertebrate-liolopid cophyly because *Dracovermis* is sister to the liolopids infecting snakes and amphibians.

We examined adult alligators, 20 from eastern South Carolina (Crawl Creek, Santee River), 8 from southern Alabama (Mobile Bay), 5 from Pascagoula River (Mississippi) and Mississippi Sound (northern Gulf of Mexico) (SAB, unpublished data) as well as 15 juvenile alligators from the type locality for *D. occidentalis* (Rockefeller Wildlife Refuge, Cameron Parish, Grand Chenier, Louisiana). Of those, only one adult alligator from Mobile Bay was infected. Scott et al. (1997), the only other report of *D. occidentalis* since 1978, documented infections (prevalence = 1 of 25; intensity = 2) of *D. occidentalis* in adult alligators from the Trinity River, Texas. Their analysis showed that infection by *D. occidentalis* was significantly higher among adult alligators (no juvenile alligator was infected). The present publication is the first to examine a large number of juvenile alligators for a liolopid infection. Our data and that of Scott et al. (1997) indicate that juvenile alligators lack infections of *D. occidentalis*. We suspect that this could be related to a dietary shift of adult alligators eating large aquatic vertebrates (e.g., fishes, reptiles, mammals) (Delany, 1990; Delany et al., 1999; Platt et al., 1990; Scott et al., 1997; Taylor, 1986; Wolfe et al., 1987) that could be the second intermediate host for *D. occidentalis*. Regardless of the mechanism(s), our results clearly show that alligators from different areas have different parasites and that certain parasite species can be rare across the known geographic range of the alligator.

Acknowledgements: We thank Brett Warren, Steve Ksepka, Steve Curran, and Kamila Cajiao-Mora (all Aquatic Parasitology Laboratory) for their help necropsying alligators, the Alabama Department of Conservation and Natural Resources (ADCNR) for allowing us to collect during the hunt, the hunters who allowed us to sample their trophies, Anna Phillips, Chad Walter, Kathryn Ahlfeld, and William Moser (all Department of Invertebrate Zoology, National Museum of Natural History, Smithsonian Institution, Washington, DC) for loaning type material and curating our museum specimens.

Literature Cited

Anderson GR, Barker SC (1998). Inference of phylogeny and taxonomy within the Didymozoidae (Digenea) from the second internal transcribed spacer (ITS2) of ribosomal DNA. Syst Parasitol 41: 87–94.

Ashley D, Caldwell J (2013) World trade in crocodilian skins 2009-2011. UNEP-WCMC. Cambridge https://www.louisianaalligators.com/uploads/1/0/4/8/104800207/worldtradeincroc77-88_firstreport.pdf. Accessed 01 September 2013.

Bhutta MS, Khan D (1975) Digenetic trematodes of vertebrates from Pakistan. Bull of the Dep of Zool Univ of the Panjab 8: 1–175.

Brooks DR, Overstreet RM (1978) The family Liolopidae (Digenea) including a new genus and two new species from crocodilians. Int. J Parasitol 8: 267–273.

Chattopadhyaya DR (1970) Studies on the trematode parasites of reptiles found in India. (Digenetic flukes from the marine snakes of the coast of Bombay). Helminthologia11: 35–62.

Chernomor O, Von Haeseler A, Minh BQ (2016) Terrace aware data structure for phylogenomic inference from supermatrices. Syst Bio 65: 997–1008.

Cribb TH, Adlard RD, Bray RA (1998) A DNA-based demonstration of a three-host life-cycle for the Bivesiculidae (Platyhelminthes: Digenea). Int J for Parasitol 28: 1791–1795.

Delany MF (1990) Late summer diet of juvenile American alligators. J of Herp 24: 418–421.

Delany MF, Linda SB, Moore CT (1999) Diet and condition of American alligators in 4 Florida lakes. In Proc of the Annu Conf of the Southeast Assoc of Fish and Wildl Agencies, 53: 375–389.

Dutton HR, DuPreez LH, Urabe M, Bullard SA (2022) *Paraharmotrema karinganiense* n. gen., n. sp. (Digenea: Liolopidae) infecting the intestine of serrated hinged terrapin (*Pelusios sinuatus*), East African black mud turtle (*Pelusios subniger*), and South African helmeted turtle (*Pelomedusa galeata*) and a phylogenetic hypothesis for liolopid genera. Int J Parasitol: Parasites Wildl 17: 43–52.

Elsey RM, Woodward AR (2010) American Alligator *Alligator mississippiensis*. Crocodiles. Status Survey and Conservation Action Plan. 3rd edn, ed. by S.C. Manolis and C. Stevenson. Crocodile Specialist Group: Darwin, pp 1–4.

Hoang DT, Chernomor O, Von Haeseler A, Minh BQ, Vinh LS (2018) UFBoot2: improving the ultrafast bootstrap approximation. Molec Bio and Evol 35: 518–522.

Jelden D, Robert WG, Jenkins AM, Caldwell J (2014) Crocodilians and the Convention on International Trade in Endangered Species of Wild Fauna and Flora (CITES)–update

February 2014. In: Crocodiles. Proc. 17th Working Meeting IUCN Crocodile Specialist Group. http://www.iucncsg.org/365_docs/attachments/protarea/Jeld-b0b18719.pdf. Accessed 01 Feb 2014.

Kalyaanamoorthy S, Minh BQ, Wong TK, Von Haeseler A, Jermiin LS (2017) ModelFinder: fast model selection for accurate phylogenetic estimates. Nat Methods 14: 587–589.

Katoh K, Standley DM (2013) MAFFT multiple sequence alignment software version 7: improvements in performance and usability. Molec Bio and Evol 30: 772–780.

Littlewood DTJ, Olson PD (2014) Small subunit rDNA and the Platyhelminthes: signal, noise, conflict and compromise. In Interrelationships of the Platyhelminthes. CRC Press, Florida, pp 262–278.

Nguyen LT, Schmidt HA, Von Haeseler A, Minh BQ (2015) IQ-TREE: a fast and effective stochastic algorithm for estimating maximum-likelihood phylogenies. Molec Bio and Evol 32: 268–274.

PIJAC, Pet Industry Joint Advisory Council Newsletter, President's Message, (2013) https://www.cga.ct.gov/2013/PDdata/Tmy/2013HB-06323-R000220-Michael%20Maddox,%20Esq.,%20Pet%20Industry%20Joint%20Advisory%20Council-TMY.PDF. Accessed 19 Feb 2013.

Platt SG, Brantley CG, Hastings RW (1990) Food habits of juvenile American alligators in the upper Lake Pontchartrain estuary. Gulf of Mexico Sci 11: 4.

Rambaut A, Suchard MA, Xie D, Drummond AJ (2018) FigTree v1.4.4. Available at: http://tree.bio.ed.ac.uk/ software/figtree. Accessed 25 November 2018.

Scott TP, Simcik SR, Craig TM (1997) Endohelminths of American alligators (*Alligator mississippiensis*) from southeast Texas. J Helm Soc Wash 64: 258–262.

Taylor D (1986) Fall foods of adult alligators from cypress lake habitat, Louisiana. In Proc of the Annu Conf of the Southeast Assoc of Fish and Wildl Agencies, 40: 338–341.

Thorbjarnarson JB, Messel H, King FW, and Ross JP (1992) Crocodiles: an action plan for their conservation. International Union for Conservation of Nature and Natural Resources, Switzerland, pp 1–136.

Wang PQ (1987) Four new species of digenetic trematodes from the amphibians and reptiles of Fujian. Acta Herp Sinica 6: 71–77.

Wolfe JL, Bradshaw DK, Chabreck RH (1987) Alligator feeding habits: new data and a review. Gulf of Mexico Sci, 9: 1.

Figure Legends

Fig. 1 *Dracovermis occidentalis* Brooks and Overstreet, 1978 emend. Dutton and Bullard, 2024 (Digenea: Liolopidae Odhner, 1912) infecting intestine of American alligator, *Alligator mississippiensis* Daudin, 1802 (Crocodilia: Alligatoridae) from Mobile Bay, Alabama. Scale values aside bars. (**A**) Body of voucher (USNM No. 1718009) showing oral sucker (os), pharynx (ph), esophagus (e), nerve cord (nc), excretory system (ex), ventral sucker (vs), vitellarium (vt), cirrus (c), metraterm (m), seminal vesicle (sv), anterior testis (at), ovary (o), posterior testis (pt), and excretory pore (ep). Ventral View. (**B**) Light micrograph body of voucher (USNM No. 1718009). Ventral View

Fig. 2 *Dracovermis occidentalis* Brooks and Overstreet, 1978 emend. Dutton and Bullard, 2024 (Digenea: Liolopidae Odhner, 1912) infecting intestine of American alligator, *Alligator mississippiensis* Daudin, 1802 (Crocodilia: Alligatoridae) from Mobile Bay, Alabama. Scale values aside bars. (**A**) Genitalia of voucher (USNM No. 1718009) showing pars prostatica (pp), cirrus (c), genital pore (gp), metraterm (m), egg (e), seminal vesicle (sv), anterior testis (at), ovary (o), uterus (u), vitelline reservoir (vr), oötype (oö), oviduct (ov), Mehlis' gland (Mg), and posterior testis (pt). Ventral View. (**B**) Light micrograph genitalia of voucher (USNM No. 1718009) Ventral View

Fig. 3 Large subunit ribosomal (*28S*) DNA phylogeny (Maximum Likelihood). Values aside nodes are ultrafast bootstrap replicates (UFBoot). Scalebar indicates the number of substitutions per site. *Dracovermis occidentalis* Brooks and Overstreet, 1978 emend. Dutton and Bullard, 2024 is shown in bold and GenBank accession numbers follow each taxon

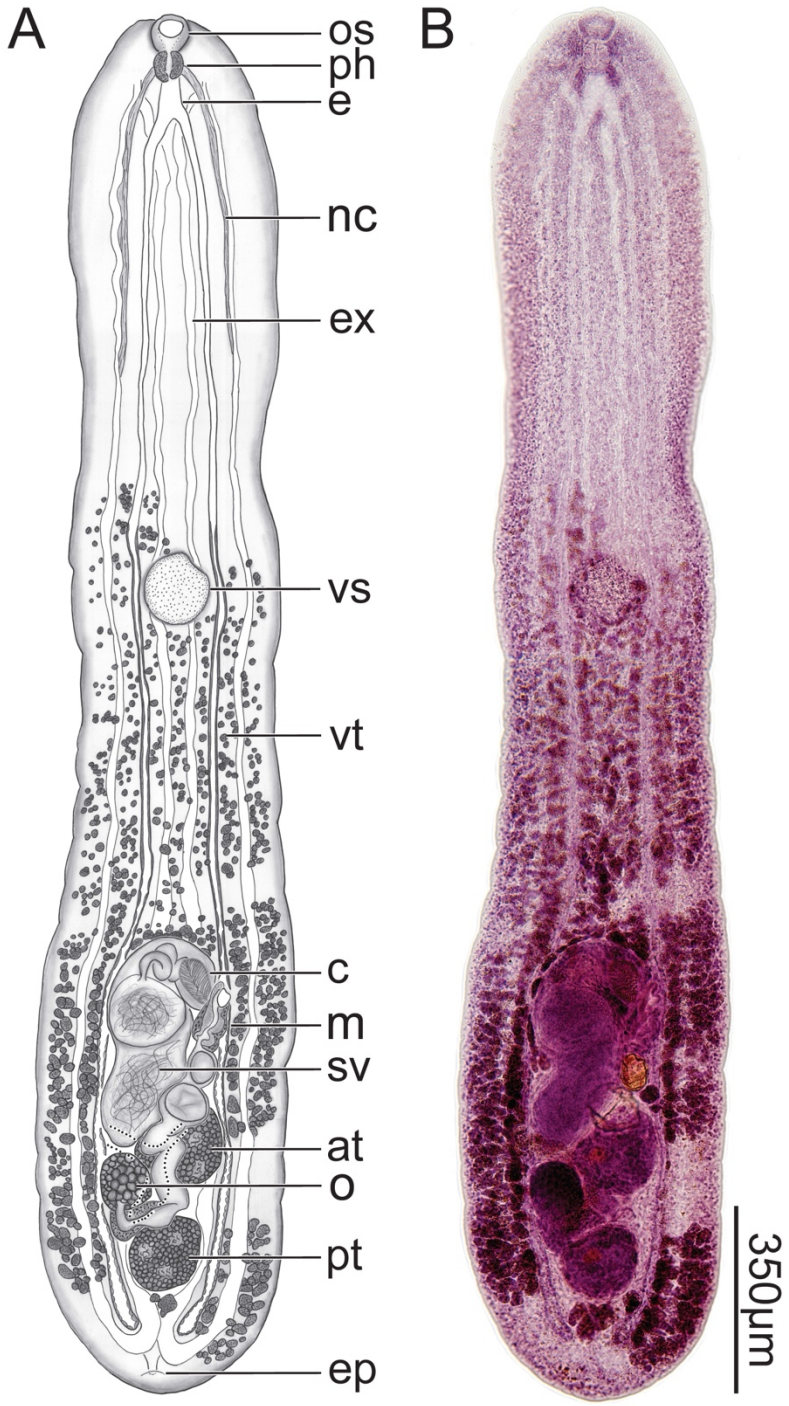
A
os
ph
e
nc
ex
vs
vt
c
m
sv
at
o
pt
ep
B
350µm

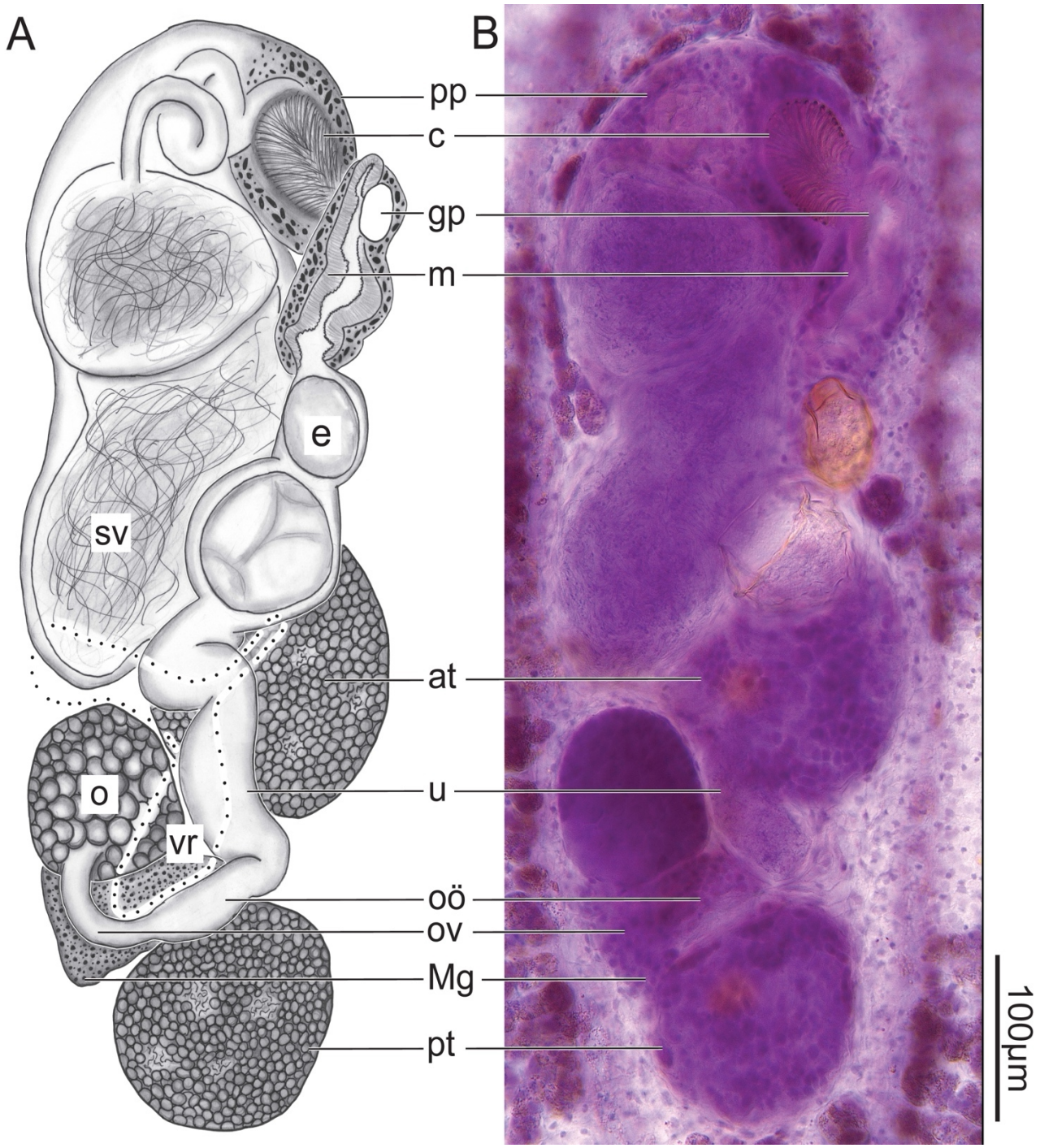
A
B
pp
c
gp
m
e
sv
at
u
o
vr
oö
ov
Mg
pt
100µm

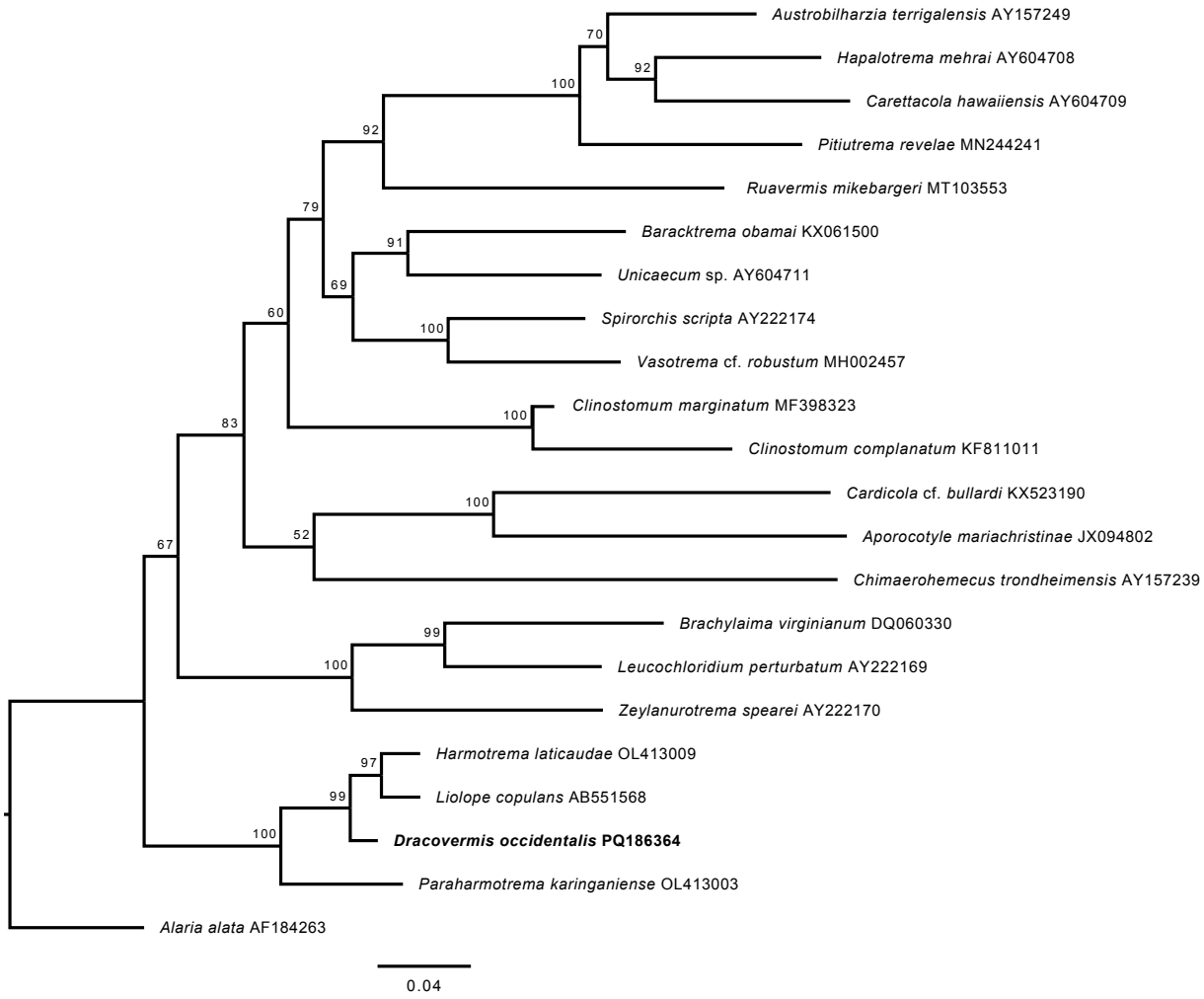
Austrobilharzia terrigalensis AY157249
Hapalotrema mehrai AY604708
Carettacola hawaiiensis AY604709
Pitiutrema revelae MN244241
Ruavermis mikebargeri MT103553
Baracktrema obamai KX061500
Unicaecum sp. AY604711
Spirorchis scripta AY222174
Vasotrema cf. *robustum* MH002457
Clinostomum marginatum MF398323
Clinostomum complanatum KF811011
Cardicola cf. *bullardi* KX523190
Aporocotyle mariachristinae JX094802
Chimaerohemecus trondheimensis AY157239
Brachylaima virginianum DQ060330
Leucochloridium perturbatum AY222169
Zeylanurotrema spearei AY222170
Harmotrema laticaudae OL413009
Liolope copulans AB551568
***Dracovermis occidentalis* PQ186364**
Paraharmotrema karinganiense OL413003
Alaria alata AF184263
70
92
100
92
79
91
69
60
100
100
83
100
52
67
99
100
97
99
100
0.04

CHAPTER 3: New genus and species of Liolopidae Odhner, 1912 (Platyhelminthes: Digenea) infecting Nile crocodile, *Crocodylus niloticus* (Laurenti, 1768) (Crocodilia: Crocodylidae) in the Kavango River, Namibia

***Accepted in Parasitology International (18 January 2025)**

Authors: Haley R. Dutton, Francois J. Jacobs, Piet C. Beytell, Edward C. Netherlands, Louis H. DuPreez, and Stephen A. Bullard

Abstract

A large adult (male) Nile crocodile, *Crocodylus niloticus* (Laurenti, 1768) (Crocodilia: Crocodylidae) (500−650 kg; 4,100 mm total length) from a site (18°08'24.5"S, 21°40'58.4"E) on the Kavango River (Namibia) was opportunely examined herein for parasitic infection and found to be infected in the intestine by *Ngubuvangandu francoisjacobsi* Dutton and Bullard n. gen., n. sp. (Digenea: Liolopidae). The new genus and species differs from all other liolopids by the combination of having a linguiform body that is ~3× longer than wide, a weakly muscular ventral sucker (with pre- and post-ventral sucker distances equal), lobed testes that nearly span the intercecal space and that occupy the posterior 1/3 of the body, a posterior testis that occupies the space between the tips of the posterior ceca, an ovary abutting the anterior testis, a vitellarium that extends slightly anterior to the ventral sucker (not reaching cecal bifurcation), and a uterus that traverses the intercecal space immediately anterior to the anterior testis. We herein reassign 2 previously-named crocodilian liolopids formerly of *Dracovermis* Brooks and Overstreet, 1978 to the new genus: *Ngubuvangandu brayii* (Baylis, 1940) Dutton and Bullard, 2024 (infecting the west African slender snouted crocodile, *Mecistops cataphractus* Cuvier, 1825 in the Congo River) and *Ngubuvangandu rudolphii* (Tubangui and Masilungan, 1936) Dutton and Bullard, 2024 (infecting the saltwater crocodile, *Crocodylus porosus* Schneider, 1801 in the Philippines). The phylogenetic analysis recovered the new genus sister to *Liolope* Cohn, 1902.

That clade was sister to *Harmotrema* Nicoll, 1914, with *Dracovermis* sister to the clade and *Paraharmotrema* Dutton and Bullard, 2022 sister to all liolopids analyzed. This result demonstrates that the crocodilian liolopids are paraphyletic; rejecting the notion that natural groups of liolopids can be defined by the definitive host they infect (i.e., no evidence of phylogenetic host specificity of liolopid genera/lineages). This is the first liolopid described from the Nile crocodile and only the second liolopid species described from an African crocodilian.

1. Introduction

The Nile crocodile, *Crocodylus niloticus* (Laurenti, 1768) (Crocodilia: Crocodylidae) is among the largest and most iconic crocodiles in the world and the largest crocodile in Africa. The Nile crocodile has immense cultural (Aust et al. [1]), economic (Lindsey et al. [2,3]), ecological (Mazzotti et al. [4]), and conservation importance (Somaweera et al. [5]) throughout sub-Saharan Africa. Yet surprisingly little is known about its parasites. Less surprising is that much less is known overall about the parasites infecting other African crocodile species, i.e., 2 species of *Crocodylus* Laurenti, 1768; 2 species of *Mecistopus* Gray, 1844; and 2 species of *Osteolaemus* Cope, 1861. Of note regarding recent taxonomic studies with the Nile crocodile *sensu lato*, two species are now accepted: *C. niloticus* ranging throughout western and southern Africa and the west African crocodile, *Crocodylus suchus* Geoffroy, 1807 overlapping with *C. niloticus* within the Niger and Congo River Basins (west-central Africa) (Hekkala et al. [6,7]).

Regarding the family of digeneans we report herein (Liolopidae Odhner, 1912), complete and comprehensive taxonomic accounts (species descriptions) of liolopids infecting crocodiles are nearly wholly lacking. The lack of complete and detailed morphological descriptions in this family of digeneans makes differentiating genera challenging in general, and our assessment is

that most species need to be recollected and redescribed (Dutton et al. [8,9]). Even a character as basic and fundamental as body shape and general orientation of genitalia has been confused in the Liolopidae because several descriptions of liolpids are based on cold-fixed (highly contracted) and poorly stained specimens. Previous to our work with liolopids (Dutton et al. [8,9]), only one sequence of one lioloipid species (*Liolope copulans* Cohn, 1902; type species) was available. Dutton et al. [8] published sequences of a species of *Harmotrema* Nicoll, 1914 and *Paraharmotrema* Dutton and Bullard, 2022. Dutton et al. [9] published a sequence for the type species of *Dracovermis* Brooks and Overstreet, 1978, and the present study provides nucleotide sequences for a new genus. The remaining liolopid genus, *Helicotrema* Odhner, 1912, is not represented by a nucleotide sequence; however, the types for all liolopid genera aside from *Harmotrema* and *Helicotrema* have been sequenced and are publicly available now. Still, the testing of hypotheses about liolopid-crocodile cophyly and biogeography requires extensive additional taxon sampling. Another impediment is that, as stated above, we lack necessary morphological information for many liolopids. Another typical impediment that is true for seemingly all groups of parasites is that no specimen from the Indian sub-continent is available for loan.

The scarcity of parasitological information from Nile crocodiles throughout its known distribution is perhaps related to the difficulty in capturing large predators that maim, kill, and eat people. In addition to being a human predator, sampling them is treacherous because they range in large, fast flowing rivers where they cohabitate with the hippopotamus, *Hippopotamus amphibius* Linnaeus, 1758, which can attack and kill people (Aust et al. [1]). It also ranges in stagnant backwaters and deltaic wetlands. The Nile crocodile is protected under law, and is recognized as a protected game species in Namibia under the Nature Conservation Ordinance No

4 of 1975, allowing trophy hunting of the species only with the issuing of a hunting license and with an export quota of 25 per year in Namibia (Combrink et al. [10]). CITES Appendix II allows the trade of no more than 1,600 Nile crocodile skins from Namibia, which originate from both trophy hunting and ranching (Lyet et al. [11]).

From the parasitological perspective and perhaps explaining the paucity of parasite studies involving Nile crocodiles, even if one is present when and where a Nile crocodile is available for necropsy, the parasitologist still must rapidly (within 1 hr) separate the organs/tissues and stabilize them in citrated saline at a cool temperature such that parasite specimens remain alive long enough to heat-kill for taxonomic study. High quality microscopes are required to do a thorough and complete necropsy, i.e., examining the skin, eye and conjunctival sac, brain, head cavities, mouth, esophagus and trachea, lungs, kidney, liver, spleen, stomach, intestine, cloaca, heart, blood, and body cavity, and live parasite specimens must be cared for and ultimately allocated for fixation in formalin and preservation in ethanol. With four highly experienced parasitologists, the necropsy of a large Nile crocodile can take 8-10 hrs (totaling 80-100 total hrs of effort for a single Nile crocodile). In our experience, the Nile crocodile has been among the most difficult hosts to gain access to and among the most challenging to obtain high quality parasite specimens from.

In the present study, we report a new genus and species of Liolopidae from the intestine of a Nile crocodile from the Kavango River, Namibia. We also correct some errors in the literature, provide a revised diagnosis of Liolopidae, and reassign two previously named crocodilian liolopids to the new genus.

2. Materials and methods

2.1. Crocodile collection, parasite specimen collection, preparation, and deposition

Two Nile crocodiles were examined for this study. A large adult (male) Nile crocodile (500−650 kg; 4,100 mm total length), estimated to between 75 and 100 years of age, from a site (18°08'24.5"S, 21°40'58.4"E) on the Kavango River (Namibia) and a small juvenile Nile crocodile from the Kwando River (Namibia) (17°52'34.2"S 23°20'28.4"E) was examined on 10 February 2024. Only the large Nile crocodile from the Kavango River was infected but both Nile crocodiles were processed the same. The digestive tract was excised intact, sliced longitudinally to expose the lumen, heat killed at 65C, decanted and placed into acrylic settling columns where the sediment was observed in a petri dish under the dissecting scope and examined for trematodes. Trematodes intended for morphology as whole-mounts were observed microscopically and fixed following Dutton et al. [8]. Whole mounts were examined and illustrated using an Olympus BX53 microscope (Olympus Corporation, Shinjuku City, Tokyo, Japan) equipped with differential interference contrast, measured using an ocular micrometer, and illustrated using a drawing tube. Measurements are reported in micrometers (μm) as the range followed by the mean, +/− standard deviation, and sample size in parentheses. Vouchers were deposited in the National Museum of Natural History's Invertebrate Zoology Collection (Smithsonian Institution, USNM Collection Nos. XXXXX–XXXXX). Classification and anatomical terms for liolopids follow Dutton et al. [8].

2.2. DNA extraction, amplification, sequencing, and phylogenetic analysis

Total genomic DNA was extracted from 1 EtOH-preserved specimen. DNA extraction, primers used, PCR amplification, sequencing, sequence assembly and analysis follow that of Dutton et al. [8,9]. We amplified the *28S*, *18S*, *ITS2,* and *CO1* for the new species, we also

amplified the *18S* and *CO1* for *Paraharmotrema karinganiense* Dutton and Bullard, 2022 from the same extract from Dutton et al., [8] to generate a more complete genetic library for this group. The *28S* phylogenetic analysis included a sequence from the current study, the remaining liolopid sequences that were available on GenBank (Dutton et al. [8,9]), a subset of taxa from the Schistosomatoidea Stiles & Hassall, 1898, Brachylaimidae Dujardin, 1843, and Diplostomoidea Poirier, 1886, and *Transversotrema patialense* (Soparkar, 1924) Crusz and Sathananthan, 1960 as the outgroup. Sequences were aligned with the multiple alignment tool using fast Fourier transform (MAFFT) (Katoh and Standley [12]) and trimmed to the length of the shortest sequence presented herein (1,237 base pairs [bp]) in Geneious Prime Software version 2023.0.4 (Geneious Corp., Auckland, New Zealand). Aligned sequences were reformatted and exported from .fasta to .phy to run a maximum likelihood tree (ML). The ML was inferred with IQTREE v.1.16.12 (Nguyen et al. [13]). Substitution model testing was done with ModelFinder (Kalyaanamoorthy et al. [14]) as implemented in IQTREE. After model testing, tree inference was done using best-fitting substitution models (Chernomor et al. [15]). Default tree search parameters were used, except perturbation strength was set to 0.2, and 500 iterations had to be unsuccessful to stop the tree search. Tree inference was performed 20 times with only the tree with the best log-likelihood score reported. Support for relationships was measured with 1000 ultrafast bootstrap replicates (UFBoot) (Hoang et al. [16]). The inferred phylogenetic tree was visualized using FigTree v1.4.4 (Rambaut et al. [17]) and further edited with Adobe Illustrator (Adobe Systems) for visualization purposes.

3. Results

3.1 Liolopidae Odhner, 1912, emended

Body small or moderately large, elliptical, linguiform or slender; tegument unarmed. Oral sucker and pharynx present; esophagus short or indistinct; pre-pharyngeal portion of esophagus indistinct. Ceca long, nearly reaching posterior body end. Ventral sucker variously distanced from anterior body end. Testes round, oval or irregular in outline, tandem, separate, usually well separated, occupying posterior, middle or anterior third of body. Cirrus-sac between ventral sucker and anterior testis, enveloping bipartite seminal vesicle, pars prostatica, and spinose cirrus. External seminal vesicle predominantly absent. Genital atrium present. Genital pore opening in hindbody (posterior to ventral sucker), submedian or lateral. Ovary irregular, intertesticular. Seminal receptacle absent. Laurer's canal present or indistinct. Uterine seminal receptacle present or indeterminate. Uterus distributing in hindbody and principally posterior to cirrus-sac and genital pore. Metraterm robust. Vitellarium follicular, surrounding ceca to various extent. Excretory system with terminal or dorsoterminal excretory pore, post-testicular Y-shaped vesicle and paired inter- and extracaecal tubules united anteriorly and posteriorly. Infecting intestine of amphibians and reptiles.

Type genus: *Liolope* Cohn, 1902

Accepted genera: Helicotrema Odhner, 1912; *Dracovermis* Brooks and Overstreet, 1978; *Harmotrema* Nicoll, 1914; *Paraharmotrema* Dutton and Bullard, 2022.

3.2 Ngubuvangandu Dutton and Bullard n. gen.

Diagnosis: Body linguiform, approximately 3× longer than wide, having slightly tapered anterior end, having broadly rounded posterior end, with maximum breadth at midbody. Oral sucker smaller than ventral sucker, ventral, bowl shaped. Ventral sucker weakly muscular, in middle of body (pre- and post-ventral sucker distances equal), inter-cecal, not spanning inter-

cecal space. Pre-pharyngeal portion of esophagus indistinct. Intestine comprising paired ceca extending posteriad approximately in parallel with lateral body margin, nearly reaching posterior body end, lacking diverticula and out-pocketings, bowing laterad at level of common genital pore and testes. Gonads inter-cecal, in posterior 1/3 of body. Testes posterior to ventral sucker, lobed, tandem, medial, inter-cecal, nearly spanning breadth of intercecal space, in posterior 1/3 of body; anterior testis flanked by cirrus sac and ovary; posterior testis at level of cecal tips. Cirrus sac inter-cecal, transverse or oblique, between ventral sucker and anterior testis, containing bipartite seminal vesicle, and spined eversible cirrus with small spines. Common genital pore sinistral, ventral to sinistral ceca, post-acetabular, level with anterior testis. Ovary entire, dextral, inter-testicular, inter-cecal, abutting anterior testis. Vitellarium confluent throughout distribution, nearly spanning breadth of hindbody, extending from midway between ventral sucker and cecal bifurcation to posterior body end, not extending anteriad to level of intestinal bifurcation. Uterus convoluted, dorsal to ovary, ventral to anterior testis, transverse anterior to anterior testis, dorsal to cirrus/cirrus spines; uterine seminal receptacle present. Excretory system comprising lasso configuration dextrally and sinistrally (excretory system having a pair of ducts, each having an anterior cyclocoel-like portion). Intestinal parasites of crocodilians.

Differential diagnosis: Body linguiform (vs. elongate in *Helicotrema*, *Paraharmotrema*, *Dracovermis*, and *Harmotrema*), approximately 3× longer than wide, having slightly tapered anterior end, having broadly rounded posterior end, with maximum breadth at midbody. Ventral sucker weakly muscular (vs. strongly muscular in *Liolope*); pre- and post-ventral sucker distances equal (vs. not equal in *Paraharmotrema*, *Liolope*, *Dracovermis*, *Helicotrema*, and *Harmotrema*). Testes lobed (vs. smooth in *Liolope* [except *L. dollfusi* with lobed testes],

Helicotrema, *Harmotrema*, and *Dracovermis*), in posterior 1/3 of body (vs in anterior half of body in *Helicotrema*), nearly spanning breadth of intercecal space; posterior testis at level of cecal tips (vs anterior to level of cecal tips in *Paraharmotrema*, *Liolope*, *Dracovermis*, *Helicotrema*, and *Harmotrema*). Ovary dextral, abutting anterior testis (vs. lobed and nearest posterior testis in *Paraharmotrema*; far separated in *Harmotrema* and *Helicotrema*). Vitellarium extending anteriad to ventral sucker, not reaching level of cecal bifurcation (vs. distributing from ventral sucker to posterior body end in *Paraharmotrema* and *Helicotrema*; vs. extending to level of cecal bifurcation in *Liolope*; vs. extending to level of ventral sucker in *Dracovermis* [except *D. nicolli* that extends to the oral sucker] and *Harmotrema* [except *H. infecundum* that extends anterior to ventral sucker]). Uterus ventral to anterior testis (like *Harmotrema* spp. except *Harmotrema infecundum* that has a uterus lateral to the anterior testis) and *Paraharmotrema*; transverse anterior to anterior testis (vs not transverse to the anterior testis in *Helicotrema*, *Harmotrema*, *Paraharmotrema*, and *Dracovermis*). Infecting the intestine of crocodilians.

Type species: Ngubuvangandu francoisjacobsi Dutton and Bullard n. sp.

Other species: Ngubuvangandu brayii (Baylis, 1940) Dutton and Bullard, 2024 (infecting the west African slender snouted crocodile, *Mecistops cataphractus* Cuvier, 1825 in the Congo River system) and *Ngubuvangandu rudolphii* (Tubangui and Masilungan, 1936) Dutton and Bullard, 2024 (infecting the saltwater crocodile, *Crocodylus porosus* Schneider, 1801 in the Philippines).

ZooBank registration: XXXXXXXX-XXX

Etymology: The genus name *Ngubuvangandu* combines "*Ngubu*," which honors the fellowship and scientific discovery we experienced as a team while working and learning

together in the powerful wilderness of Namibia, and "*vangandu*," which is a word for 'crocodile' in the group of Kavango languages.

3.3 Ngubuvangandu francoisjacobsi Dutton and Bullard n. sp. (Figs. 1−X)

3.3.1 Light microscopy of adult based on 4 whole-mounted adult specimens: USNM collection nos. XXXXXXX–XXXXXXX (Based on light microscopy of the heat-killed, formalin-fixed, stained, whole-mounted holotype and 3 paratypes)

Body 2,150−2,325 (2,206± 80; 4) long, 680−760 (735 ± 38; 4) in maximum width at level of the ventral sucker, 2.9−3.2 (3 ± 0.1; 4) longer than wide. Oral sucker 40−125 (91 ± 38; 4) long or 2−5% (4% ± 2%; 4) of body length, 90−125 (115 ± 17; 4) wide or 13−16% (16% ± 2%; 4) of maximum body width, oral sucker spines absent. Ventral sucker weakly muscular, 170−195 (179 ± 11; 4) long or 8% (8% ± 0%; 4) of body length, 175−185 (179 ± 5; 4) wide or 32−43% (39% ± 5%; 4) of maximum body width; 1: 1.4−2.0 (1.6 ± 0.3; 4) to oral sucker width ratio. Forebody 930−990 (955 ± 26; 4) long or 43−45% (43% ± 1%; 4) of total body length. Nerve commissure ventral to esophagus, 170−220 (191 ± 22; 4) or 7−10% (9% ± 1%; 4) of body length from anterior body end. Pharynx 90−130 (111 ± 19; 4), 115−130 (123 ± 6; 4) wide; 1: 0.7 −1 (0.9 ± 0.2; 4) oral sucker to pharynx width ratio. Esophagus 175−225 (200 ± 20; 4) long post pharyngeal, 20−40 (29 ± 9; 4) wide; esophageal gland indistinct. Intestine bifurcating 225−270 (245 ± 20; 4) or 10−12% (11% ± 1%; 4) of body length from anterior body end.

Anterior testis 150−240 (195 ± 37; 4) long or 7−11% (9% ± 2%; 4) of body length, 275−335 (316 ± 28; 4) wide or 37−49% (43% ± 5%; 4) of body width at level of ventral sucker; inter-testicular space 50−100 (81 ± 24; 4) long or 2−5% (4% ± 1%; 4) of body length. Posterior testis 225−275 (256 ± 24; 4) long or 10−13% (12% ± 1%; 4) of body length, 225−325 (290 ± 45;

4) wide or 30−48% (40% ± 8%; 4) of body width at level of ventral sucker, 50−140 (95 ± 40; 4) or 2−6% (4% ± 2%; 4) of body length from posterior body end. Cirrus sac slightly curved, semilunar, 350−450 (397 ± 41; 4) long or 16−21% (18% ± 2%; 4) of body length, 100−150 (122 ± 26; 4) wide or 15−21% (18% ±2%; 4) body width at level of genital pore, 620−725 (666 ± 54; 4) length to body end or 29−33% (30% ±2%; 4) of body length. Internal seminal vesicle bipartite, comprising proximal and distal portions; proximal portion variable in size depending on amount of sperm, 50−125 (95 ± 32; 4) long, 90−95 (93 ± 2; 4) wide; distal portion ovoid,75−150 (116 ± 31; 4) long or 3−7% (5% ± 1%; 4) of body length, 63−100 (78 ± 16; 4) wide. Cirrus beginning at end of distal portion of internal seminal vesicle, beginning as a coiled duct, 113−225 (157 ± 48; 4) long or 31−58% (40% ± 13%; 4) of cirrus sac length, 38−53 (46 ± 7; 4) wide; cirrus spines curved, tapering, 5−10 (8 ± 2; 4) long; pars prostatica indistinct, prostatic gland-cells present surrounding cirrus; genital atrium indistinct, usually obscured by terminal genitalia.

Ovary 105−150 (135 ± 21; 4) long or 5−7% (6% ± 1%; 4) of body length, 125−155 (138 ± 12; 4) wide or 16−23% (19% ± 3%; 4) of body width; post-ovarian space 330−400 (360 ± 30; 4) or 15−18% (16% ± 1%; 4) of body length. Uterus convoluted, 625−925 (800 ± 127; 4) long, 75−125 (88 ± 25; 4) wide; uterine seminal receptacle present. Eggs oblong, 125−130 (128 ±3; 15) long, 55−75 (68 ± 10; 15) wide; numbering 9−13 (10 ± 2; 4) per specimen; a single developing egg dorsal to or immediately posterior to ovary in 3 of 4 specimens. Metraterm 175−250 (231 ± 38; 4) long, 60−100 (85 ± 18; 4) wide. Total uterus/metraterm length 315−450 (396 ± 58; 4) long or 14−21% (18% ± 3%; 4 of body length. Common genital pore 600−650 (620 ± 24; 4) or 27−30% (28% ± 1%; 4) of body length from posterior body end, 13−15 (14 ± 1; 4) in diameter. Vitellarium comprising series of irregularly-shaped follicles, distributing from

390−590 (470 ± 94; 4) or 27−30% (28% ± 1%; 4) from anterior to end of body, confluent posteriorly; transverse vitelline duct dorsal, 315−400 (354 ± 35; 4) in breadth 20−75 (40 ± 25; 4) wide; primary vitelline collecting duct 50−100 (74 ± 21; 4) long, 25−75 (50 ± 20; 4) wide, inserting dorsal to ovary.

Excretory system with extra- and intercecal tubules; 1,800−1,875 (1,843 ± 36; 4) long, both intercecal branches joining at level of ceca tips; excretory pore subterminal.

3.3.2 Taxonomic summary

Type and only reported host: Crocodylus niloticus (Laurenti, 1768) (Crocodilia: Crocodylidae), the Nile crocodile.

Type and only reported locality: A site (18°08'24.5"S, 21°40'58.4"E) on the Kavango River, Kavango East Region, Namibia.

Specimens and sequences deposited: Holotype (USNM XXXXX); paratypes (USNM XXXXXX−XXXXXX); *28S* (GenBank Nos. XXXXXX), *18S* (GenBank Nos. XXXXXX), *ITS2* (GenBank Nos. XXXXXX), and *CO1* sequences (GenBank Nos. XXXXXX).

Site in host: Intestine.

Prevalence and intensity: One of two Nile crocodiles was infected with 5 specimens of *N. francoisjacobsi*.

Etymology: The species name "*francoisjacobsi*" honors our admired colleague and friend, Dr. Francois Jakob Jacobs, for leading us in the field, teaching us about the natural history and ecology of eastern Namibia, hosting us in Divundu during our stay, and protecting us from predators on land and water.

3.3.3 Taxonomic remarks

Ngubuvangandu francoisjacobsi differs from all other liolopid genera by the combination of having a linguiform body that is ~3× longer than wide, a weakly muscular ventral sucker (with pre- and post-ventral sucker distances equal), lobed testes that nearly span the intercecal space and that occupy the posterior 1/3 of the body, a posterior testis that occupies the space between the tips of the posterior ceca, an ovary abutting the anterior testis, a vitellarium that extends slightly anterior to the ventral sucker (not reaching cecal bifurcation), and a uterus that traverses the intercecal space immediately anterior to the anterior testis. Species of *Helicotrema*, *Paraharmotrema*, *Dracovermis*, and *Harmotrema* have a much more elongate body. The ventral sucker of species of *Liolope* is strongly muscular, and the pre- and post-ventral sucker distances are not equal in *Paraharmotrema*, *Liolope*, *Dracovermis*, *Helicotrema*, and *Harmotrema*. The testes are smooth in *Liolope*, *Helicotrema*, *Harmotrema*, and *Dracovermis* (an exception is *L. dollfusi* that reportedly has lobed testes); the testes are in the anterior half of the body in *Helicotrema*; and the posterior testis are far anterior to the cecal tips in *Paraharmotrema*, *Liolope*, *Dracovermis*, *Helicotrema*, and *Harmotrema*. The ovary is non-abutting but nearest the posterior testis in *Paraharmotrema* and far separated in *Harmotrema* and *Helicotrema*. The vitellarium distributes from the ventral sucker to the posterior body end in *Paraharmotrema* and *Helicotrema*; extends to the level of the cecal bifurcation in *Liolope*; and extends to the level of the ventral sucker in *Dracovermis* [except *D. nicolli* that extends to the oral sucker] and *Harmotrema* [except *H. infecundum* that extends anterior to ventral sucker]). Uterus not transverse to anterior testis in *Helicotrema*, *Harmotrema*, *Paraharmotrema*, and *Dracovermis*.

We herein reassign two previously-named crocodilian liolopids formerly of *Dracovermis* Brooks and Overstreet, 1978 to the new genus: *Ngubuvangandu brayii* (Baylis, 1940) Dutton and

Bullard, 2024 (infecting the west African slender snouted crocodile, *Mecistops cataphractus* Cuvier, 1825 in the Congo River system) and *Ngubuvangandu rudolphii* (Tubangui and Masilungan, 1936) Dutton and Bullard, 2024 (infecting the saltwater crocodile, *Crocodylus porosus* Schneider, 1801 in the Philippines). Both of these trematodes fit the generic diagnosis of *Ngubuvangandu*. Dutton et al. [9] regarded *Dracovermis nicollii* Mehra, 1933 as a *species inquirendum*.

We observed that the size, shape, and distribution of cirrus spines across liolopid genera could be a useful differential diagnostic feature for some genera (Fig. 2). These spines are challenging to characterize because they are associated with an eversible structure, are curved, and orient dorso-ventrally in whole-mounted specimens. Observing the live liolopid would be greatly beneficial to understanding the fine anatomy of these spines, and we suggest that future workers make an effort to photograph and illustrate the spines from live specimens or specimens fixed and mounted in a semi-permanent mounting medium and clearing agent like Grey-Wess mounting medium. We did not do this because we had too few specimens to commit any to semi-permanent mounting.

3.4 Phylogenetic analysis

Our *28S* sequence of *N. francoisjacobsi* comprised 1,331 nucleotides and differed from that of *Dracovermis occidentalis* Brooks and Overstreet, 1978 (see Dutton et al. [9]) (GenBank No. PQ186364; 1,270 bp) by 57 bp (4%); from *Paraharmotrema karinganiense* Dutton and Bullard, 2022 (GenBank No. OL413003; 1,623 bp) by 106 bp (8%); from *Liolope copulans* (Cohn,1902) (see Baba et al [18]) (GenBank No. AB551568; 1,303 bp) by 38 bp (3%); and from *Harmotrema laticaudae* Yamaguti, 1933 (OL413009 GenBank No.; 1,303 bp) by 46 bp (4%).

The phylogenetic analysis recovered the new genus sister to *Liolope* Cohn, 1902 (Fig. 3). That clade was sister to *Harmotrema* Nicoll, 1914, with *Dracovermis* sister to that clade and *Paraharmotrema* Dutton and Bullard, 2022 sister to all liolopids analyzed (Fig. 3).

4. Discussion

The present study demonstrates that the crocodilian liolopids are paraphyletic; rejecting the notion that a natural group of liolopids can be defined by the definitive host they infect. This also rejects the notion of phylogenetic host specificity of liolopid genera/lineages. However, it is noteworthy that the species reassigned to the new genus all infect crocodylids (Crocodylidae Cuvier, 1807), making the species in the new genus all parasites of "true crocodiles", whereas *Dracovermis* remains monotypic and includes a species that infects the American alligator (Alligatoridae Gray, 1844) (Dutton et al. [9]). Additional taxon sampling and subsequent phylogenetic analyses that include additional sequences will change this tree topology. However, at present, because so few taxa have been sequenced across liolopid genera, the existing data fail to suggest that liolopids are co-evolving with the main ectotherm lineages that they have come to mature in and use as definitive hosts.

Although only one liolopid life cycle is known (*L. copulans*; Baba et al. [18]), knowledge of the intermediate hosts for any species is critical to understanding liolopid natural history. Like the results of Dutton et al. [9], the small juvenile crocodile was not infected whereas the large adult crocodile examined herein was infected. Dutton et al. [9], which examined many more hosts than in the present study, suggested that the difference in parasite infection prevalence between young and old alligators could be related to an ontogenetic shift in diet or to an uneven geographic distribution of the intermediate hosts. Testing that for liolopids and Nile crocodiles

would require extensive temporal-spatial sampling, which is not likely feasible given the conservation status of the Nile crocodile. Further, as with any apex predator, the parasite component community of geographic populations of Nile crocodiles could help shed light on environmental quality given that high parasite diversity can correlate with high biodiversity of free living aquatic invertebrates and vertebrates. Additionally, parasitological information can provide insights into local food web dynamics if parasite life cycles are known.

The phylogenetic position of the Liolopidae has become recently more intriguing based on the results of Cutmore et al. [19], who used Transversotrematidae Witenberg, 1944 as an outgroup and who recovered Liolopidae sister to all other ingroup trematode taxa (indicating liolopids could be an early branching digenean lineage). This result is not necessarily surprising given their morphological affinities to the blood flukes and diplostomoids. Dutton et al. [8,9] recovered a monophyletic Liolopidae with high support values and as an early branching group within the early branching clade.

Acknowledgements: We thank Amanda Robinson and Anna Phillips (Department of Invertebrate Zoology, National Museum of Natural History, Smithsonian Institution, Washington, D.C.) for loaning type material and curating our museum specimens.

Funding: This study was supported by Southeastern Cooperative Fish Parasite and Disease Project (Auburn University), the US Fish and Wildlife Service (Department of Interior), United States Department of Agriculture (National Institute of Food and Agriculture), Federal Aid in Sport Fish Restoration (Alabama Department of Conservation and Natural Resources, Inland and Marine Resources Divisions), and the Alabama Agricultural Experiment Station (Auburn University, College of Agriculture). Field work was supported by the Kwando Carnivore Trust of Namibia.

Literature Cited

[1] P. Aust, B. Boyle, R. Fergusson, T. Coulson, The impact of Nile crocodiles on rural livelihoods in northeastern Namibia, S. Afr. J. of Wildl. Res., 39 (2009) 57–69.

[2] P.A. Lindsey, P.A. Roulet, S.S. Romanach, Economic and conservation significance of the trophy hunting industry in sub-Saharan Africa, Biol. Conserv. 134 (2007) 455–469.

[3] P.A. Lindsey, J. Barnes, V. Nyirenda, B. Pumfrett, C.J. Tambling, W.A. Taylor, M.T.S. Rolfes, The Zambian wildlife ranching industry: scale, associated benefits, and limitations affecting its development, PloS One. 8 (2013) e81761.

[4] F.J. Mazzotti, G.R. Best, L.A. Brandt, M.S. Cherkiss, B.M. Jeffery, K.G. Rice, Alligators and crocodiles as indicators for restoration of Everglades ecosystems, Ecol. Indic. 9 (2009) S137–S149.

[5] R. Somaweera, J Nifong, A. Rosenblatt, M.L. Brien, X. Combrink, R.M. Elsey, G Grigg, Magnusson, W.E., F.J. Mazzotti, A. Pearcy, S.G. Platt, The ecological importance of crocodylians: towards evidence-based justification for their conservation, Biol. Rev. 95 (2020) 936–959.

[6] E. Hekkala, M.H. Shirley, G. Amato, J.D. Austin, S. Charter, J. Thorbjarnarson, K.A. Vliet, M.L. Houck, R. Desalle, and M.J. Blum, An ancient icon reveals new mysteries: mummy DNA resurrects a cryptic species within the Nile crocodile, Molec. Ecol. 20 (2011) 4199–4215.

[7] E.R. Hekkala, M.L. Aardema, A. Narechania, G. Amato, S. Ikram, M.H. Shirley, K.A. Vliet, S.W. Cunningham, M. T.P. Gilbert, and O. Smith, The secrets of Sobek–A crocodile mummy mitogenome from ancient Egypt, J. of Archaeol. Sci.: Rep. 33 (2020) 102483.

[8] H.R. Dutton, L.H. DuPreez, M. Urabe, S.A. Bullard, *Paraharmotrema karinganiense* n. gen., n. sp. (Digenea: Liolopidae) infecting the intestine of serrated hinged terrapin (*Pelusios sinuatus*), East African black mud turtle (*Pelusios subniger*), and South African helmeted turtle (*Pelomedusa galeata*) and a phylogenetic hypothesis for liolopid genera, Int. J. Parasitol: Parasites Wildl. 17 (2022) 43–52.

[9] H.R. Dutton, J.H. Brule, S.A. Bullard, A.M. Kelly, Redescription of *Dracovermis occidentalis* (Digenea: Liolopidae) infecting American alligator, *Alligator mississippiensis* from the Bon-Secour River (Mobile–Tensaw River Delta, Alabama, USA) and a revised phylogeny for Liolopidae, Paristol. Res. 123:326 (2024) 1–8.

[10] X. Combrink, C. Lippai, R. Fergusson, Nile Crocodile *Crocodylus niloticus*, Crocodiles. Status Survey and Conservation Action Plan. Crocodile Specialist Group: Darwin. Fourth

ed., International Union for Conservation of Nature and Natural Resources, Switzerland, 2019.

[11] A. Lyet, R. Slabbert, W.F. Versfeld, A.J. Leslie, P.C. Beytell, P. Du Preez, Using a binomial mixture model and aerial counts for an accurate estimate of Nile crocodile abundance and population size in the Kunene River, Namibia, Afr. J. of Wildl. Res. 46 (2016) 71–86.

[12] K. Katoh, D.M. Standley, MAFFT multiple sequence alignment software version 7: Improvements in performance and usability, Mol. Biol. Evol. 30 (2013) 772–780.

[13] L.T. Nguyen, H.A. Schmidt, A. Von Haeseler, B.Q. Minh, IQ-TREE: a fast and effective stochastic algorithm for estimating maximum-likelihood phylogenies, Molec. Bio. and Evol. 32 (2015) 268–274.

[14] S. Kalyaanamoorthy, B.Q. Minh, T.K. Wong, A. Von Haeseler , L.S. Jermiin, ModelFinder: fast model selection for accurate phylogenetic estimates, Nat. Methods, 14 (2017) 587–589.

[15] O. Chernomor, A. Von Haeseler, B.Q. Minh, Terrace aware data structure for phylogenomic inference from supermatrices, Syst. Bio. 65 (2016) 997–1008.

[16] D.T. Hoang, O. Chernomor, A. Von Haeseler, B.Q. Minh, L.S. Vinh, UFBoot2: improving the ultrafast bootstrap approximation, Molec. Bio. and Evol. 35 (2018) 518–522.

[17] A. Rambaut, M.A. Suchard, D. Xie, A.J. Drummond, FigTree v1.4.3. Available at: http://tree.bio.ed.ac.uk/ software/figtree. Accessed 25 November 2018.

[18] T. Baba, M. Hosoi, M. Urabe, T. Shimazu, T. Tochimoto, H. Hasegawa, *Liolope copulans* (Trematoda: Digenea: Liolopidae) parasitic in *Andrias japonicus* (Amphibia: Caudata: Cryptobranchidae) in Japan: Life cycle and systematic position inferred from morphological and molecular evidence, Parasitol. Int. 60 (2011) 181–192.

[19] S.C. Cutmore, D.T.J Littlewood, M. Arellano-Martínez, C. Louvard, T.H. Cribb, Evidence that a lineage of teleost-infecting blood flukes (Aporocotylidae) infects bivalves as intermediate hosts, Int. J. for Parasitol. 53 (2023) 13–25.

Figure Legends

Figs. 1 *Ngubuvangandu francoisjacobsi* Dutton and Bullard, 2024 (Digenea: Liolopidae Odhner, 1912) infecting intestine of Nile crocodile, *Crocodylus niloticus* (Laurenti, 1768) (Crocodilia: Crocodylidae), from the Kavango River (northeastern Namibia). Scale values aside bars. (**A**) Body of holotype (USNM No. XXXXX) showing oral sucker (os), pharynx (ph), nerve cord (nc), esophagus (e), excretory system (ex), vitellarium (vt), ventral sucker (vs), seminal vesicle (sv), cirrus spines (cs), anterior testis (at), ovary (o), egg (eg), and posterior testis (pt). Ventral view. (**B**) Genitalia of paratype (USNM No. XXXXX) showing seminal vesicle (sv), cirrus spines (cs), metraterm (m), common genital pore (cp), uterus (u), anterior testis (at), ovary (o), vitelline reservoir (vr), egg (eg), and posterior testis (pt). Ventral View.

Figs. 2 Cirrus spines of liolopids. Scale bars at 10um. (**A**) Cirrus spines of *Ngubuvangandu francoisjacobsi* Dutton and Bullard, 2024 (USNM No. XXXXXXX). (**B**) Cirrus spines of *Dracovermis occidentalis* Brooks and Overstreet, 1978 (USNM No. 1718009). (**C**) Cirrus spines of *Harmotrema eugari* Tubangui and Masilungan, 1936 (USNM No. 1357428) (**D)** Cirrus spines of *Harmotrema laticaude* Yamaguti, 1933 (USNM No. 1371864). (**E)** Cirrus spines of *Paraharmotrema karinganiense* Dutton and Bullard, 2022 (USNM No. 1659278).

Fig. 3 Phylogenetic relationships of Liolopidae Odhner, 1912. Reconstructed using a Maximum Likelihood analysis using the large subunit ribosomal DNA (*28S*) gene. New sequence is shown in bold and GenBank accession number, host icons aside taxa.

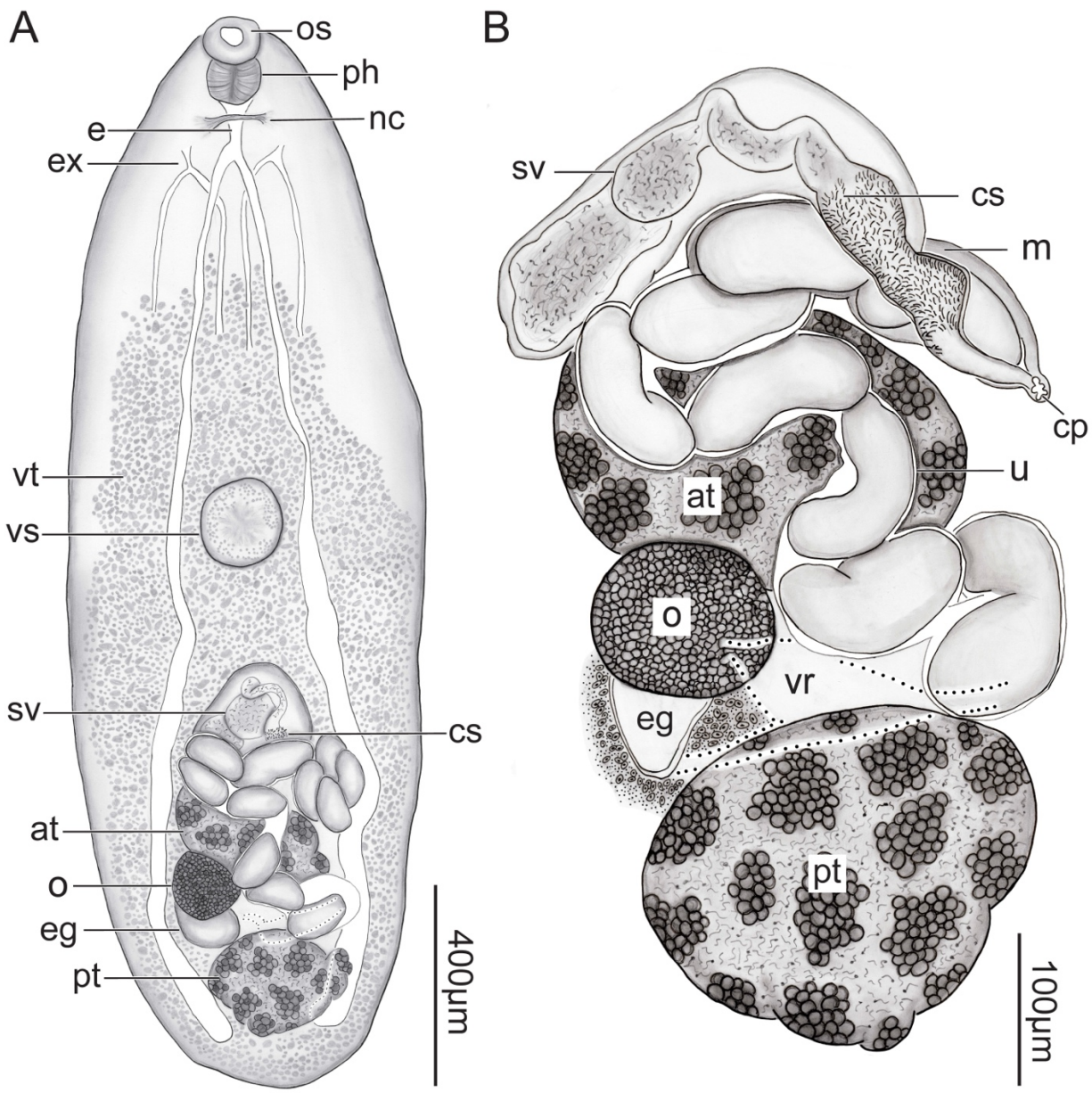
A
os
ph
nc
e
ex
vt
vs
sv
cs
at
o
eg
pt
400µm
B
sv
cs
m
cp
u
at
o
vr
eg
pt
100µm

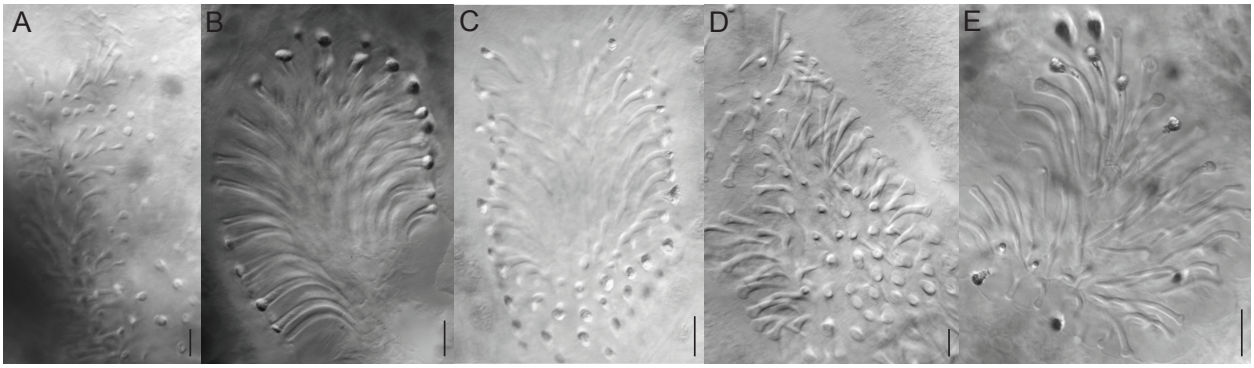
A
B
C
D
E

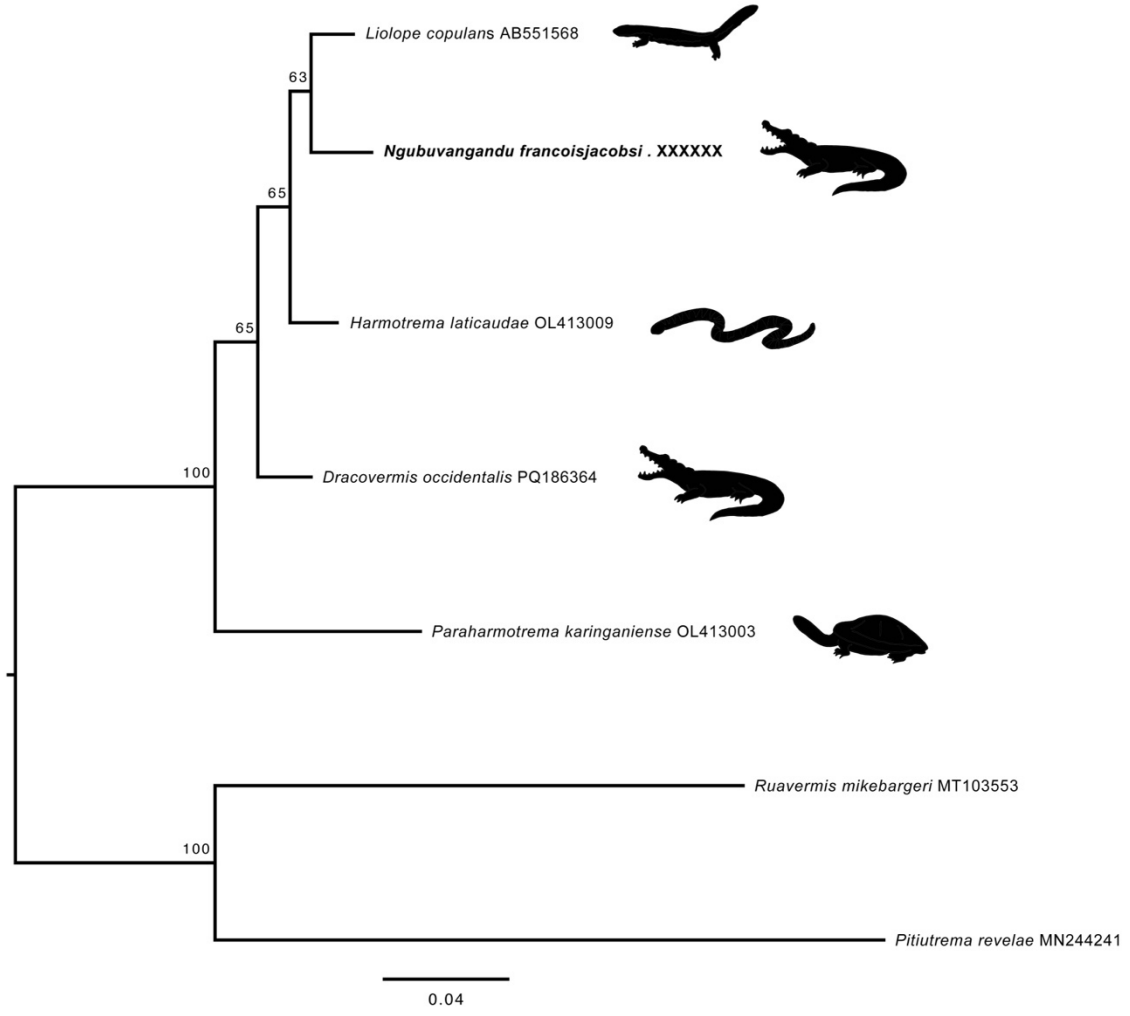
Liolope copulans AB551568
63
Ngubuvangandu francoisjacobsi . XXXXXX
65
Harmotrema laticaudae OL413009
65
100
Dracovermis occidentalis PQ186364
Paraharmotrema karinganiense OL413003
Ruavermis mikebargeri MT103553
100
Pitiutrema revelae MN244241
0.04

CHAPTER 5: FIRST RECORD OF A POLYSTOME (MONOGENOIDEA: POLYSTOMATIDAE) INFECTING A CROCODILIAN: *LATERGATOR LOUISDUPREEZI* N. GEN., N. SP. FROM THE EYE OF AN AMERICAN ALLIGATOR, *ALLIGATOR MISSISSIPPIENSIS* DAUDIN, 1802 (CROCODILIA: ALLIGATORIDAE) IN A NORTH-CENTRAL GULF OF MEXICO SALTMARSH (ROCKEFELLER WILDLIFE REFUGE)

***In Review at the Journal of Parasitology (14 January 2025)**

Authors: Haley R. Dutton and Stephen A. Bullard

ABSTRACT

During July 2021 through June 2024, we necropsied 35 American alligators from Louisiana, Alabama, and South Carolina (including Gulf of Mexico and Atlantic Ocean river basins). The eye of one wild-caught American alligator measuring 1450 mm in total length and captured from saltmarsh habitat within the Rockefeller Wildlife Refuge (Grand Chenier, Louisiana) on 19 July 2021 was infected by *Latergator louisdupreezi* n. gen., n. sp. (Monogenoidea: Polystomatidae). The new species resembles species of Polystomoidinae Yamaguti, 1963 and Oculotrematinae Yamaguti, 1963. It is readily differentiated from species of Polystomoidinae by the combination of having circular haptoral suckers with skeletal elements but that lack hamuli and deep incisions between suckers; ceca having anterior, medial, and lateral diverticula; a compact testis that occupies a small proportion of the intercecal space (vs. a broad testis that spans the intercecal space); a sinistral and intercecal ovary (vs. an ovary that is ventral to the sinistral cecum) having a proximal oviduct extending mediad and then posteriad (vs. proximal oviduct extending anteriad); a uterus that is small (occupying a minute portion of the intercecal space), medial, and located close to the cecal bifurcation; and vaginal pores that open laterally at level of or slightly posterior to the level of the testis. It differs from species of Oculotrematinae by having vaginae and lacking hamuli. No other nominal polystome has this

combination of features, and therefore the erection of a new genus for the new species is wholly warranted. We lack a nucleotide sequence for the new species because we used the only specimen we collected as a heat-killed, formalin-fixed, stained wholemount (holotype) for taxonomic study that prioritized morphology. Without a nucleotide sequence (and phylogenetic analysis) we herein refrain from emending an existing subfamily or proposing a new subfamily to accommodate the new genus. This is the first record of a polystome infecting a crocodilian and the first definitive record of an ectoparasitic polystome infecting a host captured in saltwater.

INTRODUCTION

Numerous surveys and taxonomic studies have documented a phylogenetic diversity of parasites infecting the American alligator, *Alligator mississippiensis* Daudin, 1802 (Crocodilia: Alligatoridae) throughout its endemic range in the Southeastern United States (Hazen et al., 1978; Tellez et al., 2018). Despite these extensive efforts to explore the parasite diversity of this charismatic host, no member of the Polystomatidae has yet been reported from the American alligator. Remarkably, no crocodilian has been reported as a host for this lineage of tetrapod-infecting monogenoids (Du Preez et al., 2023). Herein, we provide the first description of a polystome that infects the eye of a crocodilian (the American alligator).

MATERIALS AND METHODS

During July 2021 through June 2024, we necropsied 35 American alligators from Louisiana, Alabama, and South Carolina. The eye of one wild-caught sub-adult American alligator measuring 1450 mm in total length and captured from saltmarsh habitat of the Rockefeller Wildlife Refuge (Grand Chenier, Louisiana) on 19 July 2021 was infected by the polystomatid described herein. The soft tissue within each eye socket of the infected American alligator was excised as a single mass using hemostats and a scalpel, placed in a petri dish with

ambient freshwater, and examined using a dissecting microscope. We observed this polystomatid specimen alive and attached to the conjunctiva (soft tissue immediately below the eye globe) using a dissecting microscope. No other host species was sampled in our laboratory on that day, and no American alligator necropsied during the aforementioned study period had cohabitated with another aquatic animal. The polystome was removed from the conjunctiva alive using fine forceps and horsehair artist's brushes, placed on a glass slide, gently cover-slipped without pressure, and observed alive with the aid of an Olympus BX51 compound microscope (Olympus, Tokyo, Japan) equipped with differential interference contrast (DIC) optical components. After being observed, the slide with the specimen was exposed to a flame from a hand-held butane lighter for 2 seconds immediately before 10% neutral buffered formalin (n.b.f.) was applied to the slide to fix the heat-killed specimen. The specimen was left overnight in n.b.f. before being rinsed with freshwater, stained in Van Cleave's hematoxylin, dehydrated with a graded EtOH series, made basic at 70% EtOH with lithium carbonate and butyl-amine, dehydrated in absolute EtOH, exposed to a few drops of xylene (to confirm complete dehydration of the specimen before exposure to clove oil), cleared with clove oil, and permanently mounted on a glass slide using Canada balsam. The whole-mount was photographed, examined, and illustrated (Figs. 1–5) with the aid of an Olympus BX51 compound microscope equipped with differential interference contrast (DIC) optical components and a drawing tube. Measurements were obtained with a calibrated ocular micrometer (as straight line distances along the course of each duct) and are reported in micrometers (μm). The holotype was deposited in the National Museum of Natural History’s Invertebrate Zoology Collection (Smithsonian Institution, USNM Collection No. XXXXX). Polystome classification follows Du Preez et al. (2023).

DESCRIPTION

***Latergator* n. gen.**

(Figs. 1–5)

Diagnosis: Body approximately equally tapering anteriorly and posteriorly (not obviously pyriform), becoming confluent with dorsal center of haptor, lacking eyespots in adult. Haptor large (haptor diameter larger than maximum body width), comprising 3 pairs of discoid suckers each bearing skeletal elements, lacking hamuli, lacking deep incisions between suckers; marginal hooklets 16 in number, with handle and blade approximately equal in length, having relatively short guard. Mouth ventral, subterminal, comprising a broad (wider than long) and ovoid opening. False oral sucker present. Esophagus comprising funnel-shaped opening anteriad, narrowing posteriad and coursing through pharynx, emerging from pharynx and extending posteriad a short distance (bucco-esophageal canal present) before connecting to intestinal bifurcation. Pharynx medial, spheroid. Intestine bifurcating a short distance posterior to pharynx, terminating immediately anterior to level of haptor margin in posterior body end, not becoming confluent with corresponding cecum (cyclocoel absent), having diverticulae extending anteriad, laterad, and mediad, lacking anastomoses. Testis single, medial, oblong, intercecal, compact (not spanning intercecal space), pre-equatorial (in anterior half of body), having smooth margins, not diffuse nor reticular. Vas deferens not-convoluted, straight, medial, extending anteriad before becoming confluent with seminal vesicle. Seminal vesicle straight (not-convoluted), relatively thick-walled. Vitellarium follicular, distributing in 2 diffuse fields principally between intestinal ceca and body margin, not extending into haptor or posterior body extremity, lacking pre-equatorial bodies. Ovary sinistral, compact, oblong, wholly intercecal and pretesticular, having smooth margins. Proximal oviduct extending mediad and then posteriad (vs. proximal oviduct extending anteriad). Vaginae paired, having canals forming a bow shape (inverse u-shaped),

arching around testis and away from ovary, thick-walled portion of vaginal duct immediately proximal to pore relatively short; vaginal pores opening laterally (on lateral body margin), nearly post-testicular (at level of posterior margin of testis), slightly muscular. Uterus medial, compact (small; occupying small portion of intercecal space), pre-gonadal (near cecal bifurcation), sacciform (not tubiform), a vase-shaped and relatively thin-walled and weakly muscular (pyriform) duct comprising distal segment of female genitalia. Egg not observed. Genital pore median, immediately postero-ventral to intestinal bifurcation, having a single ring of 10 coronet spines. Egg formation chamber present. Infecting eye of American alligator.

Differential diagnosis: Body lacking eyespots in adult. Haptor having 3 pairs of discoid suckers each bearing skeletal elements, lacking hamuli, lacking deep incisions between suckers. Intestine lacking cyclocoel, having diverticulae extending anteriad, laterad, and mediad. Testis single, compact (not spanning intercecal space), not diffuse or reticulate. Vitellarium not extending into haptor. Ovary wholly intercecal and pretesticular; proximal oviduct extending mediad and then posteriad (vs. proximal oviduct extending anteriad). Vaginal pores opening laterally (on lateral body margin) at level of posterior margin of testis. Uterus medial, occupying small portion of intercecal space, pre-gonadal, sacciform. Coronet spines comprising a single ring of 10 spines.

Taxonomic summary

Type and only nominal species: *Latergator louisdupreezi* n. sp.

ZooBank registration: XXXXXXX-XXXXXXXX-XXXXXXX

Etymology: Given that we searched for years and in many American alligators only to find a single polystome specimen, the genus name "*Latergator*" foretells that, sooner or later, more

American alligators will be examined for polystome infections. Further, the results herein obviously justify examining other crocodilians on other continents for polystome infections.

***Latergator louisdupreezi* n. sp.**

(Figs. 1−5)

Description of adult (measurements and illustrations based on the heat-killed, stained, whole-mounted holotype): Entire monogenoid (body and haptor) measuring 3,250 long; body elongate, 2,650 long, 900 in maximum width at midline, 860 in maximum width at level of vaginal ducts, 3.6× longer than wide (Figs. 1, 2). Haptor 860 long or 32% of body length, 920 wide; haptoral suckers highly contractile and muscular, 280−310 (298 ± 12; 6) in diameter. Hamuli not observed. Haptoral hooklets 16 in number (Fig. 4). Mouth terminal, directed slightly ventral. False oral sucker (no strong muscular component) 210 long (from anterior end of body to start of the pharynx), 460 wide. Pharynx approximately spheroid, 270 long, 270 wide (Figs. 1, 2). Intestine U-shaped, comprising 2 ceca, bifurcating immediately posterior to pharynx or 515 or 16% of body length from anterior body end; ceca 1825 long or 69% of body length, extending posteriad approximately in parallel with respective lateral body margin, terminating 100 or 4% of body length from anterior margin of haptor (Figs. 1, 2). Testis 170 long, 115 wide, having smooth margins, occupying middle 1/3 of body, (anterior margin of testis 960 or 36% of body length from anterior body end) (Figs. 1, 2). Vas deferens medial, extending directly anteriad for 310, 8 wide, dorsal to terminal female genitalia (Figs. 1−3). Seminal vesicle prominent, filled with sperm, markedly laterally expanded proximal to terminal genitalia, 110 long or 4% of body length, 55 wide or 6% of body width (Figs. 1−3). Ovary 175 long, 100 wide, 740 or 28% of body length from anterior body end (Figs. 1−3). Vitellarium indistinct or loosely dispersed throughout space surrounding ceca. Oviduct 100 long, 30 wide (Figs. 1−3). Genito-intestinal canal 250 long,

13 wide, extending antero-mediad from sinistral intestinal cecum to sinistral vaginal duct (Figs. 2). Vaginae with a thick-walled dilated distal portion that connects to vaginal pore (Figs. 1−3), converging medially at level of the oviduct and genito-intestinal canal (870 or 33% of body length from anterior body end); proximal portions of vaginae 475 long or 53% of body width, 15 wide; distal portions of vaginae muscular, thick-walled, perhaps functioning as a sphincter, 88 long, 20 wide (Figs. 1−3); vaginal pores marginal, opening 1,075 or 41% of body length from anterior body end. Oötype surrounded by Mehlis' gland, 38 long, 20 wide. Uterus 213 long, 55 wide, extending anteriad before curving mediad (Figs. 1−3). Egg not observed. Genital bulb 53 long, 50 wide, medial, immediately posterior to or at level of cecal bifurcation, spined (having genital coronet); genital coronet comprising 10 spines, 525 or 20% of body length from anterior body end; coronet spines 7 long, 4 wide at base, hooked (Fig. 5). Excretory vesicles paired, lateral to ceca, pores at level of anterior caeca at cecal bifurcation (Figs. 1, 2).

Taxonomic summary

Type and only known host: *Alligator mississippiensis* (Daudin, 1802) (Crocodilia: Alligatoridae), American alligator.

Site in host: Conjunctiva of eye.

Type locality: Rockefeller Wildlife Refuge (29°43'45.8"N 92°49'07.1"W), Grand Chenier, Louisiana, north-central Gulf of Mexico.

Specimen deposited: Holotype (USNM XXXXX).

Prevalence and intensity of infection: A single (1) American alligator was infected with 1 specimen of *L. louisdupreezi*.

Etymology: The specific epithet "*louisdupreezi*" honors our close friend and mentor Prof. Louis Heyns Du Preez (Northwest University, Potchefstroom, North-West Province,

South Africa) for his unparalleled contributions to polystome taxonomy. Equally, the name is also in gratitude for his unending generosity and enthusiasm for teaching us about the natural history of southern Africa's herpetofauna.

DISCUSSION

The new genus is clearly morphologically distinct from all other accepted polystome genera. Monotypic Concinnocotylinae Pichelin, Whittington, and Pearson, 1991 (type *Concinnocotyla* Pichelin, Whittington, and Pearson, 1991) has hamuli, haptoral sucker type 4 (*sensu* du Preez et al., 2023) and skeletal elements (suckers not circular in outline), an intestine having short 'anterior ceca' and a pair of distinctive bi-laterally symmetrical out pocketings directed laterad, a cyclocoel, and numerous testes. Species of this group infect the gill and buccal cavity of the Australian lungfish, *Neoceratodus forsteri* (Krefft, 1870). The new genus is readily differentiated from this genus by lacking a cyclocoel. Diplorchiinae Yamaguti, 1963 (type *Diplorchis* Ozaki, 1931, *Neodiplorchis* Yamaguti, 1963; *Parapolystoma* Ozaki, 1935; *Pseudodiplorchis* Yamaguti, 1963) has 2 pairs of eyespots in the adult, a pair of testes or multiple testes, and a massive uterus that is sinuous or saccate and that spans the intercecal space. Species of this group infect the urinary bladder of frogs. The new genus differs from these genera by lacking eyespots and having a single testis and a compact, elongate uterus. Eupolystomatinae Yamaguti, 1963 (type *Eupolystoma* Kaw, 1950; *Madapolystoma* Du Preez, Verneau, Raharivololoniaina, and Vences, 2010; and *Kankana* Raharivololoniaina, Verneau, Berthier, Vences, and Du Preez, 2011) has a confluent intestine posteriorly (cyclocoel present) that extends into the haptor, an anterior pair of haptoral suckers separated by the intestinal diverticulum that extends posteriad from the cyclocoel, a follicular testis, a sacciform uterus that extends the full length of the body, non-operculate eggs having a soft membrane and exhibiting

intra-uterine development, and vaginae in the anterior end of the body approximately at level of cecal bifurcation. Species of this group infect the urinary bladder of frogs. The new genus is easily differentiated from these genera by lacking a cyclocoel and having a non-follicular testis, a compact and elongate uterus, and vaginal pores nearly posterior to the testis.

Monotypic Nanopolystomatinae Du Preez, Landman, and Verneau, 2023 (type *Nanopolystoma* Du Preez, Wilkinson, and Huyse, 2008) has hamuli, smooth intestinal ceca (lacking diverticula), a broad testis spanning the intercecal space, a sinistral ovary ventral to the sinistral cecum and immediately medial to the sinistral vaginal pore, a uterus holding a single egg, and vaginal pores that are well anterior to the testis and at level of the ovary. Species of this group infect the urinary bladder and phallodeum of caecilians. The new genus differs from *Nanopolystoma* by having a compact testis not spanning the intercecal space, an intercecal ovary, and vaginal pores that are posterior to or at level of the posterior margin of the testis. Polystomatinae Gamble, 1896 (type *Polystoma* Zeder, 1800; *Indopolystoma* Chaabane, Verneau, and Du Preez, 2019; *Mesopolystoma* Vaucher, 1981; *Metapolystoma* Combes, 1976; *Neoriojatrema* Imkongwapang and Tandon, 2010; *Protopolystoma* Bychowsky, 1857; *Riojatrema* Lamothe-Argumedo, 1963; *Sundapolystoma* Lim and Du Preez, 2001; *Wetapolystoma* Gray, 1993) has haptoral suckers arranged in 2 bilateral rows of 3 suckers each (suckers not arranged in a contiguous/uninterrupted ring), extensively diverticulate ceca (ceca having anastomoses) having long (longer than the ceca width) diverticulae that extend laterad and mediad, a massive uterus, and pre-ovarian vaginal pores. Species of this group infect the urinary bladder of frogs. The new genus is obviously distinct from these genera by having a compact uterus among other features. Monotypic Pseudopolystomatinae Yamaguti, 1963 (type *Pseudopolystoma* Yamaguti, 1963) has extensively diverticulate ceca, an extensively reticulate

(net-like) and extra-cecal testis, and a vitellarium that fills the body space and distributes posteriad into the haptor (separating all 3 pairs of haptoral suckers). Members of this genus infect the urinary bladder of a salamander. The new genus is obviously distinct from *Pseudopolystoma* by lacking a reticulate and extracecal testis. Monotypic Sphyranurinae Price, 1939 (type *Sphyranura* Wright, 1879) has a haptor comprising a pair of suckers, large hamuli, a cyclocoel, and numerous intercecal testes. Members of this genus infect the gill and body surface (about the insertion of the limbs) of salamanders. Sphyranurines are clearly distinct from the new genus by having only 1 pair of haptoral suckers.

Based on the character states established for each of the polystomatid subfamilies by Du Preez et al. (2023), the new genus and species is closely allied with members of both the Polystomoidinae Yamaguti, 1963 and the Oculotrematinae Yamaguti, 1963. Polystomoidinae (type *Polystomoides* Ward, 1917 *sensu* Chaabane et al. 2022; *Apaloneotrema* Du Preez and Verneau, 2020; *Aussietrema* Du Preez and Verneau, 2020; *Fornixtrema* Du Preez and Verneau, 2020; *Manotrema* Du Preez, Domingues, and Verneau, 2022; *Pleurodirotrema* Du Preez, Domingues, and Verneau, 2022; *Polystomoidella* Price, 1939; *Polystomoides* Ward, 1917; *Uropolystomoides* Tinsley and Tinsley, 2016; *Uteropolystomoides* Tinsley, 2017) has smooth ceca (lacking anastomoses and diverticulae), pre-ovarian vaginal pores, and a genital bulb having up to 130 genital spines as well as lacks a uterus (except in *Uteropolystomoides*, which has a sacciform uterus holding up to 20 eggs). Members of this group infect the conjunctival sac, urinary bladder, buccal cavity (oral region), and cloaca of turtles. Monotypic Oculotrematinae (type *Oculotrema* Stunkard, 1924) has smooth ceca that are asymmetrical (cyclocoel absent) and terminate well anterior to the haptor, no hamuli, a broad uterus with up to 62 eggs, an unarmed genital bulb, and no vaginal pores or vaginae evident. This group of polystomes infects the eye

and beneath the eyelids of the common hippopotamus, *Hippopotamus amphibius* Linnaeus, 1758 (Mammalia: Artiodactyla). The new genus resembles the genera assigned to Polystomoidinae by having a haptor with 3 pairs of suckers, lacking hamuli (*Apaloneotrema*, *Aussietrema*, *Fornixtrema*, *Pleurodirotrema* are the only polystomoidine genera that lack hamuli), a compact (elongate or spheroid) uterus located close to the cecal bifurcation and that occupies a minute portion of the intercecal space, and a vitellarium that does not extend posteriad into the haptor as well as by lacking a cyclocoel. Further, the new genus resembles monotypic Oculotrematinae by having 3 pairs of suckers, lacking hamuli, a uterus that is limited to the anterior region of the intercecal space immediately posterior to the cecal bifurcation, and a pre-haptoral vitellarium.

The new genus is readily differentiated from members of Polystomoidinae by the combination of having circular haptoral suckers with skeletal elements but that lack hamuli and deep incisions between suckers; ceca having anterior, medial, and lateral diverticula; a compact testis that occupies a small proportion of the intercecal space (vs. a broad testis that spans the intercecal space); a sinistral and intercecal ovary (vs. an ovary that is ventral to the sinistral cecum) having a proximal oviduct that extends mediad and then posteriad (vs. proximal oviduct directed anteriad); a uterus that is small (occupying a minute portion of the intercecal space), medial, and located close to the cecal bifurcation (egg not observed in the present specimen of the new genus); and vaginal pores that open laterally (on the lateral body margin) at level of or slightly posterior to the level of the testis (post-ovarian). Further, the new genus is readily differentiated from *Oculotrema* by having vaginae and lacking hamuli. No other diagnosed polystome genus has this combination of features, and so the erection of a new genus for the new species is wholly warranted. Because taxa are diagnosed with morphology, the lack of nucleotide data for this taxon is immaterial concerning the justification for the new genus.

Without a nucleotide sequence (and phylogenetic analysis) we herein refrain from emending an existing subfamily or proposing a new subfamily to accommodate the new genus. However, based on its morphological attributes, we predict that nucleotide sequences of the new species will clade near those of polystomes that infect turtles and the common hippopotamus. A phylogenetic affinity between *Oculotrema* and *Latergator* n. gen. would be interesting because of the fact that these species (both assigned to monotypic genera) comprise the only known polystomes that infect non-amphibian, non-turtle hosts. Indeed, it was extremely exciting for us to find a polystome infecting the eye of a crocodilian because no previous study had done so and we were specifically searching for polystomes. Despite searching for several years, we were able to collect only a single specimen of the new species despite our examinations of a relatively large number of American alligators from rivers and coastal habitats associated with both the Gulf of Mexico and Northwestern Atlantic Ocean basins. Because we observed the living polystome attached to the soft ocular tissue (conjunctiva) of the infected American alligator and because no other host had been kept with the infected American alligator, we concluded that the polystome we described had naturally infected (*sensu stricto*) that individual American alligator in the saltmarsh. Yet, from an evolutionary biology perspective, we cannot be certain that this polystome is not more common (higher prevalence) and numerous (higher intensity) on turtles sympatric with American alligators in southern Louisiana. The polystome we describe herein is clearly a new genus, but we cannot comment on its level of host specificity. Using the evidence in-hand, we speculate that, given its morphological similarity to *Oculotrema* (see above), the new species is a parasite of principally crocodilians. Future studies should obtain a nucleotide sequence for this polystome (conduct a phylogenetic analysis) and test its level of host specificity

among turtles and American alligators in southeastern United States saltmarshes in order to confirm that the polystome is an evolutionary partner with the American alligator.

Noteworthy regarding the natural history of polystomes is that the present report is evidently the first definitive record of a polystome being collected from saltwater. American alligators can move across a range of salinities but are abundant in saltmarsh. A polystome infecting the eye of a saltmarsh crocodilian like the American alligator could be an evolutionary link to this polystome lineage crossing over from a freshwater tetrapod into estuarine or marine tetrapods. Only 2 other host species infected by ectoparasitic polystomes (infecting buccal cavity and eye) in some part of their geographic distribution are known to enter saltwater or reside within or frequent estuaries or coastlines. First, Price (1939) reported *Polystomoides coronatus* (Leidy, 1888) Ozaki, 1935 (originally as *"coronatum"*) infecting the "*mouth, nostrils, and (?) urinary bladder*" (page 84 of Price [1939]) from a phylogenetically diverse list of hosts, including one of interest herein, which he reported only as "*terrapin*" (page 84 of Price [1939]). We cannot know what host this was or if the site of infection was internal (urinary bladder) or external (mouth, nostrils), but the only turtle commonly called a 'terrapin' in the United States is the diamondback terrapin, *Malaclemys terrapin* (Schoepff, 1793) (Cryptodira: Emydidae). The diamondback terrapin is an obligate saltmarsh endemic, and it is the only turtle species that ranges exclusively in saltmarsh of the Gulf of Mexico and northwestern Atlantic Ocean (Gibbons et al., 2001). If Price (1939) collected a specimen of *P. coronatus* from the eye of the diamondback terrapin, that report therefore is the first such report of a polystome from a host living in saltwater (an estuary or littoral/ oceanic locality). Unfortunately, we cannot confirm the locality, host species, nor site of infection from Price (1939).

Secondly, the fascinating *Oculotrema hippopotami* Stunkard, 1924 infects the eye of the common hippopotamus in Africa (Stunkard, 1924; Du Preez and Moeng, 2004; Du Preez et al., 2023). In the southeastern Atlantic Ocean off Gabon, common hippopotami are known to enter and remain in the surf zone of high energy beach of oceanic salinity. However, at present, no record of a polystome from a hippopotamus sampled in the ocean exists. Finding such an infection could reverse the assumption that *O. hippopotami* (as a lineage) is a freshwater polystome rather than a marine derived lineage that host-switched to a common hippopotamus. In fact, all host records for polystomes (Du Preez et al., 2023) originate from freshwater despite some of their hosts being associated with marine or estuarine waters. Hence, to our knowledge the present study is the only definitive report of an ectoparasitic polystome infecting a host sampled within a saltmarsh. Another polystome, an endoparasitic species, *Riojatrema cerrocoloradense* (Nasir and Fuenes-Zambrano, 1983) Du Preez, Landman, and Verneau, 2023 (originally as *R. cerrocoloradensis*) infects the urinary bladder of the marine toad, *Rhinella marina* (Linnaeus, 1758) in South America (Nasir and Fuenes-Zambrano, 1983). The infections status of marine toads throughout their inland and coastal range is indeterminate. As indicated by Du Preez et al. (2023), examinations of other coastal, euryhaline, and wholly marine tetrapods (e.g., turtles, crocodilians, mammals) could reveal hitherto innominate polystome taxa.

ACKNOWLEDGMENTS

We thank Ruth Elsey (formerly Rockefeller Wildlife Refuge, Louisiana Department of Wildlife and Fisheries) for helping us obtain permissions to sample American alligators from the Rockefeller National Wildlife Refuge; Brett Warren, Steve Ksepka, Steve Curran, and Kamila Cajiao-Mora (all Aquatic Parasitology Laboratory) for helping necropsy American alligators; and Anna Phillips, Kathryn Ahlfeld, and William Moser (all Department of Invertebrate Zoology, National Museum of Natural History, Smithsonian Institution) for curating our museum specimens. This study was supported by Southeastern Cooperative Fish Parasite and Disease Project (Auburn University), the US Fish and Wildlife Service (Department of Interior), United States Department of Agriculture (National Institute of Food and Agriculture), Federal Aid in Sport Fish Restoration (Alabama Department of Conservation and Natural Resources, Inland and Marine Resources Divisions), and the Alabama Agricultural Experiment Station (Auburn University, College of Agriculture).

LITERATURE CITED

Du Preez, L. H. and I. A. Moeng. 2004. Additional morphological information on *Oculotrema hippopotami* Stunkard 1924 (Monogenea: Polystomatidae) parasitic on the African hippopotamus. African Zoology 39: 225–233.

Du Preez, L. H., W. J. Landman, and O. Verneau. 2023. Polystomatid Flatworms: State of knowledge and future trends. Zoological Monographs Volume 9. Springer. H. Feldhaar and A. Schmidt-Rhaesa (eds). 645 pages.

Gibbons, J. W., J. E. Lovich, A. D. Tucker, N. N. Fitzsimmons, and J. L. Greene. 2001. Demographic and ecological factors affecting conservation and management of the diamondback terrapin (*Malaclemys terrapin*) in South Carolina. Chelonian Conservation and Biology 4: 66–74.

Hazen, T. C., J. M. Aho, T. M. Murphy, G. W. Esch, and G. D. Schmidt. 1978. The parasite fauna of the American alligator (*Alligator mississippiensis*) in South Carolina. Journal of Wildlife Diseases, 14, 435–439.

Nasir, P. and J. L Fuentes Zambrano. 1983. Algunos trematodos monogeneticos venezolanos. Rivista di Parassitologia 44: 335–380.

Price, E.W. 1939. North American monogenetic trematodes. IV. The family Polystomatidae (Polystomatoidea). Proceedings of the Helminthological Society of Washington 6: 80–92.

Stunkard, H. W. 1924. A new trematode, *Oculotrema hippopotami* n. g., n. sp., from the eye of the hippopotamus. Parasitology 16: 436–440.

Tellez, M., and H. Sung. 2018. Unveiling the host-parasite dynamic of alligators and their endoparasites. *In* American Alligators: Habitats, Behaviors, and Threats, S. C. Henke and C. Eversole (eds). Nova Science: New York, NY, USA 175–214.

FIGURE LEGENDS

Figures 1, 2. *Latergator louisdupreezi* n. gen., n. sp. (holotype) from the eye of an American alligator, *Alligator mississippiensis* (Crocodilia: Alligatoridae) from Rockefeller Wildlife Refuge, Louisiana, USA. Scale value aside bars. (**1**) Line drawing of whole body (USNM XXXXX), ventral view. **(2)** Photomicrograph of whole body (USNM XXXXX), ventral view. (Abbreviations: excretory vesicle (ev), false oral sucker (fos), genital bulb (gb), Mehlis' gland (mg), ovary (ov), pharynx (ph), seminal vesicle (sv), testis (t), uterus (ut), vaginae (v)).

Figures 3–5. *Latergator louisdupreezi* n. gen., n. sp. (holotype) from the eye of an American alligator, *Alligator mississippiensis* (Crocodilia: Alligatoridae) from Rockefeller Wildlife Refuge, Louisiana, USA. Scale value aside bars. (**3**) Genitalia (USNM 1625443), ventral view. (**4**) Haptoral hooklet (USNM XXXX), lateral view. (**5**) Genital coronet spines (USNM XXXX), ventral view. (Abbreviations: genital bulb (gb), genital spines (gs), genito-intestinal canal (gc), Mehlis' gland (mg), ovary (ov), oötype (oo), seminal vesicle (sv), testis (t). uterus (ut), vas deferens (vd)).

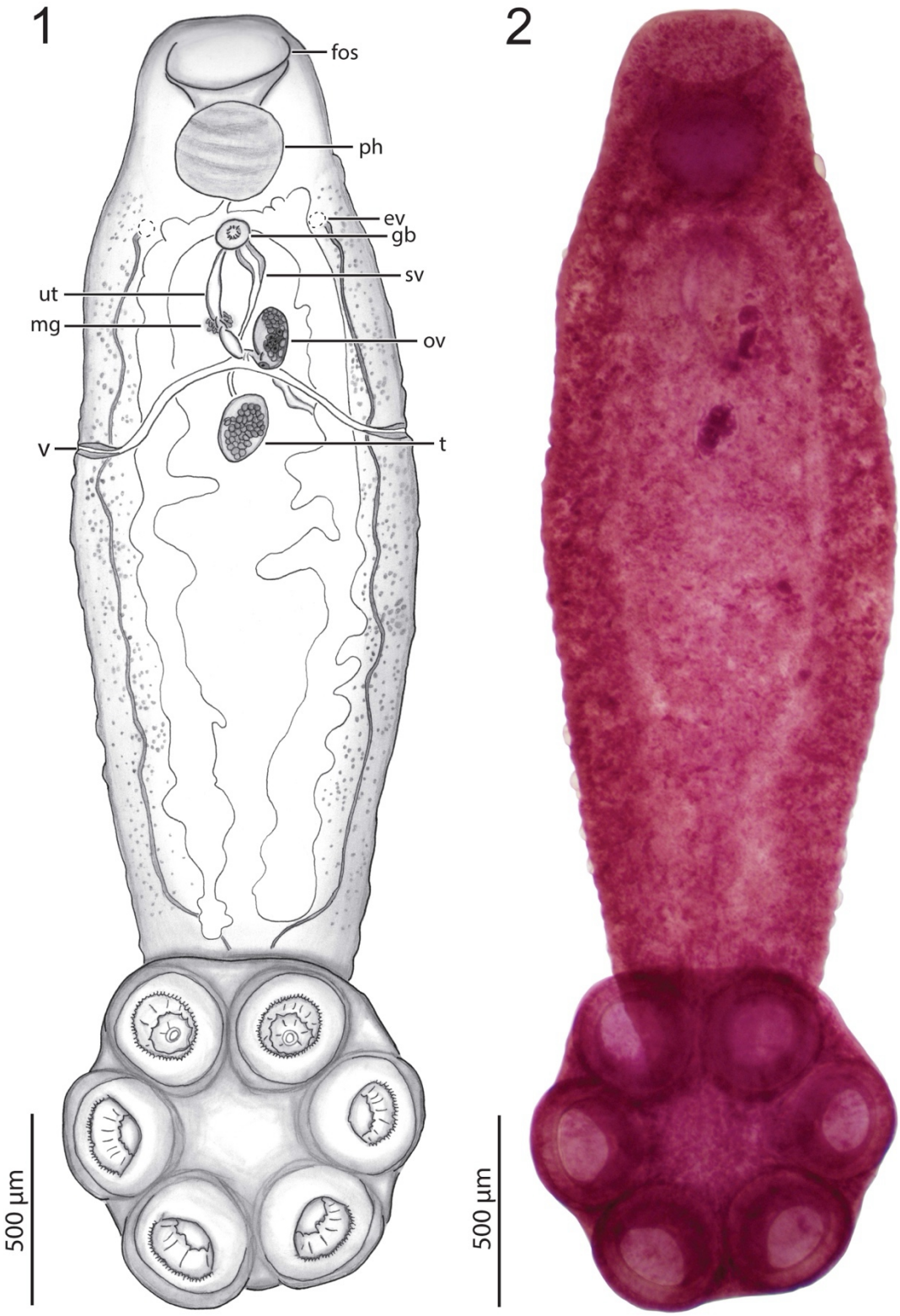
1
fos
ph
ev
gb
sv
ut
mg
ov
v
t
500 µm
2
500 µm

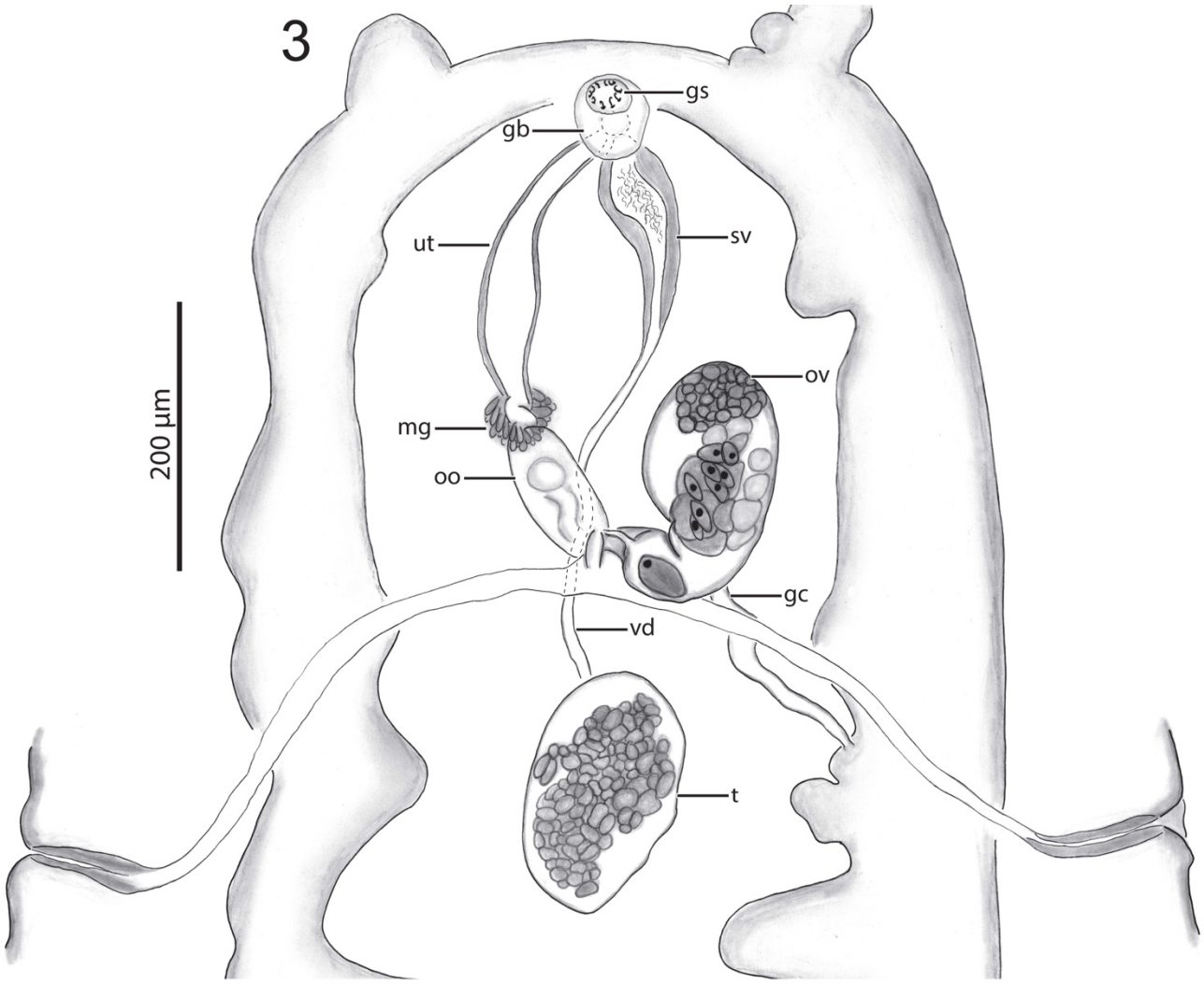
3
gs
gb
ut
sv
ov
mg
oo
gc
vd
t
200 µm

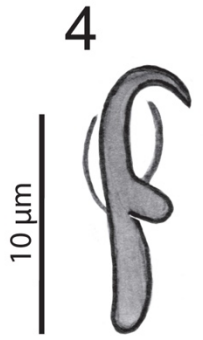
4
10 µm

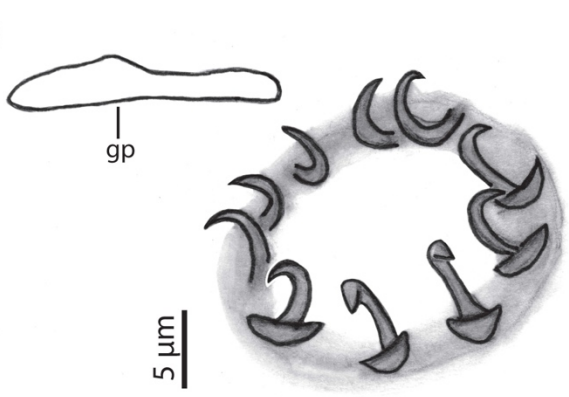
5
gp
5 µm

CHAPTER 6: NEW REDESCRIPTION OF *POLYSTOMA NEARCTICUM* PAUL, 1935 (MONOGENOIDEA: POLYSTOMATIDAE) INFECTING URINARY BLADDER OF COPE'S GRAY TREEFROG, *DRYOPHYTES CHRYSOSCELIS*, FROM AN ALABAMA BEAVER POND AND PHYLOGENETIC ANALYSIS OF *POLYSTOMA* SPP.

***Formatted for the Journal of Parasitology**

Authors: Haley R. Dutton Stephen A. Bullard, Louis H. Du Preez, and Anita M. Kelly

ABSTRACT

We herein redescribe *Polystoma nearcticum* Paul, 1935 (Monogenoidea: Polystomatidae) based on our examination of its holotype (AMNH 281) and vouchers (AMNH 1429.3−1429.5) plus new specimens that we collected from the urinary bladder of several Cope's gray treefrogs, *Dryophytes chrysoscelis* (Anura: Hylidae) that we captured from Old Pal Pond, a beaver pond (32°42'0"N; 85°46'20"W) in Wind Creek, Tallapoosa River (Walnut Hill, Alabama). The only other congener infecting a North American frog is *Polystoma cinereum* Du Preez, Verneau and Gross, 2007 (an objective synonym and replacement name for the already occupied *Polystoma floridana*). We provisionally assigned our specimens to *Polystoma* Zeder, 1800 (type species *Polystoma integerrimum* [Fröhlich, 1791] Rudolphi, 1808), a polyphyletic taxon needing revision, because they have a diverticulate intestine, cyclocoel (intestine confluent posteriorly), 3 pairs of haptoral suckers, a single pair of hamuli, a single diffuse testis, a tubiform uterus with <20 eggs, and a pre-equatorial ovary. We identified our specimens as conspecific with *P. nearcticum* because our specimens matched Paul's original description and were indistinguishable from the holotype and existing vouchers of *P. nearcticum*. Our two new *28S* sequences (1,381 bp and 1,385 bp) of *P. nearcticum* were identical to each other and nearly identical to that of *P. nearcticum* (AM157210; 99.7% similar; 5 bp differences) and *P. cinereum* (AM157211; 99.6% similar; 6 bp differences). The *28S* phylogenetic analysis recovered the

Polystoma spp. of North American treefrogs as monophyletic, and all nominal *Polystoma* spp. infecting frogs of the Americas were recovered in a clade with monotypic *Wetapolystoma* Gray, 1993. The "*Polystoma*" spp. of North American treefrogs was a clearly distinct lineage that was recovered as a crown group (clade) in a clade sister to that of frog polystomatids from Europe and Africa, including the type species *P. integerrimum.* This result indicates that a new genus could be warranted for the North American polystomatids that infect treefrogs and that are currently assigned to *Polystoma.* Our new *CO1* sequence (446 bp) of *P. nearcticum* was similar to that of *P. nearcticum* (AM913865; 97% similar; 11 bp differences) and *P. cinereum* (AM913869; 96.1% similar; 13 bp differences). The *CO1* phylogenetic analysis recovered the sequence identified as *P. integerrimum* (JF699306) as sister to the North American treefrog *Polystoma* spp. This contrasted starkly with the *28S* analysis that recovered that sequence of *P. integerrimum* in relatively unrelated clade. This result suggested that either the *28S* or, more likely based on morphology, the *CO1* sequence for *P. integerrimum* was misidentified and instead was sourced from a specimen of a new species that shares a common ancestor with the polystomatids (*P. nearcticum* and *P. cinereum*) that infect North American treefrogs (Hylidae). This is the first record of a frog polystomatid from Alabama and only the second record of a species of *Polystoma* (or any frog polystomatid) from the Southeastern United States. Our taxonomic and phylogenetic results highlight the need to diagnose morphological differences between the "*P. integerrimum* clade" (which must be regarded as *Polystoma* because it contains the type species) and the "North American treefrog polystomatid clade" recovered in the nucleotide-based analyses (the latter comprising the anticipated new genus).

INTRODUCTION

Species of Polystomatidae Gamble, 1896 (Monogenoidea) comprise endoparasitic and ectoparasitic flatworms that primarily infect the skin, gills, urinary bladder, cloaca, eyes, and oral cavity of amphibians, turtles, the American alligator, *Alligator mississippiensis* Dutton and Bullard, 2025 (Crocodilia: Alligatoridae) (see Dutton and Bullard *in review*), and the Australian lungfish, *Concinnocotyla australensis* (Reichenbach-Klinke, 1966) (Ceratodontiformes: Neoceratodontidae) (Pichelin, 1995; Du Preez et al., 2024**)** . Du Preez et al. (2024) comprises a monograph of the Polystomatidae that provides a synoptical review of the natural history of polystomatids and includes a taxonomic key to the accepted genera (all of which are reviewed and diagnosed in the same work). Based on the information compiled in Du Preez et al. (2024), the highest polystomatid species diversity so far documented is in frogs and toads (Anura). Perhaps related to the fact that they infect tadpoles and adult frogs that depend upon lentic pond habitats, their life cycles are distinctive relative to other monogenoids that infect fishes swimming in still waters or residing in flowing water. Anuran polystomatids produce an egg that hatches a ciliated oncomiracidium that can infect the gill of a tadpole or the urinary bladder of an adult frog. The polystomatid infecting the tadpole is often termed a "neotenic" individual but the term seems a misnomer since, although there is no well-developed genital system, no larval feature is retained in that stage (which can reach up to 5 mm in total length on the gill of a tadpole).

In general, little is known about the polystomatid parasites of North America, and the same is true for those of Central America and South America, where the relatively high anuran endemism and biodiversity alone foretells the presence of many innominate polystomatids (Table 1). Only two frog-infecting species of *Polystoma* Zeder, 1800 (both infecting tree frogs [Hylidae]) have been described from North America: *Polystoma nearcticum* Paul, 1935 and

Polystoma cinereum Du Preez, Verneau and Gross, 2007 (formerly *Polystoma floridana*) (Du Preez et al., 2007). Herein, towards sorting the taxonomy of *Polystoma* spp. and further exploring the diversity of frog polystomatids in the Southeastern United States, we provide a taxonomic redescription of *P. nearcticum* based on a study of the holotype and newly-collected specimens from Cope's gray treefrog, *Dryophytes chrysoscelis* (Cope, 1880) (Anura: Hylidae) in Alabama. We also provide phylogenetic analyses (*28S*, *CO1*) that complement our morphological analyses, report a new host and locality record, and present a synoptical table of records for polystomatids infecting anurans in the Americas.

MATERIALS AND METHODS

During May and June 2022, we collected 6 Cope's gray treefrogs by hand from a beaver pond (32°42'0"N; 85°46'20") in Wind Creek, Tallapoosa River (Walnut Hill, Alabama). Frogs were transported to the laboratory in Tupperware containers with ambient water and screened for the presence of polystomatid eggs in the water. Frogs releasing polystomatid eggs were euthanized by immersion in MS-222 until movement ceased. Each frog was dissected with aid of a stereozoom dissecting microscope in a petri dish with physiological saline solution. Polystomatids in the lumen of the urinary bladder were removed alive using fine forceps and horsehair brushes, heat-killed on a glass slide using a butane hand lighter, fixed in 5% neutral buffered formalin for morphology and others separately preserved in 95% non-denatured ethanol (EtOH) for DNA extraction and sequencing. For morphology a subset of specimens were rinsed with water, stained in Van Cleave's hematoxylin, dehydrated with a graded EtOH series, made basic at 70% EtOH with lithium carbonate and butyl-amine, dehydrated in absolute EtOH and xylene, cleared with clove oil, and permanently mounted on glass slides using Canada balsam. The lithium carbonate and butyl-amine steps that we normally take (Dutton et al., 2021, 2023)

caused the black residue (probably haematin) in the intestine to dissipate thereby making the course of the intestine relatively difficult to follow. For that reason, 4 additional specimens were stained without lithium carbonate and butyl-amine and 2 specimens were cleared, which conserved the haematin and made tracking the intestine easier. Whole mounts were examined and illustrated with the aid of a compound microscope (Olympus BX51 [Olympus, Shinjuku, Tokyo, Japan]) equipped with differential interference contrast (DIC) optical components and a drawing tube. Measurements were obtained with a calibrated ocular micrometer (as straight-lines along the course of each duct) and are reported in micrometers (μm) as the range followed by the mean, +/− standard deviation, and sample size in parentheses. A formalin-fixed specimen intended for scanning electron microscopy (SEM) was rinsed in distilled water, dehydrated in a graded ethanol series, critical point dried in liquid CO2, mounted on an SEM aluminum stub with double-sided carbon tape, sputter coated with gold-palladium (19.32 g/cm3; 25 mA), and viewed with a Zeiss EVO 50VP SEM (Carl-Zeiss, Oberkochen, Germany). Specimens were deposited in the National Museum of Natural History's Invertebrate Zoology Collection (Smithsonian Institution, USNM Collection Nos. XXXXX–XXXXX). Classification and anatomical terms for polystomatids follow Du Preez et al. (2024). Frog identification, scientific and common names follows Guyer and Bailey (2023). Frogs were identified as *D. chrysoscelis* using the key in Guyer and Bailey (2023) by having webbing behind toes to about half way along fourth toe; large toe pads; granular ventral skin; light spot below each eye; light yellow or orange interspaces between dark markings on thigh; and a warty dorsum.

Total genomic DNA was extracted from 2 EtOH-preserved and microscopically-identified polystomatids from the same infected hosts using a Qiagen DNeasy Blood and Tissue Kit (Qiagen, Valencia, California, USA) following the manufacturer's protocol; however, the

proteinase-K incubation period was extended overnight and we used 100 µL of elution buffer to increase the final DNA concentration. Amplification and sequencing of 2 genetic markers were investigated for genetic analysis. Amplification and sequencing of the *28S* and the *COX1* genes used the following primer sets: *28S* (LSU5 [5′-TAGGTCGACCCGCTGAAYTTAAGCA-3′] and 1500R [5′-GCTATCCTGAGGGAAACTTCG-3′] [Littlewood and Olson, 2001], *COX* (COI-ASmit1, [5'-TTTTTTGGGCATCCTGAGGTTTAT-3'] and ASmit2 [5'-TAAAGAAAGAACATAATGAAAATG-3'] (Littlewood et al. 1997).The thermocycling profile for both genes comprised 5 min at 95 C for denaturation, 35 repeating cycles at 95 C for 1 min for denaturation, 45 C for 1 min for annealing, and 72 C for 2 min for extension followed by a final 10 min at 72 C for extension. All PCR reactions were carried out in a ProFlex PCR System (Applied Biosystems, Waltham, MA). PCR products (10 µ1) were verified on a 1% agarose gel and stained with ethidium bromide. PCR products were purified with the QIAquick PCR Purification Kit (Qiagen) according to the manufacturer's protocols except that the last elution step was performed with autoclaved nanopure H2O rather than with the provided buffer. Purified DNA concentration was estimated using a NanoDrop™ One Microvolume UV-Vis Spectrophotometer (Thermo Fisher Scientific Inc., Waltham, Massachusetts). Purified DNA samples were prepared for sequencing with a total volume of 15 ml (2 µl 10 mM primer + purified DNA + purified water) with volumes of purified DNA and water depending on DNA sample concentration. DNA sequencing was conducted by GENEWIZ (Azenta Life Sciences, South Plainfield, New Jersey). All nucleotide sequences were deposited in GenBank (XXXXXX).

The phylogenetic analyses included the sequences from the current study, and the other available polystome sequences on GenBank. Sequence assembly and analysis of chromatograms

were assembled using the multiple alignment tool using fast Fourier transform (MAFFT) component (Katoh and Standley, 2013) in Geneious Prime Software version 2023.0.4 (Geneious Corp., Auckland, New Zealand). Aligned sequences were reformatted and exported from .fasta to .phy to run an maximum likelihood tree (ML). The ML was inferred with IQTREE v.1.16.12 (Nguyen et al., 2015). Substitution model testing was done with ModelFinder (Kalyaanamoorthy et al., 2017) as implemented in IQTREE. After model testing, tree inference was done using best-fitting substitution models (Chernomor et al., 2016). Default tree search parameters were used, except perturbation strength was set to 0.2 and 500 iterations had to be unsuccessful to stop the tree search. Tree inference was performed 20 times with only the tree with the best log-likelihood score reported. Support for relationships was measured with 1000 ultrafast bootstrap replicates (UFBoot) (Hoang et al., 2018). The inferred phylogenetic tree was visualized using FigTree v1.4.4 (Rambaut et al., 2014) and further edited for visualization purposes with Adobe Illustrator (Adobe Systems).

RESULTS

Polystoma nearcticum (Figs. 1−10)

Description of adult (based on 7 heat-killed, stained whole-mounted adult specimens [USNM XXXXXXX–XXXXXXX] and the holotype [AMNH No. 281]. Measurements for the holotype are in brackets following the measurements of our newly-collected specimens): Body, 3,500−6,175 (5,406 ± 1,030; 7) [6,650] long including haptor, 2,775−5,500 (4,233 ± 969; 7) [5,630] long without haptor, 950−2,000 (1,393 ± 357; 7) [1,975] in maximum width, 670−1,200 (932 ± 187; 7) [1,250] wide at level of vaginal ducts, 3.1−4.3× (3.7 ± 0.4; 7) [3.4×] longer than wide (Fig. 1). Haptor, 700−1,075 (864 ± 144; 7) [1,020] long or 16−20% (17% ± 1%; 7) [15%] of body length, 1,075−2,000 (1,396 ± 321; 7) [1,900] wide; haptor length to body length ratio 0.2

(0.2 ± 0; 7) [0.2]; haptoral suckers 280−350 (317 ± 31; 7) [350] in diameter; hamuli having skeletal “hat” on curve of blade, 275−550 (352 ± 90; 7) [355] in total length, 110−150 (129 ± 17; 7) [165] guard length, 140−205 (162 ± 23; 7) [195] handle length, 50−70 (61 ± 7; 7) [65] blade length, 80−90 (87 ± 5; 7) [75] wide from tip of blade; marginal hooklets 23−25 (23 ± 1; 7) [23] in total length, 8−10 (8 ± 1; 7) [not visible in holotype] wide at thumb, 10−13 (12 ± 2; 7) [13] shaft (posterior end to thumb) length, 10−13 (12 ± 1; 7) [8] thumb to tip length; cuticular loops 5−8 (7 ± 2; 5) [13] long, 5 (5 ± 0; 5) [5] wide (Figs. 3, 4, 7). Mouth subterminal, directed slightly ventral. Oral sucker 215−300 (251 ± 34; 7) [300] long, 340−470 (383 ± 44; 7) [440] wide. Pharynx pyriform, 210−300 (236 ± 32; 7) [330] long, 180−250 (219 ± 23; 7) [250] wide (Fig. 1). Intestine bifurcating immediately posterior to pharynx 410−550 (473 ± 57; 7) [590] from anterior body end, 2,830−5,150 (4,195 ± 920; 7) [5,700] long or or 81−89% (83% ± 3%; 7) [86%] of body length, with anterior, lateral and medial diverticula creating a network of anastomoses; caeca confluent posteriorly, extending into haptor but never extending dorsal to suckers (Figs. 1–3).

Testis [not visible in holotype] 880−2,125 (1,404 ± 456; 7) long, 830−1,675 (1,261 ± 336; 7) wide, ventral to cecae, thin follicular network of vas deferens with irregular margins, does not stain well, extends from just posterior to the vitello-vaginal duct occupying the middle third of the body proper 1,280−2,050 (1,649 ± 305; 7) or 37−47% (39% ± 3%; 7) of body length from anterior body end (Figs. 1, 10). Seminal vesicle prominent, filled with sperm, beginning where vas deferens join at anterior end of testis, medial to slightly sinistral, extending anteriad dorsal to terminal female genitalia, 900−1,750 (1,249 ± 283; 7) [1,775] or 26−35% (30% ± 3%; 7) [32] of body length, 40−75 (56 ± 14; 7) [23] wide, making a dextral turn at the level of the ovary, with thickened walls as vesicle narrows closer to the genital bulb (Figs. 1–3).

Ovary 400−700 (576 ± 104; 7) [780] long, 210−400 (307 ± 63; 7) [340] wide, 675−1,375 (1,002 ± 235; 7) [1,300] or 11−20% (14% ± 3%; 7) [14] of body length from anterior body end, some specimens exhibiting enantiomorphism (4 specimens with a sinistral ovary and 3 specimens with a dextral ovary) (Figs. 1–4). Vitellarium distributed throughout the body starting at the level of anterior diverticula around pharynx, ending to level of cyclocoel in haptor. Oviduct extending from ovary to vitello-vaginal duct that descends from both vaginae and joins in middle of body posterior to ovary, 125−240 (188 ± 35; 7) [200] long, 10−30 (23 ± 7; 7) [20] wide (Figs. 1, 8). Genito-intestinal canal 300−675 (446 ± 126; 7) [400] long, 30−50 (41 ± 9; 7) [80] wide, on same side as ovary dorsal to the vitelline duct, joining intestinal cecum to vitello-vaginal duct dorsally 1,125−1,950 (1,531 ± 325; 7) [2,125] or 34−41% (36% ± 2%; 7) [38%] of body length from anterior body end (Figs. 1, 8). Vaginae 2, paired, comprising a distal mound that appears glandular that feeds into a think-walled duct that overlays the vitelline duct ventrally, converging medially at level of the vitelline duct, oviduct and genito-intestinal canal. Vaginal mounds 138−325 (197 ± 64; 7) [375] long, 625−1,150 (841 ± 181; 7) [1,100] or 18−23% (20% ± 1%; 7) [20%] of body length from anterior body end, 40−75 (61 ± 11; 7) [65] wide, 550−1,075 (803 ± 167; 7) [1,400] from anterior margin of testis; vaginal ducts 500−900 (703 ± 158; 7) [975] long, 25−35 (28 ± 4; 7) [25] wide (Figs. 1, 8, 9). Oötype thin walled, beginning after constriction with Mehlis' gland surrounding, 325−550 (432 ± 73; 7) [450] long, 58−125 (100 ± 23; 7) [75] wide. Uterus convoluted, thick walled 1,500−2,900 (2,143 ± 461; 7) [3,425] long, 50−80 (64 ± 13; 7) [65] wide, ventral to seminal vesicle, extending anteriorly until genital atrium in the genital bulb (Figs. 1, 8). Eggs not observed. Genital bulb muscular, 75−95 (84 ± 7; 7) [110] long, 75−100 (89 ± 9; 7) [105] wide, medial, posterior to cecal bifurcation, comprising 8-9 (8 ± 0; 7) [9] spines, 460−710 (594 ± 96; 7) [720] or 12−17% (14% ± 2%; 7)

[13%] of body length from anterior body end; genital spines 25−35 (27 ± 4; 7) [25] long (Figs. 5, 6). Excretory pores dorsal, subterminal, directly anterior to paired vaginal mounds (Figs. 1, 2).

Taxonomic summary

Type host: *Dryophytes versicolor* (LeConte, 1825) (Anura: Hylidae), gray treefrog.

Additional hosts: Table 1

Type locality: Saugatuck River, Weston, Connecticut, U.S.A.

Other localities: Table 1

New locality reported herein: Old Pal Pond, a beaver pond (32°42'0"N; 85°46'20"W) on the private property of HRD and SAB in Wind Creek, Tallapoosa River (Walnut Hill, Alabama).

Specimens examined: Holotype (AMNH 281) and vouchers (AMNH 1429.3−1429.5) of *Polystoma nearcticum* Paul, 1935.

Specimens and sequences deposited: Vouchers (USNM XXXX−XXXXX); GenBank Nos. (XXXXXX−XXXXXX).

Site in host: Luminal wall of urinary bladder.

Prevalence and intensity: 3 of 6 (50%) Cope's gray treefrogs were infected with 4, 4, and 5 specimens of *P*. *nearcticum*, respectively.

Taxonomic remarks

We provisionally assigned our specimens to *Polystoma* Zeder, 1800, a polyphyletic taxon needing revision, because they have a diverticulate intestine, a cyclocoel (intestine confluent posteriorly), 3 pairs of haptoral suckers, a single pair of hamuli, a single diffuse testis, a tubiform uterus with <20 eggs, and a pre-equatorial ovary (Du Preez et al., 2024). We identified our specimens as conspecific with *P. nearcticum* because our specimens matched its original

description by Paul (1935, 1938) and were indistinguishable from the holotype (AMNH 281-1) and existing vouchers (AMNH 1429.3−1429.5). Although not all of the features we describe herein were included in the original description of *P. nearcticum*, we confirmed the presence of these features in all specimens.

As indicated above, we found no evidence that our specimens comprised a new species. However, the quality of our specimens allowed us to clearly visualize and illustrate the testis (Figs. 1, 10). Although the testis is typically easily stained and fairly obvious in monogenoids, polystomatids can be challenging in this regard and many museum specimens simply are not taxonomically useful beyond assigning them to a group of genera. As a result, even a feature as fundamental as testis shape in many species of *Polystoma* is indeterminate and excluded or ambiguous in published descriptions. In our specimens of *P. nearcticum*, the testis is rectangular, well-delineated, and occupies the anterior half of the body space posterior to the terminal genitalia (middle 1/3 of the body proper). The testis in our specimens clearly does not extend posteriad to the level of the haptor. Paul (1938) reported that the testis extended from the 'vitello-vaginal ducts' to the haptor in his general account of *P. nearcticum*. We cannot know if he made that observation based on a live specimen or a stained/unstained specimen (or if that specimen was part of the type series or was the holotype) but suspect he might have presumed and over-generalized its shape based on his observations of the testis of other polystomatids. Because we could not discern the testis in the holotype nor any voucher specimen of *P. nearcticum*, we cannot know (with the specimens in-hand) if testis shape differentiates our specimens from the type series of *P. nearcticum* from Paul (1935). Based on the uncanny morphological similarity of seemingly every other feature present in our specimens and the museum specimens we borrowed, we took a conservative approach and consider our specimens conspecific with those

of Paul (1935). A future worker should collect new specimens of *P. nearcticum sensu stricto* from the type locality and type host, base their description on heat-killed and formalin-fixed specimens that have been well-stained and whole-mounted, obtain high quality (long) sequences for *28S, CO1*, *ITS2*, and *18S*, and deposit specimens and sequences in a museum and GenBank, respectively.

This is the first record of a polystomatid from Alabama and only the second record of a species of *Polystoma* (or any frog polystomatid) from the Southeastern United States.

Phylogenetic results

Our two new *28S* sequences (1,381 bp and 1,385 bp) of *P. nearcticum* were identical to each other and nearly identical to that of *P. nearcticum* (AM157210; 99.7% similar; 5 bp differences) and *P. cinereum* (AM157211; 99.6% similar; 6 bp differences) (Fig. 11). The *28S* phylogenetic analysis recovered the *Polystoma* spp. of North American treefrogs as monophyletic. All nominal *Polystoma* spp. infecting frogs of the Americas (North, Central, and South America) were recovered in the same clade along with *Wetapolystoma almae* Gray, 1993 (Fig. 11). The "*Polystoma*" spp. of North American treefrogs was a clearly distinct lineage that was recovered as a crown group (clade) in a clade sister to that of frog polystomatids from Europe and Africa, including the type species *P. integerrimum.* This result indicates that a new genus could be warranted for the North American polystomatids that infect treefrogs and that are currently assigned to *Polystoma.*

Our new *CO1* sequence (446 bp) of *P. nearcticum* was similar to that of *P. nearcticum* **(**AM913865; 97% similar; 11 bp differences) and *P. cinereum* **(**AM913869; 96.1% similar; 13 bp differences) (Fig. 12). The *CO1* phylogenetic analysis recovered the sequence identified as *P. integerrimum* (JF699306; a nonugen sourced from a polystome collected in France) as sister to

the North American treefrog *Polystoma* spp., contrasting starkly with (contradicting) the *28S* analysis that recovered *P. integerrimum* in a clade that includes European and African frog polystomatids. This result suggested that either the *28S* or, more likely based on morphology, the *CO1* sequence for *P. integerrimum* was misidentified and instead was sourced from a specimen of a new species that shares an immediate common ancestor with the polystomatids (*P. nearcticum* and *P. cinereum*) that infect North American treefrogs.

DISCUSSION

The description above includes important features related to the fine anatomy of the male and female reproductive tracts that could result in likening *P. nearcticum* to *P. cinereum* and differentiating them from all of the other species of *Polystoma* (tantamount to proposing a new genus for *P. nearcticum* and *P. cinereum* and designating *P. nearcticum* as the type species). The urge to do so is strong because they infect related frogs in North America and clearly comprise a distinct lineage (based on *28S* and *CO1*) that is markedly diverged from the other nominal species of *Polystoma*; which is a paraphyletic group with uncertain affinities with species of *Wetapolystoma* Gray, 1993 and *Metapolystoma* Combes, 1976. The named species of *Polystoma* cannot all belong to *Polystoma* without synonymizing the morphologically distinct *Wetapolystoma* and *Metapolystoma*; thereby creating an even larger catch-all genus that does not motivate the discovery of morphological features that can assign the existing species of *Polystoma* to new, morphologically well-diagnosed and monophyletic genera. Yet, despite all of these perspectives and the large amount of genetic divergence between the "*P. nearcticum* and *P. cinereum* clade" and the "*P. integerrimum* clade" (which objectively defines the included taxa as *Polystoma sensu stricto*) (Figs. 11, 12), the lack of high quality museum specimens of *P. integerrimum* blocks further study of the concept of *Polystoma*. Lacking a functional and

phylogenetically real diagnosis for *Polystoma* makes the proposal of a new genus within the group a daunting task. On the other hand, proposing a new genus for *P. nearcticum* and *P. cinereum* facilitates the later sorting out of clearly genetically unrelated polystomatids currently assigned to *Polystoma*. To address these issues, overall, we need better specimens, additional detailed descriptions, and more collections of polystomatids from frogs in North America.

Correspondingly important regarding the systematic revision of *Polystoma* (or any genus), each GenBank sequence deposited should be accompanied by the taxonomic evidence of its identity. Few researchers deposit voucher specimens in museums to accompany the nucleotide sequences they upload to GenBank. This is unfortunate because these workers could be a source for taxonomically-valuable specimens that can address confounded molecular trees using morphology. Yet, molecular taxonomists routinely submit taxonomically-baseless sequences to GenBank; which perhaps causes more confusion than help since many species/sequences are misidentified in GenBank and have led some workers to erroneous phylogenetic conclusions.

Frog polystomes could be a nice model to study host specificity among monogenoids. Historically, monogenoids have been generally regarded as highly host-specific; infecting a single host species or taxonomists historically biasing their decisions based on the host infected (Combes 1966, 1968; Tinsley 1973; Kok & Du Preez, 1987; Du Preez & Kok, 1997; Whittington et al. 1999, 2000). So much so that the early literature on the taxonomy of Monogenoidea would include the identity of the host as justification for the new species. Some authors even would concede that their specimens were morphologically indistinguishable from all named congeners but, because they were collected from a new host, they were described as a new species anyway. Although using the identity of the host to diagnose species or genera (or code cladograms) is

rightly rejected nowadays, the dogma of high host specificity in monogenoids has by-and-large withstood the test of time. Based on our experiences, we agree that monogenoids should be regarded as highly host specific relative to many trematodes, for example. However, detailed taxonomic studies that rely on morphology to diagnose species and that include nucleotide-based phylogenetic evidence as a complementary source of information indicate that sample size is correlated with the likelihood of finding the parasite on additional hosts.

Several monogenoids, in fact, exhibit low host specificity, and good examples can be found within the Gyrodactylidae Cobbold, 1864, Dactylogyridae Bychowsky, 1933, Monocotylidae Taschenberg, 1879, Capsalidae Baird, 1853, and Polystomatidae. *Gyrodactylus cichlidarum* Paperna, 1968 (Gyrodactylidae) infects Nile tilapia, *Oreochromis niloticus*, (Linnaeus, 1758) (Cichliformes: Cichlidae) but also infects guppies (Poeciliidae) and other livebearers (Brule et. al, 2024). *Cichlidogyrus sclerosus* Paperna and Thurston, 1969 (Dactylogyridae) primarily infects African cichlids (Cichlidae) but has likely been co-introduced with its tilapia hosts due to aquaculture production and the aquarium trade (Brule et. al, 2025) and has spilled over into native fish communities. *Cathariotrema selachii* (MacCallum, 1916) Johnston and Tiegs, 1922 (Monocotylidae) exhibits low host specificity to littoral and offshore whaler sharks (Carcharhinidae) and epipelagic mackerel sharks (Lamnidae) (Bullard et al., 2019). *Empruthotrema dasyatidis* Whittington and Kearn, 1992 (Monocotylidae) infects 10 species of sharks and rays across four orders (Bullard et al., 2021). *Neobenedenia melleni* (MacCallum, 1927) (Capsalidae) infects dozens of fish species across most major actinopterygian lineages (Bullard et al. 2000, Bullard et al., 2021). Among polystomatids, North American species are thought to be generally host-specific to their freshwater turtle hosts. However, *Polystomoides orbicularis* (Stunkard, 1916) (formerly *Neopolystoma orbiculare*)

infects 12 turtle species of 6 genera and 4 families (Verneau et al., 2011; Dutton et al., 2021; Du Preez et al., 2024). Verneau et al. (2011) reported that turtle polystomatids exhibit reduced host specificity in confinement. This was also documented by MacCallum (1918), who reported *N. orbiculare* infecting 2 species of turtles assigned to 2 genera at the New York Aquarium (Dutton et al., 2021; Du Preez et al., 2024). Regarding our results herein, the morphological and nucleotide differences between *P. nearcticum* and *P. cinereum* indicate very little evolutionary change between these taxa, and if one considers the *CO1* data to comprise intraspecific variation (what else could it be if the specimens are morphologically identical?), there would be a good justification to synonymize them. If that occurred, there would be a single species of *Polystoma*, *P. nearcticum,* infecting frogs in North America. Already, *P. nearcticum* has been reported from 7 species of frogs in 3 genera and 2 families (tree frogs [Hylidae]; American spadefoot toads [Scaphiopodidae]). Interestingly, *Polystoma nearcticum* and *P. cinereum* have both been reported from the urinary bladder of the North American green treefrog, *Dryophytes cinereus* (Schneider, 1799) (Hylidae) (Table 1). Hence, taken together, the polystomatids promise to be a good system with which to further tests notions of host specificity within the Monogenoidea.

The notion of exploring the evolution of polystomatid lineages and life cycles in response to the life history and habitat of the frogs they infect is exciting to us. We think that the sort of ephemeral aquatic habitats that harbor some frogs and polystomatids could provide a unique insight on their life cycles. Ponds created by the construction of dams by North American beavers, *Castor canadensis* Linneaus, 1758 (Rodentia: Castoridae) are common throughout Wind Creek and other low-order streams of the Tallapoosa River. They impound streams and create lentic aquatic systems ("beaver ponds") comprising good habitat for frogs, tadpoles, and evidently the polystomatids that infect them. In the present study, we collected the infected frogs

from Old Pal Pond, which no longer exists because the North American beavers maintaining its dam have left the area and moved to an adjacent creek. Since collecting the infected frogs, we observed Old Pal Pond transition from a 3 acre pond with at least 16 frog species (HRD, SAB, LHD personal observations) to a dry, lowland area (with no frog calling day or night) adjacent to a flowing stream. We assume that the frogs and polystomatids have been extirpated from that immediate area because we cannot hear frogs calling at any time of day there now; however, other beaver ponds in nearby low order streams have not been surveyed and will likely harbor infected frogs. Colonization of a new pond by a polystomatid would seemingly depend on immigration of infected frogs. We wonder if other mechanisms might also contribute to dispersal and survival of polystomatids that infect frogs in ephemeral habitats, e.g., frogs eaten by birds and whose polystomatid eggs are shed in the feces of the bird. Regardless, we think that a lot needs to be learned about the lives of polystomatids in lentic ephemeral freshwater habitats of Alabama.

As a general comment concerning a current trend in flatworm taxonomy, we noticed that *CO1* sequences are being used to differentiate morphologically-indistinguishable specimens and name new species. In some instances, the morphologically identical specimens are also identical (100% similarity) to each other in the *28S*. So, workers are naming new species based on a unique *CO1* sequence despite the fact that another widely used and phylogenetically informative gene (*28S*) is identical and there is no discernible morphological difference between the sets of specimens. We cannot accept this as reasonable, adequate justification for a species. It does not make sense biologically and forces the *CO1* taxonomist to simply accept at face value that each and every unique *CO1* sequence must, by definition, represent a new species. This is leading to a sort of superficial taxonomy where morphological differences are secondary to *CO1* sequences,

despite example after example of morphologically identical specimens being named according to each unique sequence. Oftentimes these studies define the morphologically identical set of species as a group of "cryptic species" as defined by their *CO1* diversity.

Based on our experiences with flatworm morphology and phylogenetics, we regard the *CO1* as hypervariable and do not think it should be used as a taxonomic barcode without first diagnosing the new taxon using taxonomically-significant morphological features. All flatworms exhibit some level of intraspecific morphological variability. The species diagnosis defines the limits of that intraspecific morphological variation (which necessitates having well-stained, whole-mounted, heat-killed, formalin-fixed specimens), i.e., the species was diagnosed by using a set of discerned, discrete, conserved morphological features. Further, we think it is a methodological fact that, in this day and age, that sequencing a gene (or a genome) and producing a phylogenetic analysis is, quite frankly, vastly less costly and methodologically easier than obtaining the funding, permits, personnel, equipment, and expertise to separate live parasites (intact) from rare and elusive hosts before spending hours in a remote area in challenging physical (sometimes dangerous) conditions dissecting the host, micro-manipulating the parasite specimens in the few hosts that are infected (if any are infected at all), heat-killing them, fixing them, transporting them across borders, staining them, mounting them, and then finally beginning a proper taxonomic study of them; which can take months or years (and even then you might not have enough good material for morphology).

ACKNOWLEDGMENTS

We thank John Brule, Kamila Cajiao-Mora (both Aquatic Parasitology Laboratory) for SEM assistance, Ed Netherlands (Department of Zoology and Entomology, University of the Free State) for helping collect frogs; Anna Phillips, Kathryn Ahlfeld, and William Moser (all Department of Invertebrate Zoology, National Museum of Natural History, Smithsonian Institution) for curating our museum specimens; and Estefania Rodriguez and Lily Berniker (American Museum of Natural History) for sending the holotype and vouchers of *P. nearcticum*. This study was supported by the Southeastern Cooperative Fish Parasite and Disease Project (Alabama Department of Conservation and Natural Resources), United States Fish and Wildlife Service, and the Alabama Agriculture Experiment Station.

LITERATURE CITED

Bolek, M. G., and Coggins, J. R. 1998. Endoparasites of Cope's gray treefrog, *Hyla chrysoscelis*, and western chorus frog, *Pseudacris t. triseriata*, from southeastern Wisconsin. Journal-Helminthological Society Washington, 65, 212–218.

Brule, J. H., Warren, M. B., Dutton, H. R., Truong, T. N., Ksepka, S. P., Curran, S. S., Shurba J. A., Lawson L. L., and Bullard, S. A. 2024. First taxonomic description of a gyrodactylid, *Gyrodactylus cichlidarum* Paperna, 1968 (Monogenoidea) infecting Nile tilapia, *Oreochromis niloticus* (Linnaeus, 1758)(Cichlidae) in the United States. BioInvasions Record 13: 1.

Brule, J. H., Warren, M. B., and Bullard, S. A. 2025. First report of a dactylogyrid, *Cichlidogyrus sclerosus* Paperna & Thurston, 1969 (Monogenoidea) infecting Nile tilapia, *Oreochromis niloticus* (Linnaeus, 1758)(Cichliformes: Cichlidae) in the United States, with a review of host and locality records in its invasive range and a phylogenetic analysis. Journal of Helminthology 99: e17.

Bullard, S. A., Benz, G. W., Overstreet, R. M., Williams Jr, E. H., and Hemdal, J. 2000. Six new host records and an updated list of wild hosts for *Neobenedenia melleni* (MacCallum) (Monogenoidea: Capsalidae). Faculty Publications from the Harold W. Manter Laboratory of Parasitology 407.

Bullard, S. A., Warren, M. B., and Dutton, H. R. 2021. Redescription of *Cathariotrema selachii* (MacCallum, 1916) Johnston and Tiegs, 1922 (Monogenoidea: Monocotylidae), emendation of monotypic *Cathariotrema* Johnston and Tiegs, 1922, and proposal of Cathariotrematinae n. subfam. based on morphological and nucleotide evidence. The Journal of Parasitology 107: 481–513.

Caballero, C., Zerecero, E.C. 1941. Una nueva especie de Polystoma (Trematoda: Polystomatidae) parasito de la vejiga urinaria de *Hyla baudinii* (Dum. y Bibr.). Anales del Instituto de Biología, Universidad Nacional Autónoma de México, 12, 615–621.

Campbell, R.A. 1967. A comparative study of the parasites of certain Salientia from Pocahontas state park, Virginia. Virginia Journal of Science 19: 13–20.

Campbell, R.A. 1969. An unusual infection of *Polystoma nearcticum* (Paul, 1938). Virginia Journal of Science 20: 174–175.

Chernomor, O., Von Haeseler A., and Minh B.Q. 2016. Terrace aware data structure for phylogenomic inference from supermatrices. Systematic Biology 65: 997–1008.

Combes, C. 1966. Recherches expérimentales sur la spécificité parasitaire des polystomes de *Rana temporaria* et *de Pelobates cultripes* (Cuv.). Bulletin de la Société Zoologique de France 91: 439–444.

Combes, C. 1968. Biologie, écologie des cycles et biogéographie de digènes et monogènes d'amphibiens dans l'est des Pyrénées. Mémoires du Muséum National d'Histoire Naturelle, Série A Zoologie, Fascicule unique 51: 1–195.

Combes, C., Laurent, R.F. 1978. Deux nouveaux Polystomatidae (Monogenea) de l'Argentine. Acta Zoologica Lilloana 33: 85–92.

Combes, C., Laurent, R.F. 1979. Les monogènes Polystomatidae de République Argentine: description de deux nouvelles espèces et essai de synthese. Revista Iberica de Parasitologia 79: 545–557.

Du Preez, L.H. and Kok, D.J. 1997. Supporting evidence of host-specificity among southern African polystomes (Polystomatidae:Monogenoidea). Parasitology Research 83: 558–562.

Du Preez, L. H., Verneau, O., and Gross, T. S. 2007. *Polystoma floridana* n. sp. (Monogenoidea: Polystomatidae) a parasite in the green tree frog, *Hyla cinerea* (Schneider), of North America. Zootaxa 1663: 33–45.

Du Preez, L.H., Domingues, M.V. 2019. *Polystoma knoffi* n. sp. and *Polystoma travassosi* n. sp. (Monogenea: Polystomatidae): naming museum-archived specimens from Brazil. Systematic Parasitology 96: 755–765.

Du Preez, L. H., Landman, W. J., and Verneau, O. 2024. Overview of the Polystomatidae: Systematics and Classification. In Polystomatid Flatworms: State of Knowledge and Future Trends (pp. 1–28). Cham, Switzerland: Springer International Publishing.

Dutton, H. R., Du Preez, L. H., Verneau, O., Whelan, N. V., & Bullard, S. A. 2021. First record of a polystome from alligator snapping turtle, *Macrochelys temminckii* (Cryptodira: Chelydridae) or Mississippi; with comments on "*Neopolystoma orbiculare* (Stunkard, 1916)" and its junior subjective synonyms. Journal of Parasitology, 107: 74–88.

Dutton, H. R., Bullard, S. A., & Kelly, A. M. 2023. New genus and species of Cyclocoelidae Stossich, 1902 (Platyhelminthes: Digenea) infecting the nasopharyngeal cavity of Canada goose, *Branta canadensis* (Anseriformes: Anatidae) from Western Alabama. Journal of Parasitology 109: 349–356.

Dutton, H.R., and Bullard, S.A. (*in review*) First record of a polystome (Monogenoidea: Polystomatidae) infecting a Crocodilian: *Latergator louisdupreezi* n. gen., n. sp. from the eye of an American Alligator, *Alligator mississippiensis* Daudin, 1802 (Crocodilia: Alligatoridae) in a North-Central Gulf Of Mexico saltmarsh (Rockefeller Wildlife Refuge). Journal of Parasitology.

Dyer, W.G. 1985. *Riojatrema ecuadorensis* n. sp. (Trematoda: Polystomatidae) from the urinary bladder of *Bufo typhonius* (Linnaeus, 1758). Journal of Parasitology 71: 215–217.

Goldberg, S. R., & Bursey, C. R. 2002. Helminths of the plains spadefoot, *Spea bombifrons*, the western spadefoot, *Spea hammondii*, and the Great Basin spadefoot, *Spea intermontana* (Pelobatidae). Western North American Naturalist, 62: 491–495.

Gray, M.E. 1993. *Wetapolystoma almae* n. gen., n. sp. (Monogenea: Polystomatidae) parasite of *Bufo typhonius* (Linnaeus, 1758) (Amphibia: Bufonidae) from Tropical Peru. Transactions of the Kansas Academy of Science (1903) 96: 181–185.

Guyer, C. and Bailey, M. A. 2023. Frogs and toads of Alabama. Tuscaloosa, Alabama: University of Alabama Press.

Hoang D.T., Chernomor O., Von Haeseler A., Minh B.Q., and Vinh L.S. 2018. UFBoot2: improving the ultrafast bootstrap approximation. Molecular Biology and Evolution 35: 518–522.

Kalyaanamoorthy S., Minh B.Q., Wong T.K., Von Haeseler A., Jermiin L.S. 2017. ModelFinder: fast model selection for accurate phylogenetic estimates, Nature Methods 14: 587–589.

Katoh, K. and Standley, D. M. 2013. MAFFT multiple sequence alignment software version 7: improvements in performance and usability. Molecular Biology and Evolution 30: 772–780.

Kohn, A., Combes, C., Gomes, D.C. 1978. Représentants du genre Polystoma Zeder (Monogenea) au Brésil. Bulletin du Muséum National d'Histoire naturelle 353: 227–229.

Kok, D.J. and Du Preez, L.H. 1987. *Polystoma australis* (Monogenoidea): Life cycle studies in experimental and natural infections of normal and substitute hosts. Journal of Zoology (London) 212: 235–243.

Lamothe-Argumedo, R. 1963. Trematodos de los Anfibios de Mexico. I. Sobre un nuevo genero de la familia Polystomatidae Gamble, 1896 hallado en la vejica urinaria de *Tomadactylus amulae* Günther y *Bufo simus* Schmidt. Revista de la Sociedad Mexicana de Historia Natural 24:73–88.

Lamothe-Argumedo, R. 1973. Monogéneos de los anfibios de Mexico IV. Redescripcion de *Neodiplorchis scaphiopi* (Rodgers, 1941) Yamaguti 1963. Anales Instituto de Biologia, Universidad Nacional Autonoma de Mexico, Serie Zoologia 44: 1–7.

Lamothe-Argumedo, R. 1976. Monogéneos de los anfibios de Mexico VI. Redescripcion de *Polystoma naevius* Caballero y Cerecero, 1941. Anales Instituto de Biologia, Universidad Nacional Autonoma de Mexico, Serie Zoologia 47: 1–8.

Lamothe-Argumedo, R. 1985. Monogéneos de los anfibios de México VII. Hallazgo de *Pseudodiplorchis americanus* (Rodgers y Kuntz, 1940) Yamaguti, 1963 en baja California sur, México. Anales Instituto de Biologia, Universidad Nacional Autonoma de Mexico, Serie Zoologia 56: 291–300.

Littlewood, D. T. J., Rohde, K., & Clough, K. A. 1997. Parasite speciation within or between host species?—Phylogenetic evidence from site-specific polystome Monogenoideans. International Journal for Parasitology 27: 1289–1297.

Littlewood D.T.J. and Olson P.D. 2001. Small subunit rDNA and the Platyhelminthes: signal, noise, conflict and compromise. In Interrelationships of the Platyhelminthes (pp 262–278). Boca Raton, Florida: CRC Press.

MacCallum, G. A. 1918. Studies on the Polystomatidae. Zoopathologica 1: 105–120.

Muzzall, P. M., & Kuczynski, M. C. 2017. Helminths of the eastern gray treefrog, *Hyla versicolor* (Hylidae), from a pond in southwestern lower Michigan, USA. Comparative Parasitology, 84: 55–59.

Nasir, P., Fuentes-Zambrano, J.L. 1983. Algunos trematodos monogeneticos venezolanos. Rivista di Parassitologia 44: 335–380.

Nguyen L.T., Schmidt H.A., Von Haeseler A., Minh B.Q. 2015. IQ-TREE: a fast and effective stochastic algorithm for estimating maximum-likelihood phylogenies, Molecular Biology and Evolution 32: 268–274.

Paul, A.A. 1935. *Polystoma integerrimum nearcticum* n. subsp. From the urinary bladder, genital ducts, kidneys and gills of *Hyla versicolor* Le Conte. Journal of Parasitology 21: 442.

Paul, A. A. 1938. Life history studies of North American freshwater polystomes. Journal of Parasitology 24: 489–510

Pérez-Vigueras, I. 1955. Contribucion al conocimiento de la fauna helmintologica cubana. Memorias de la Sociedad Cubana de Historia Natural 22:21–71.

Pichelin, S. 1995. The taxonomy and biology of the Polystomatidae (Monogenea) in Australian freshwater turtles (Chelidae, Pleurodira). Journal of Natural History 29: 1345–1381.

Rambaut, A., M. A. Suchard, D. Xie, and A. J. Drummond. 2014. FigTree v1.4.3. Available from: http://tree.bio.ed.ac.uk/software/figtree. Accessed 25 November 2018.

Riley, W.A. 1927. Introduction to the study of animal parasites and parasitism. Ann Arbor, Michigan: Edward Bros.

Rodgers, L.O., Kuntz, R.E. 1940. A new polystomatid monogenean fluke from a spadefoot. Wasman Collector 4: 37–40.

Rodgers, L.O. 1941. *Diplorchis scaphiopi*, a new polystomatid monogenean fluke from the spadefoot toad. Journal of Parasitology 27:153–157.

Sales, A.N., Du Preez, L.H., Verneau, O., Domingues, M.V. 2023 Morphology and molecular characterization of *Polystoma goeldii* n. sp. (Monogenea, Polystomatidae) parasite from the

urinary bladder of *Physalaemus ephippifer* (Steindachner) (Anura, Leptodactylidae). Parasitology International 92: 102685. https://doi.org/10.1016/j.parint.2022.102685

Santos, V.G.T., Amato, S.B. 2012 *Polystoma cuvieri* (Monogenea: Polystomatidae) in *Physalaemus cuvieri* (Anura, Leiuperidae) in Southern Brazil. Neotropical Helminthology 6: 1–7.

Stunkard, H.W. 1959. Induced gametogenesis in a monogenetic trematode, *Polystoma stellai* Vigueras, 1955. Journal of Parasitology 45: 389–394.

Tinsley, R.C. 1973. Observations on Polystomatidae (Monogenoidea) from East Africa with a description of *Polystoma makereri* n. sp. Zeitschrift für Parasitenkunde 42: 251–263.

Tinsley, R.C., Earle, C. 1983. Invasion of vertebrate lungs by the polystomatids *monogeneans Pseudodiplorchis americanus* and *Neodiplorchis scaphiopodis*. Parasitology 86: 501–517.

Vaira, M. 2004. Population morphological variation of the monogenean *Polystoma andinum*, parasitic in *Melanophryniscus rubriventris* (Anura, Bufonidae). Acta Parasitologica 49: 281–291.

Vaucher, C. 1981. *Mesopolystoma samiriensis* n.gen, n. sp. (Monogenea: Polystomatidae): parasite de *Osteocephalus taurinus* Steindachner (Amphibia: Hylidae) en Amazonie péruvienne. Revue suisse de zoologie 88: 797–802.

Vaucher, C. 1983. Helminthes parasites du Paraguay V: *Polystoma lopezromani* Combes et Laurent, 1979 et utilisation d'une technique inédite d'observation des hamuli chez les Polystomatidae (Monogenea). Bulletin de la Société des sciences naturelles de Neuchâtel 106: 101–107.

Vaucher, C. 1986. Helminthes parasites du Paraguay XIII: *Polystoma diptychi* n. sp. (Monogenea: Polystomatidae), parasite de *Bufo diptychus* Cope (Amphibia: Bufonidae). Bulletin de la Société des sciences naturelles de Neuchâtel 109: 5–10.

Vaucher, C. 1987. Polystomes d'Equateur, avec description de deux nouvelles espèces. Bulletin de la Société des sciences naturelles de Neuchâtel 110: 45–56.

Vaucher, C. 1990. *Polystoma cuvieri* n. sp. (Monogenea: Polystomatidae), a parasite of the urinary bladder of the leptodactylid frog *Physalaemus cuvieri* in Paraguay. Journal of Parasitology 76: 505–504.

Verneau, O., Palacios, C., Platt, T., Alday, M., Billard, E., Allienne, J.F., Basso, C., and Du Preez, L. H. 2011. Invasive species threat: parasite phylogenetics reveals patterns and processes of host-switching between non-native and native captive freshwater turtles. Parasitology 138: 1778–1792.

Whittington, I. D., Chisholm, L. A., and Rohde, K. 1999. The larvae of Monogenoidea (Platyhelminthes). Advances in Parasitology 44: 139–232.

Whittington, I. D., Cribb, B. W., Hamwood, T. E., & Halliday, J. A. 2000. Host-specificity of Monogenoidean (platyhelminth) parasites: a role for anterior adhesive areas? International Journal for Parasitology 30: 305–320.

Table 1 Anuran polystomes in the Americas genera, species, hosts, and localities

Genus	Host	Locality	Reference
Mesopolystoma samiriense Vaucher, 1981	*Osteocephalus taurinus* Steindachner, 1862 (Anura:Hylidae); Manaus Slender-Legged Treefrog	Pithecia Research Station, Rio Samiria, Peru	Vaucher, 1981; Vaucher, 1987
Neodiplorchis scaphiopodis (Rodgers, 1941)	*Spea bombifrons* (Cope, 1863) (Anura: Scaphiopodidae), Plains Spadefoot	Stillwater, Oklahoma; Arizona, USA	Rodgers, 1941; Tinsley and Earle, 1983
	Spea multiplicata (Cope, 1863) (Anura: Scaphiopodidae), New Mexico Spadefoot	Capulhuac, México, Arizona, USA	Lamothe-Argumedo, 1973; Tinsley and Earle, 1983
Polystoma andinum Combes and Laurent, 1978	*Melanophryniscus rubriventris* (Vellard, 1947) (Anura:Bufonidae), Yungas Redbelly Toad	Calilegua, Argentina	Combes and Laurent, 1978; Vaira, 2004
P. borellii Combes and Laurent, 1974	*Pleurodema borellii* (Peracca, 1895) (Anura: Leptodactylidae), Rufous Four-Eyed Frog	Tucumán, Argentina	Combes and Laurent, 1978
P. cinereum (DuPreez, Verneau & Gross, 2007)	*Dryophytes cinereus* (Schneider, 1799) (Anura: Hylidae), North American Green Treefrog	Gainesville, Florida, USA	DuPreez, Verneau and Gross, 2007; Du Preez, Landman and Verneau, 2023
P. cuvieri Vaucher, 1990	*Physalaemus cuvieri* Fitzinger, 1826 (Anura: Leptodactylidae), Cuvier's Foam Froglet	San Carlos, Paraguay; State of Santa Catarina and Rio Grande do Sul, Brazil	Vaucher, 1990; Santos and Amato, 2012
P. diptychi Vaucher, 1986	*Rhinella diptycha* (Cope, 1862) (Anura:Bufonidae), Cope's Toad	Rio Alto Parana, Puerto Presidente Stroessner, Paraguay	Vaucher, 1986
P. goeldii Sales, Du Preez, Verneau and Domingues, 2023	*Physalaemus ephippifer* (Steindachner, 1864) (Anura: Leptodactylidae), Steindachner's Dwarf Frog	Ramal do Maneta, Itabocal Village, municipality of Irituia, Pará, Brazil	Sales, Du Preez, Verneau, and Domingues , 2023
P. guevarai Combes and Laurent, 1979	*Boana pulchella* (Duméril and Bibron, 1841) (Anura: Hylidae), Montevideo Treefrog	Argentina	Combes and Laurent, 1979
P. knoffi Du Preez and Domingues, 2019	*Trachycephalus nigromaculatus* Tschudi, 1838 (Anura: Hylidae), Black-spotted Casque-headed Treefrog	Jacarepagua, Rio de Janeiro, Brazil	Du Preez and Domingues, 2019; Kohn et al., 1978
P. lopezromani Combes and Laurent, 1979	*Trachycephalus typhonius* (Linnaeus, 1758) (Anura: Hylidae), Veined treefrog or Pepper Treefrog	Province de Salta, Argentina; Paraguay	Combes and Laurent, 1979; Vaucher, 1983
P. naevius Caballero and Cerecero, 1941	*Smilisca baudinii* (Duméril and Bibron, 1841) (Anura: Hylidae), Common Mexican Treefrog	Potrero Viejo, Veracruz, Mexico	Caballero & Zerecero, 1941; Lamothe-Argumedo, 1976
P. napoense Vaucher, 1987	*Osteocephalus leprieurii* (Duméril and Bibron, 1841) (Anura: Hylidae), Cayenne Slender-legged Treefrog.	San Pablo de Kantesiya, Napo Province, Ecuador	Vaucher, 1987
P. nearcticum Paul, 1935	*Dryophytes versicolor* (LeConte, 1825) (Anura: Hylidae), Eastern Gray Treefrog	Minnesota; Weston, Conneticut; Florida; Pocahontas State Park, Virginia; Haynes Mill Pond, Virginia; Kellogg Biological Station, Michigan; St. Paul, Dynamite Pond, USA	Riley, 1927; Paul, 1935; Paul, 1938; Campbell,1967; Campbell, 1969; Muzzall and Kuczynski, 2017
	Dryophytes cinereus (Schneider, 1799) (Anura: Hylidae), North American Green Treefrog	Weston, Conneticut; Pocahontas State Park, Virginia; Haynes Mill Pond, Virginia, USA	Paul, 1938; Campbell,1967; Campbell, 1969
	Dryophytes squirellus (Daudin, 1800) (Anura: Hylidae), Squirrel Treefrog	Duke University, North Carolina, USA	USNM Invertebrate Collection Database
	Spea bombifrons (Cope, 1863) (Anura: Scaphiopodidae), Plains Spadefoot	Cochise County, Arizona, USA	Goldberg and Bursey, 2002
	Spea hammondii (Baird, 1859) (Anura: Scaphiopodidae), Western Spadefoot	California, USA	Goldberg and Bursey, 2002
	Spea intermontana (Cope, 1883) (Anura: Scaphiopodidae), Great Basin Spadefoot	Carbon County, Utah, USA	USNM Invertebrate Collection Database
	Dryophytes chrysoscelis (Cope, 1880) (Anura: Hylidae), Cope's gray treefrog	Wisconsin; Walnut Hill, Alabama, USA	Bolek and Coggins, 1998; Current Study
P. praecox Combes and Laurent, 1978	*Telmatobius oxycephalus* Vellard, 1946 (Anura:Telmatobiidae), Red-headed Water Frog	Alto Calilegua, Jujuy Province, Argentina	Combes and Laurent, 1978
P. stellai Pérez-Vigueras, 1955	*Osteopilus septentrionalis* (Duméril and Bibron, 1841) (Anura: Hylidae), Cuban Treefrog	Havana, Cuba	Pérez-Vigueras, 1955; Stunkard, 1959
P. touzeti Vaucher, 1987	*Gastrotheca riobambae* (Fowler, 1913) (Anura: Hemiphractidae), Riobamba Marsupial Frog	San Pablo de Kantesiya, Napo Province, Ecuador	Vaucher, 1987
P. travassosi Du Preez and Domingues, 2019	*Trachycephalus mesophaeus* (Hensel, 1867) (Anura: Hylidae), Porto Alegre Golden-Eyed Treefrog	Angra dos Reis, Rio de Janeiro, Brazil	Du Preez and Domingues, 2019; Kohn et al., 1978
Pseudodiplorchis americanus (Rodgers and Kuntz, 1940)	*Scaphiopus couchii* Baird, 1854 (Anura: Scaphiopodidae), Couch's Spadefoot	Lawton, Oklahoma; Arizona, USA; La Paz, Baja California Sur, México	Rodgers and Kuntz, 1940; Lamothe–Argumedo, 1985; Tinsley and Earle, 1983
Riojatrema bravoae Lamothe-Argumedo, 1963	*Eleutherodactylus nitidus* (Peters,1870) (Anura: Eleutherodactylidae), Shiny Peeping Frog; Rhinella spinulosa (Wiegmann, 1834) (Anura:Bufonidae), Warty Toad	Morelos, México	Lamothe-Argumedo, 1963
R. cerrocoloradense (Nasir and Fuentes-Zambrano, 1983)	*Rhinella marina* (Linnaeus, 1758) (Anura:Bufonidae), Cane Toad or Marine Toad	Cerro, Colorado and Cumana, Venezuela	Nasir and Fuentes-Zambrano, 1983
R. ecuadorense Dyer, 1985	Rhinella margaritifera (Laurenti, 1768) (Anura:Bufonidae), South American Common Toad	Ecuador	Dyer, 1985; Vaucher, 1987
Wetapolystoma almae Gray, 1993	*Rhinella margaritifera* (Laurenti, 1768) (Anura:Bufonidae), South American Common Toad	Peru Departamento de Madre de Dios, Provincia Tam-bopata, Cusco Amazonico, Rio Madre de Dios, ca. 15 km E Puerto Mal-donado, Peru	Gray, 1993

FIGURE LEGENDS

Figures 1−2. *Polystoma nearcticum* from Cope's gray treefrog, *Dryophytes chrysoscelis* (Anura: Hylidae) from Walnut Hill, Alabama, USA. Scale value aside bars. (**1**) Body of voucher (USNM XXXXXX) showing oral sucker (os), pharynx (ph), genital bulb (gb), excretory pores (ep), vaginae (v), ootype (oo), ovary (ov), Mehlis' gland (Mg), vitello-vaginal ducts (vvd), seminal vesicle (sv), testis (t), vitellarium (vr), haptor (h), and hamuli (hm). Ventral view. (**2**) Photomicrograph of voucher (USNM XXXXXX), showing anastomoses and cecal morphology. Ventral view.

Figure 3−6. *Polystoma nearcticum* from Cope's gray treefrog, *Dryophytes chrysoscelis* (Anura: Hylidae) from Walnut Hill, Alabama, USA. Scale value aside bars. (**3**) Haptor of voucher (USNM XXXXXX).Ventral view. (**4**) Marginal hooklets of vouchers (USNM XXXXXX–XXXXXXX). Ventral view. (**5**) Genital coronet of voucher (USNM XXXXXX). Ventral view. (**6**) Genital coronet of voucher (USNM XXXXXX). Side view.

Figure 7. *Polystoma nearcticum* from Cope's gray treefrog, *Dryophytes chrysoscelis* (Anura: Hylidae) from Walnut Hill, Alabama, USA. Scale value aside bars. Hamuli of voucher (USNM XXXXXX). Ventral view

Figure 8−10. *Polystoma* cf. *nearcticum* from Cope's gray treefrog, *Dryophytes chrysoscelis* (Anura: Hylidae) from Walnut Hill, Alabama, USA. Scale value aside bars. (**8**) Female genitalia of voucher (USNM XXXXXX) showing genital bulb (gb), excretory pores (ep), vaginae (v), uterus (ut), ootype (oo), ovary (ov), Mehlis' gland (Mg), vitello-vaginal ducts (vvd), oviduct (od), genito-intestinal canal (gc). Ventral view. (**9**) SEM of dextral vaginal mound. (**10**) Male genitalia of voucher (USNM XXXXXX), showing genital bulb (gb), genital pore (gp), seminal vesicle (sv), and testis (t). Ventral view.

Figure 11. 28S Maximum Likelihood phylogeny. Values aside nodes are posterior probability. Scale bar is in substitutions per site. GenBank numbers in parenthesis following each taxon.

Figure 12. COI Maximum Likelihood phylogeny. Values aside nodes are posterior probability. Scale bar is in substitutions per site. GenBank numbers in parenthesis following each taxon.

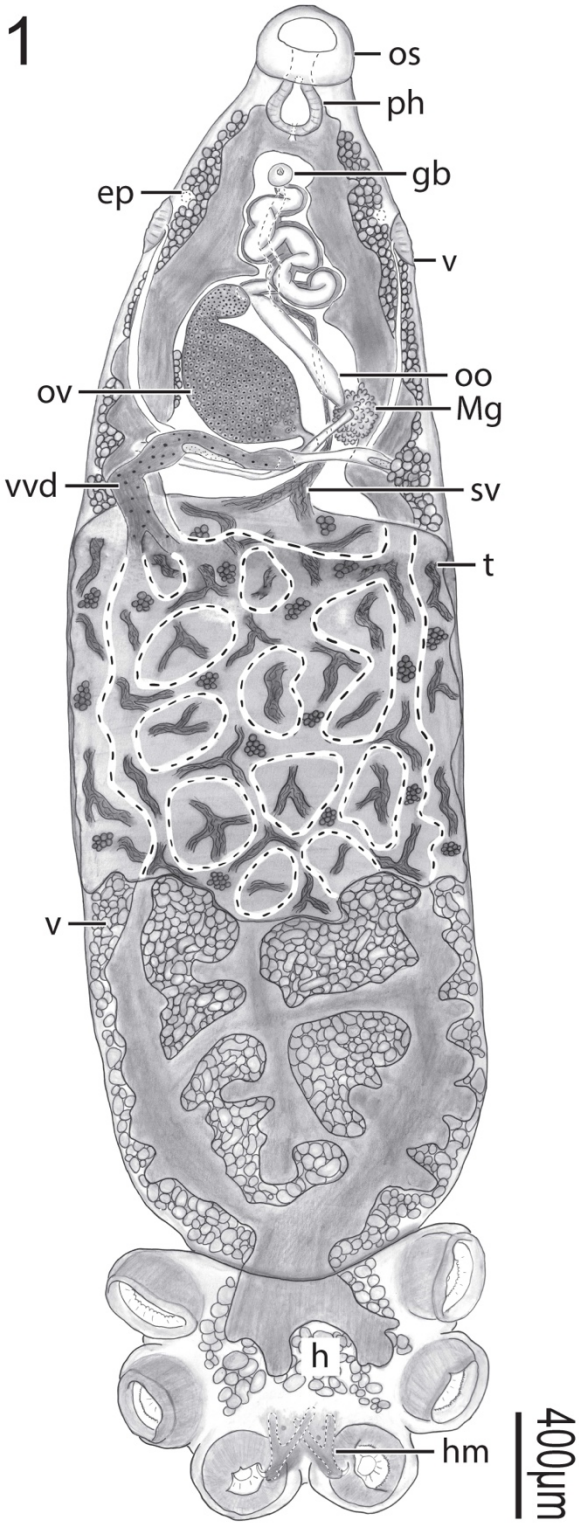
1
os
ph
gb
ep
v
oo
ov
Mg
vvd
sv
t
v
h
hm
400µm

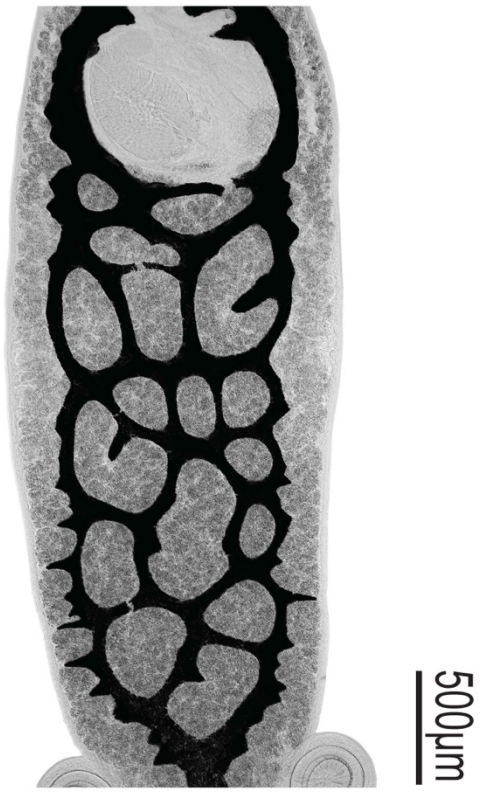
2
500µm

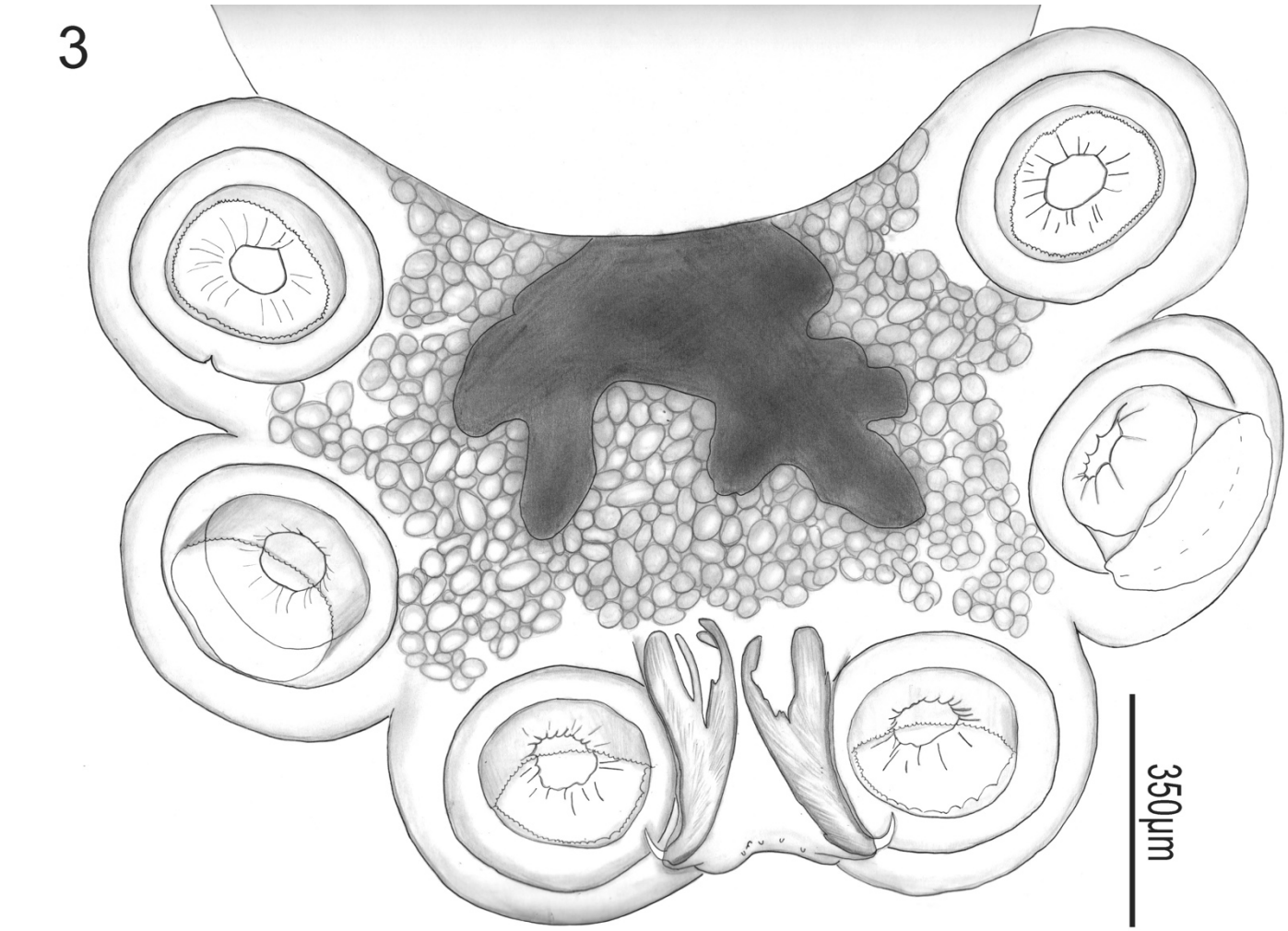
3
350µm


4
10µm

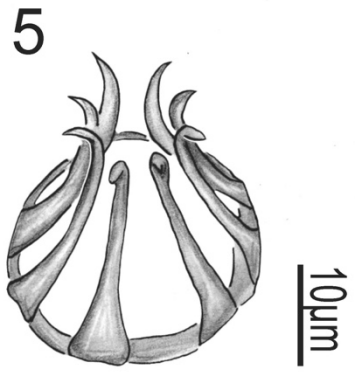
5
10µm

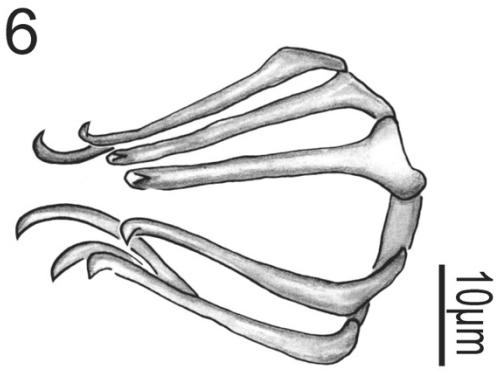
6
10µm

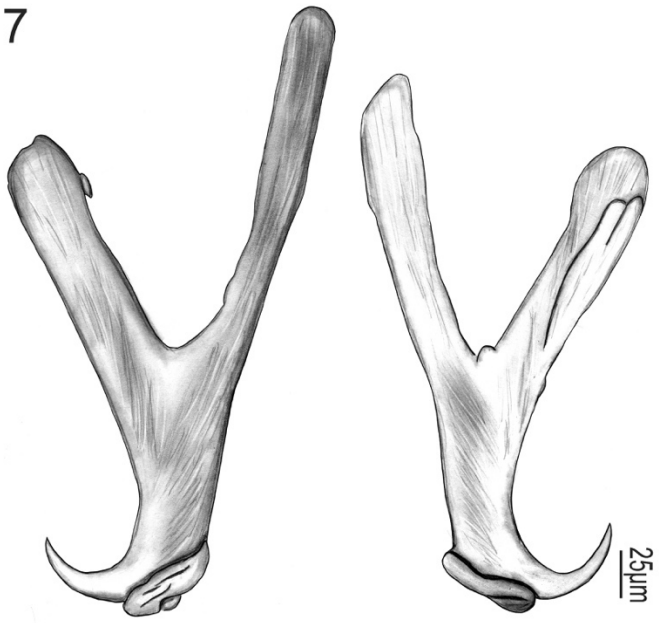
7
25µm

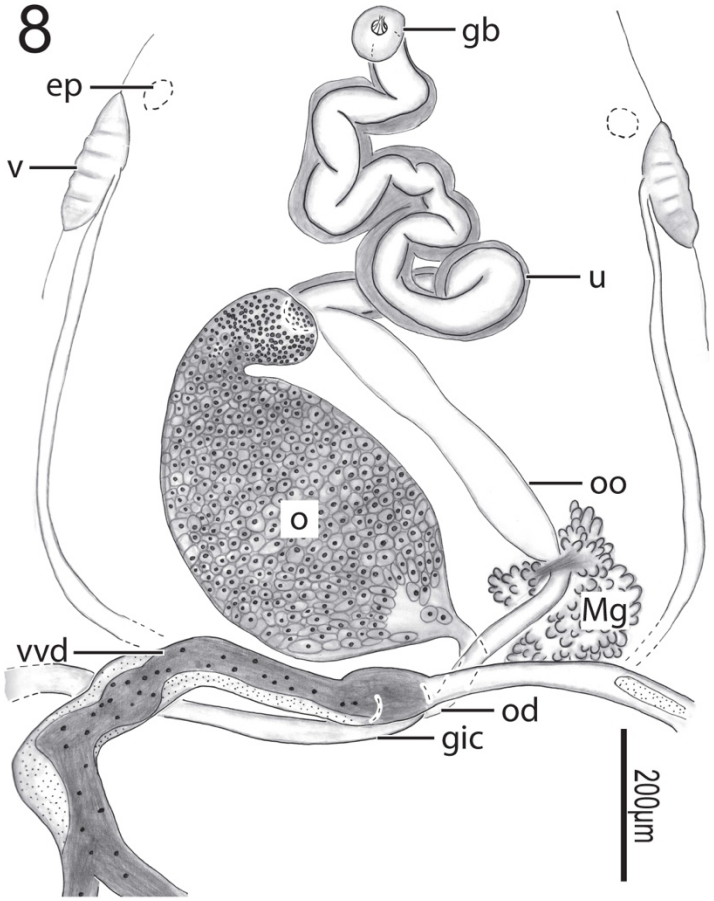
8
gb
ep
v
u
oo
o
Mg
vvd
od
gic
200µm

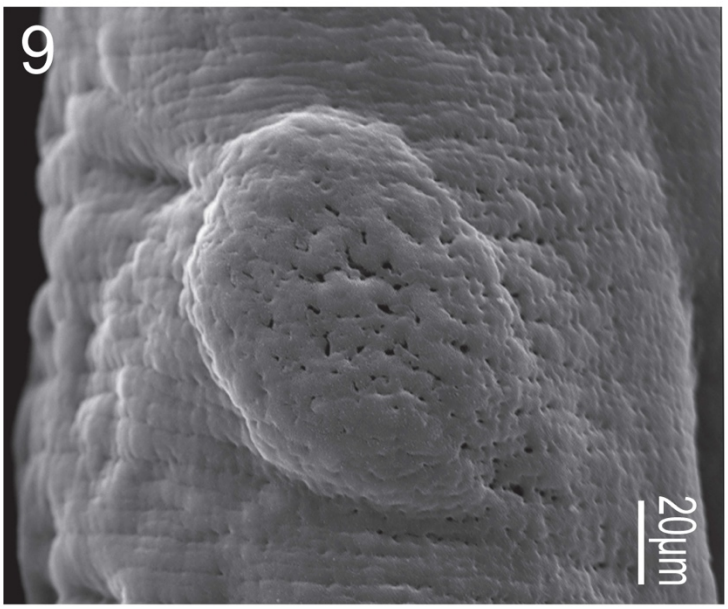
9
20µm

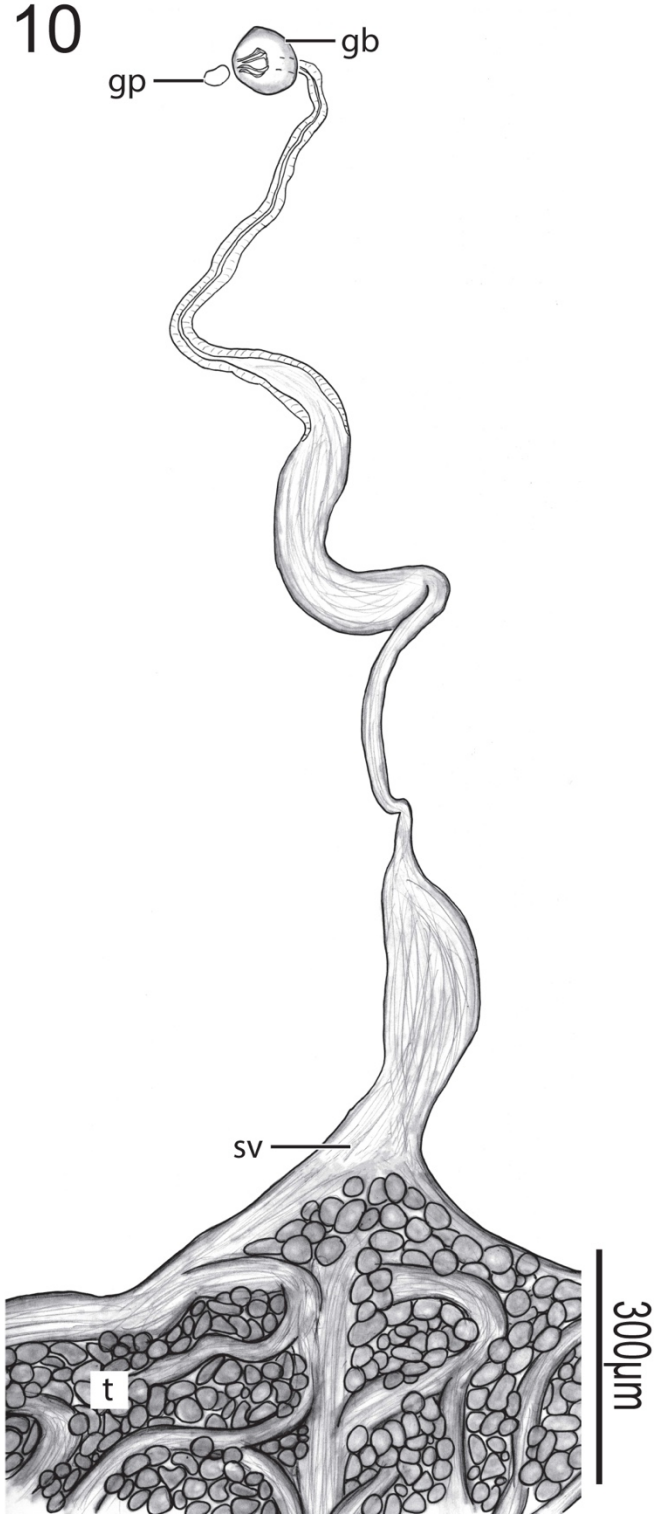
10
gb
gp
sv
t
300µm

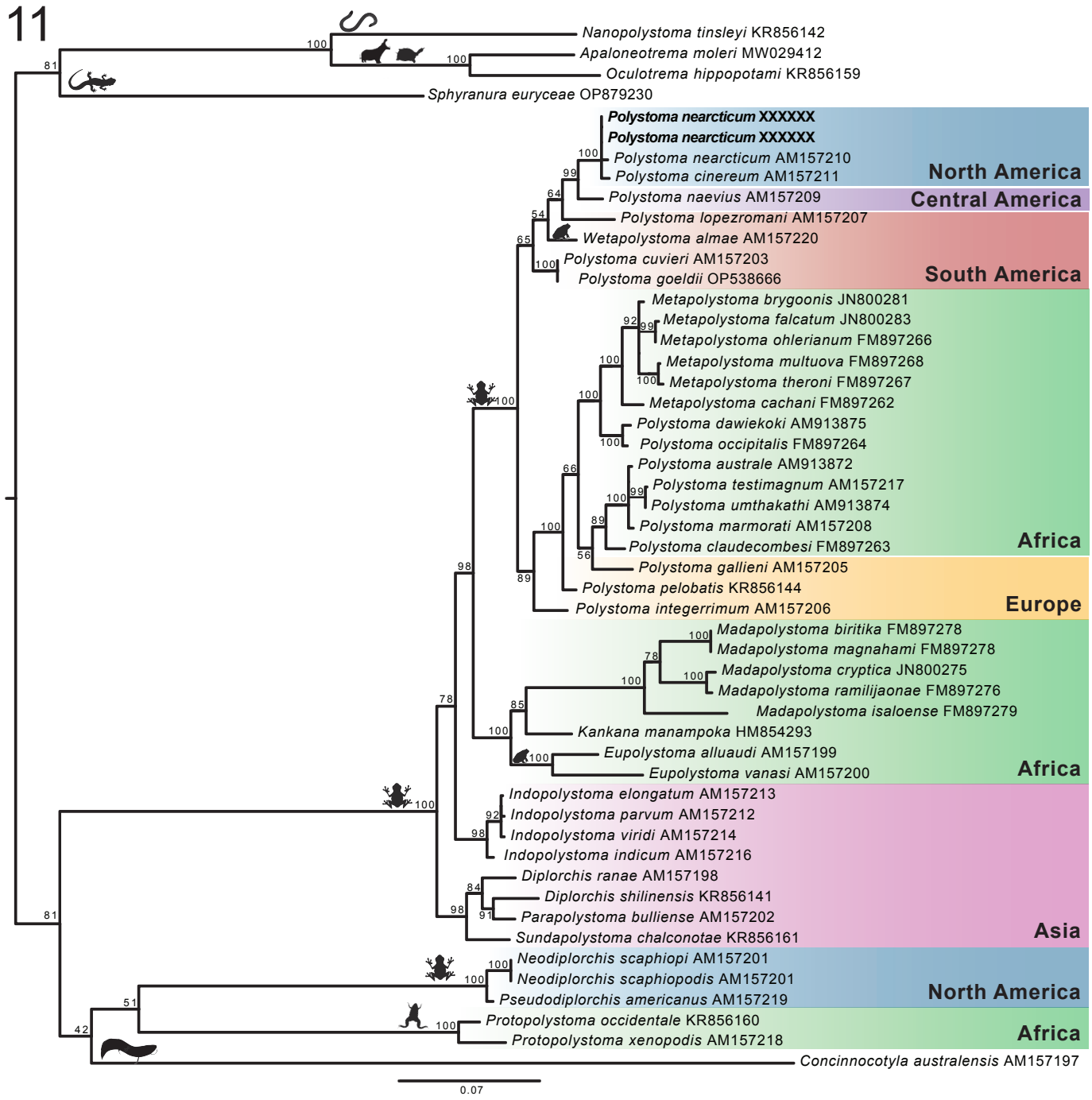
11
Nanopolystoma tinsleyi KR856142
Apaloneotrema moleri MW029412
Oculotrema hippopotami KR856159
Sphyranura euryceae OP879230
Polystoma nearcticum XXXXXX
Polystoma nearcticum XXXXXX
Polystoma nearcticum AM157210
Polystoma cinereum AM157211
North America
Polystoma naevius AM157209
Central America
Polystoma lopezromani AM157207
Wetapolystoma almae AM157220
Polystoma cuvieri AM157203
Polystoma goeldii OP538666
South America
Metapolystoma brygoonis JN800281
Metapolystoma falcatum JN800283
Metapolystoma ohlerianum FM897266
Metapolystoma multuova FM897268
Metapolystoma theroni FM897267
Metapolystoma cachani FM897262
Polystoma dawiekoki AM913875
Polystoma occipitalis FM897264
Polystoma australe AM913872
Polystoma testimagnum AM157217
Polystoma umthakathi AM913874
Polystoma marmorati AM157208
Polystoma claudecombesi FM897263
Africa
Polystoma gallieni AM157205
Polystoma pelobatis KR856144
Polystoma integerrimum AM157206
Europe
Madapolystoma biritika FM897278
Madapolystoma magnahami FM897278
Madapolystoma cryptica JN800275
Madapolystoma ramilijaonae FM897276
Madapolystoma isaloense FM897279
Kankana manampoka HM854293
Eupolystoma alluaudi AM157199
Eupolystoma vanasi AM157200
Africa
Indopolystoma elongatum AM157213
Indopolystoma parvum AM157212
Indopolystoma viridi AM157214
Indopolystoma indicum AM157216
Diplorchis ranae AM157198
Diplorchis shilinensis KR856141
Parapolystoma bulliense AM157202
Sundapolystoma chalconotae KR856161
Asia
Neodiplorchis scaphiopi AM157201
Neodiplorchis scaphiopodis AM157201
Pseudodiplorchis americanus AM157219
North America
Protopolystoma occidentale KR856160
Protopolystoma xenopodis AM157218
Africa
Concinnocotyla australensis AM157197
0.07

12

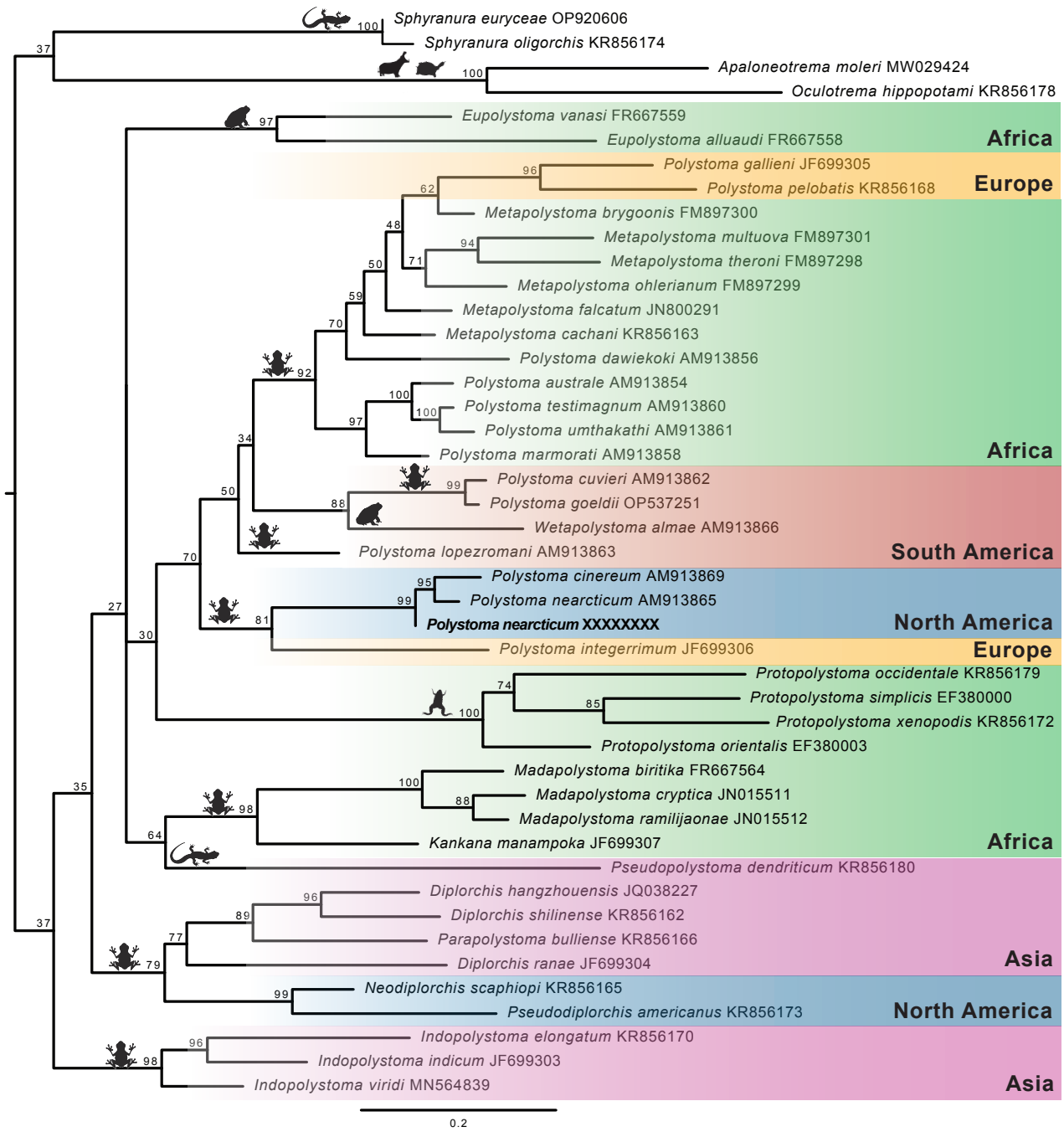
Sphyranura euryceae OP920606
Sphyranura oligorchis KR856174
Apaloneotrema moleri MW029424
Oculotrema hippopotami KR856178
Eupolystoma vanasi FR667559
Eupolystoma alluaudi FR667558
Africa
Polystoma gallieni JF699305
Polystoma pelobatis KR856168
Europe
Metapolystoma brygoonis FM897300
Metapolystoma multuova FM897301
Metapolystoma theroni FM897298
Metapolystoma ohlerianum FM897299
Metapolystoma falcatum JN800291
Metapolystoma cachani KR856163
Polystoma dawiekoki AM913856
Polystoma australe AM913854
Polystoma testimagnum AM913860
Polystoma umthakathi AM913861
Polystoma marmorati AM913858
Africa
Polystoma cuvieri AM913862
Polystoma goeldii OP537251
Wetapolystoma almae AM913866
Polystoma lopezromani AM913863
South America
Polystoma cinereum AM913869
Polystoma nearcticum AM913865
Polystoma nearcticum XXXXXXXX
North America
Polystoma integerrimum JF699306
Europe
Protopolystoma occidentale KR856179
Protopolystoma simplicis EF380000
Protopolystoma xenopodis KR856172
Protopolystoma orientalis EF380003
Madapolystoma biritika FR667564
Madapolystoma cryptica JN015511
Madapolystoma ramilijaonae JN015512
Kankana manampoka JF699307
Africa
Pseudopolystoma dendriticum KR856180
Diplorchis hangzhouensis JQ038227
Diplorchis shilinense KR856162
Parapolystoma bulliense KR856166
Diplorchis ranae JF699304
Asia
Neodiplorchis scaphiopi KR856165
Pseudodiplorchis americanus KR856173
North America
Indopolystoma elongatum KR856170
Indopolystoma indicum JF699303
Indopolystoma viridi MN564839
Asia
0.2